VNIVERSITAT DE VALÈNCIA

PhD program in Neurosciences

RD 99/2011

ANALYSIS OF STRUCTURAL PLASTICITY IN THE ADULT AND ADOLESCENT MOUSE BRAIN. EFFECTS OF ERYTHROPOIETIN

Yasmina Curto Sastre

June 2019

Dr. Juan Nácher Roselló

VNIVERSITAT DE VALÈNCIA | Facultad de Ciencias Biológicas

Departamento de Biología Celular, Funcional y Antropología Física

The supervisor of the present doctoral thesis, Dr. Juan Salvador Nácher Roselló, Doctor in Biology and Professor of the Department of Cell Biology, Functional Biology and Anthropology at the University of Valencia,

CERTIFY:

That, Ms. Yasmina Curto Sastre, graduated in Biology and MSc in Neuroscience at the University of Valencia, has carried out the present Doctoral Thesis entitled:
"ANALYSIS OF STRUCTURAL PLASTICITY IN THE ADULT AND ADOLESCENT MOUSE BRAIN. EFFECTS OF ERYTHROPOIETIN",
and that being concluded, authorizes its presentation to be judged by the corresponding court and qualified for obtaining the PhD in Neuroscience.

What I sign as required in Burjassot, on April the 10th, 2019

Dr. Juan Salvador Nácher Roselló

Para la realización de esta tesis, la autora ha sido beneficiaria de una beca predoctoral de Formación de Profesorado Universitario concedida por el Ministerio de Educación, Cultura y Deporte (FPU-13/04764) según la resolución del 18 de noviembre de 2013, de la Secretaría de Estado de Educación, Formación Profesional y Universidades.

"Lock up your libraries if you like; but there is no gate, no lock, no bolt that you can set upon the freedom of my mind."

Virginia Woolf

A MIS PADRES

A MI HERMANA

AGRADECIMIENTOS

Cuando comencé a redactar esta tesis pensé en el momento de escribir los agradecimientos, eso significaría que ya estaría todo listo y preparado. ¡Y aquí me encuentro ahora! más que nunca me vienen a la cabeza todas las personas que han hecho esto posible.

En primer lugar, quiero agradecerle a mi director, al Dr. Juan Nácher. Moltes gràcies Juan per l'oportunitat. Ets un gran investigador, però no exagero si dic que ets encara millor persona. Gràcies per la paciencia infinita, per les paraules adequades en cada moment i per la confiança. Ha estat un plaer treballar al teu laboratori.

Quiero agradecerle también al resto de profesores que forman parte del laboratorio de Neurobiología. A Emilio por sus bromas, en ocasiones pesadas, pero que siempre ha estado dispuesto a ayudarme y resolver mis dudas. A José Miguel, yo sé que echará de menos mis visitas en búsqueda de agua. Eres una enciclopedia andante y un manitas en el laboratorio. A Carlos, por esa sonrisa eterna y las palabras de ánimo. Sois los tres grandes personas y os tengo un gran cariño.

Por supuesto a mis compañeros de laboratorio! Creo que es muy importante tener un buen ambiente de trabajo y nosotros lo hemos creado. Habéis hecho que todo sea más fácil, más ameno. Quiero agradecerle en primer lugar a Clara García. Moltes gràcies Clara per la teua paciència, vas ser la primera persona en ensenyar-me com funcionava tot. Mai oblidaré les meves primeres perfusions i la perfusió que vas salvar! Gràcies per calmar-me en els meus moments d'acceleració (que són molts). Saps que sempre podràs comptar amb mi. A Maria per ser la meua partner in crime. Estàs boja i ho saps, però les millors persones ho estan. Són molts els moments que em vénen al cap, els riures al laboratori, el moment parapent i aquell home corrent i suant, els dinars i sopars... m'alegro del moment que estàs vivint ara, espero que pugue seguir compartint molts més amb tu. A Marta, que dins del desordre sempre havia molt d'ordre, ets genial Marta i arribaràs molt lluny, a la vista està. Gràcies per ser com ets i per les bones paraules sempre. A Héctor, que hem portat una vida paral·lela des de sempre. Ets tot calma i serenitat, i això s'agraeix. A Ramón, gracias infinitas por los macros pero sobre todo gracias por tu locura y tu forma de afrontar la vida. Necesitamos

a más Ramones en este mundo! A Clara Bueno, pel nostre amor-odi. Sempre serem l'equip Frozen. Ets molt gran Clara, tots els moments que recordo amb tu són amb un somriure i això diu molt de la persona que ets. Y por supuesto a Simona, mi florecilla. Hay personas que llegan a tu vida y ni te las esperas. No tengo palabras, literalmente, para agradecerte todo lo que has hecho por mí. Gracias por tu apoyo incondicional siempre, por tus consejos, por nuestros momentos y confidencias dentro del laboratorio (nuestro coffe time!) pero sobre todo por el resto de momentos que son muchos. Te quiero y lo sabes. Aquí tengo que mencionar a Ana, que vino solo unos meses y le bastó para convertirse en otra de mis florecillas. Pese a todo, siempre estaremos juntas y en un futuro quién sabe. No quiero olvidarme de toda la gente que ha formado parte del Neurolab en algún momento, Esther, Teresa, Javi, Laura, Noelia, Pablo, Esther Rodríguez… me hubiera gustado compartir más momentos con vosotras. Y por supuesto a toda la gente que empieza ahora, Julia, Yaiza… os deseo lo mejor, aunque existan momentos de bajón al final esto merece la pena, mucho ánimo chicas! Agradecerles también al resto de personas que forman la cuarta planta y que me han dado su tiempo y palabras en diferentes momentos.

Thanks very much to Dr. Ehrenreich for giving me the opportunity to work in the laboratory and for the collaborations together. Thanks to all the people in the lab, especially to Debia, my little girl, for teaching and taking care of me those months.

Por último, mi agradecimiento más sentido (se vienen lágrimas) a mis padres por todo el esfuerzo que han hecho. Por la confianza depositada, por nunca juzgar mis decisiones y apoyarme en cada paso que he dado. A mi hermana Sheila, por quererme tanto y estar siempre a mi lado. Creo que soy una afortunada por tener una familia tan unida y maravillosa como los sois vosotros. Os quiero mucho! Aquí debo incluir también a mi familia de pelo y plumas, creo que una parte de nosotros permanece dormida hasta que no descubrimos lo maravilloso que es amar a un animal, y mi corazón está lleno de huellas y pisaditas. Quiero agradecerle también a toda mi familia más cercana, a mis tíos, primos, a mis yayas… y a mis amigos por hacerme disfrutar de cada momento de esta vida, a Harry, Andreu, Paula, Olga, Nuri, Sandra, Irta...

Quiero guardarme estas últimas líneas para mencionar a mi yayo José, a quien le dedico todo el esfuerzo que he puesto en este trabajo. Ojalá pudiera compartirlo de otra forma contigo, solo quiero decirte que… lo logramos!

LIST OF CONTENTS

ABBREVIATIONS

5-HT3r	Serotonin type 3 receptor
ACC	Anterior cingulate cortex
ACd/Cg1	Dorsal cingulate cortex
ACv/Cg2	Ventral cingulate cortex
AD	Alzheimer disease
AMPA	α-amino-3-hydroxy-5-methyl-4-isoxazolepropionic acid
BDNF	Brain-derived neurotrophic factor
BZ	Benzodiazepine
CA	Cornu Ammonis
CaMKII-α	Ca(2+)/CAM-dependent protein kinase II
CB1r	Cannabinoid receptor 1
CCK	Cholecystokinin
ChABC	Chondroitinase ABC
Cl-	Chloride ion
CMP	Cytidine 5-monophosphate
CNS	Central nervous system
CSPG	Chondroitin sulfate proteoglycans
DCX	Doublecortin
DG	Dentate gyrus
dPrL	Dorsal prelimbic cortex
DZ	Diazepam
E	Embryonic day
EAAT	Excitatory amino acid transpoter
EC	Entorhinal cortex
ECM	Extracellular matrix
EGFP	Enhanced green fluorescent protein
E/I	Excitatory/inhibitory
Endo-N	Enzyme Endo-Neuraminidase-N
EPO	Erythropoietin
EPOR	Erythropoietin receptor

EPSC	Excitatory postsynaptic current
EPSP	Excitatory postsynaptic potential
FNIII	Fibronectin type III
GABA	Gamma-amynobutyric acid
GAD	Glutamic acid decarboxylase
GAT	GABA transporters
GFP	Green fluorescent protein
GIN	GFP-expressing Inhibitory Neurons
GPI	Glycosylphosphatidylinositol
HA	Hyaluronic acid
HAS	Hyaluronan synthases
HS	Hippocampo-septal cells
IG	Immunoglobulin
IL	Infralimbic cortex
IPSP	Inhibitory postsynaptic potential
IS	Interneuron-specific cells
lPFC	Lateral prefrontal cortex
LTD	Long-term depression
LTP	Long-term potentiation
mPFC	Medial prefrontal cortex
NCAM	Neural cell adhesion molecule
NMDA	*N*-methyl *D*-aspartate
nNOS	Neuronal nitric oxide synthase
NPY	Neuropeptide Y
OFC	Orbitofrontal cortex
O-LM	Oriens lacunosum-moleculare
P	Postnatal day
PBR	Polybasic region
PD	Polysialyltransferase domain
PFC	Prefrontal cortex
PNN	Perineuronal net
PNS	Peripheral nervous system

PolySia/PSA	Polysialic acid
polyST	Polysialyltransferase
PrL	Prelimbic cortex
PSD	Postsynaptic density
PV	Parvalbumin
SGZ	Subgranular zone
SOM	Somatostatin
SV	Synaptic vesicles
SVZ	Subventricular zone
SYN	Synaptophysin
TM	Transmembrane
TN	Tenascin
VGAT	Vesicular gaba transporter
VGLUT	Vesicular glutamate transporter
VIP	Vasoactive intestinal peptide
vPrL	Ventral prelimbic cortex
WFA	*Wisteria floribunda agglutinin*
YFP	Yellow fluorescent protein

LIST OF FIGURES

LIST OF TABLES

RESUMEN EN CASTELLANO

INTRODUCCIÓN

Los organismos están sujetos diariamente a cambios que ocurren en su entorno y dentro del propio organismo. Estas entradas de información del medio externo e interno son integradas y analizadas por el organismo con el fin de dar una respuesta adecuada que asegure la supervivencia. Es crucial, por tanto, que el sistema responda de forma apropiada al amplio abanico de cambios y demandas que acontecen a lo largo de la vida del organismo. En este aspecto, el sistema nervioso se destaca como uno de los principales sistemas encargados de mantener el orden interno y reaccionar con cambios adaptativos a los eventos que lo rodean. Un funcionamiento aberrante del sistema puede contribuir a las diferentes enfermedades neuropsiquiátricas que se conocen actualmente. Aunque la mayoría de los organismos poseen un sistema nervioso, la complejidad varía enormemente ofreciéndonos una excelente visión de la evolución de este sistema. En el caso de los vertebrados, ha evolucionado de tal forma que lo convierte en uno de los sistemas más sofisticados que gobiernan la vida animal. En este aspecto, el sistema nervioso se puede dividir en dos regiones principales: el sistema nervioso central (**SNC**), que está formado por el cerebro y la médula espinal, y el sistema nervioso periférico (**SNP**), compuesto por todos los nervios aferentes y eferentes que conectan cada parte del cuerpo con el SNC. Aunque el sistema nervioso está formado por un conjunto muy diverso de células, podemos destacar dos grupos principales: las neuronas y las células gliales. Las neuronas son consideradas la unidad funcional principal del sistema nervioso y fueron profundamente estudiadas por Ramón y Cajal (Ramón y Cajal, 1909), asentando las primeras bases funcionales de este complejo sistema.

A pesar de ser considerado como un sistema estático durante las últimas décadas, hoy en día se sabe que ciertas regiones conservan una marcada capacidad de remodelación, no solo durante el desarrollo sino también durante la edad adulta, aunque en menor proporción (Xerri, 2008). Dicha plasticidad está presente en condiciones normales y permite al sistema lidiar con nuevas experiencias, aprender y

reaccionar adaptativamente a diferentes factores intrínsecos o extrínsecos. Dentro de estos procesos plásticos se encuentran las alteraciones en la estructura de las neuronas, conocido como plasticidad estructural, la cual puede ser modulada, entre otros, a través de cambios en la neurotransmisión, expresión de estructuras relacionadas con la plasticidad, o el efecto de diferentes factores tróficos y hormonas. La presente tesis se centrará en la plasticidad estructural de las neuronas y su modulación a través de diferentes paradigmas, en dos de las regiones cerebrales que mantienen una marcada plasticidad incluso en cerebro adulto: la corteza prefrontal (CPF) y el hipocampo.

Descripción de las áreas de estudio

La **CPF** es una corteza asociativa ubicada en la parte anterior del lóbulo frontal del cerebro de los mamíferos (Fuster, 2015). Esta región del cerebro está implicada en la planificación del comportamiento cognitivo complejo, la memoria de trabajo, la toma de decisiones y la moderación del comportamiento social, entre otros (Carlson et al., 2006). Un mal funcionamiento de esta corteza conduce a una serie de afecciones patológicas involucradas en trastornos neuropsiquiátricos como la esquizofrenia, depresión severa o demencia (Bicks et al., 2015; Kolb and Gibb, 2015). Por otra parte, el **hipocampo** es una de las regiones más antiguas, altamente conservada en las diferentes especies (Allen and Fortin, 2013). Destaca por el papel clave que desempeña en la memoria a corto y largo plazo, pero también por su función en la navegación espacial, el comportamiento emocional y la regulación de las funciones hipotalámicas. Alteraciones que afectan la integridad de esta región están asociadas con diversos desórdenes como el Alzheimer, depresión, o esquizofrenia (Anand and Dhikav, 2012).

Tipos neuronales estudiados

En general, las neuronas pueden clasificarse atendiendo a sus características estructurales, sus propiedades electrofisiológicas y sus propiedades neuroquímicas. De esta clasificación surgen dos tipos principales de neuronas: las neuronas excitadoras (entre las que destacan las neuronas piramidales por su gran proporción) y las neuronas inhibidoras, generalmente denominadas interneuronas. Ambas poblaciones están

presentes en la CPF y el hipocampo (aunque con ciertas semejanzas y diferencias), y serán el objeto de estudio de la presente tesis.

Las **neuronas piramidales** excitadoras son más numerosas y presentan una menor diversidad en comparación con las interneuronas (Thomson, 2007). Se trata de neuronas glutamatérgicas y, por lo tanto, liberan glutamato para su comunicación, el principal neurotransmisor excitador en el cerebro (Spruston, 2008; Van Aerde and Feldmeyer, 2015). Presentan una morfología caracterizada por un cuerpo celular de forma piramidal (soma), un solo axón y dos árboles dendríticos distintos, basal y apical (Spruston, 2008). Destaca la presencia de espinas dendríticas tanto en sus dendritas apicales como basales (Hotulainen and Hoogenraad, 2010; Rochefort and Konnerth, 2012). Las espinas dendríticas son pequeñas protuberancias que constituyen el elemento postsináptico en una sinapsis. Su función principal es proveer de un compartimento local para las vías de señalización y restringir la difusión de moléculas postsinápticas (Rochefort and Konnerth, 2012). En el elemento presináptico, el axón también muestra engrosamientos membranosos llamados botones axónicos que contienen y liberan las vesículas sinápticas que albergan los neurotransmisores (Kevenaar and Hoogenraad, 2015; Spruston, 2008). Ambas estructuras constituyen los elementos post y presinápticos de una sinapsis que regulan la llegada y salida, respectivamente, de las señales de comunicación con otras neuronas.

Las **interneuronas** se caracterizan, generalmente, por la presencia de un axón corto de proyección local. Como neuronas inhibidoras, se consideran interneuronas GABAérgicas que utilizan el ácido gamma-aminobutírico (GABA) como neurotransmisor primario. Son menos numerosas, pero comprenden una amplia población (Booker and Vida, 2018; Defelipe et al., 2013). Sus diferentes dianas postsinápticas, las diferencias en el dominio subcelular, la conectividad y las propiedades intrínsecas de membrana hacen de ellas un grupo heterogéneo cuya clasificación ha sido objeto de debate hasta la fecha. En la presente tesis doctoral, se ha usado la clasificación molecular de la terminología de Petilla (Ascoli et al., 2008) la cual establece cinco tipos de interneuronas dependiendo de la expresión de diferentes proteínas quelantes de Ca^{2+} y neuropéptidos, como son: parvalbúmina, somatostatina, neuropéptido Y, péptido intestinal vasoactivo

y colecistoquinina. Para los estudios de esta tesis, han sido de principal interés las interneuronas que expresan parvalbúmina, somatostatina y colecistoquinina.

Las interneuronas que expresan **parvalbúmina** pueden clasificarse en dos grupos, células en cesto y células en candelabro, presentes tanto en la CPF como el hipocampo (Booker and Vida, 2018; Tremblay et al., 2016). Las células en candelabro hacen sinapsis exclusivamente sobre el segmento inicial del axón de las neuronas piramidales, mientras que las células en cesto deben su nombre a las cestas perisomáticas que establecen alrededor del soma y dendritas proximales de las neuronas piramidales (Defelipe et al., 2013). En esta tesis, los estudios se han centrado principalmente en este último tipo, uno de los más estudiados por sus propiedades. Las células en cesto funcionan como mecanismos de relojería controlando el disparo y precisión de las células piramidales, probablemente a través del alto número de sinapsis que cada célula en cesto puede establecer con varias neuronas piramidales. El segundo gran tipo lo componen las interneuronas que expresan el neuropéptido **somatostatina**. Están presentes en toda la corteza cerebral, incluidos la CPF (Tremblay et al., 2016) y el hipocampo (Somogyi and Klausberger, 2005). En esta tesis, se han estudiado especialmente dos subpoblaciones de interneuronas que expresan somatostatina: las células de Martinotti en la CPF y las células O-LM en el hipocampo. Este tipo de interneuronas presenta una amplia gama de morfologías, pero su función principal es inhibir la parte distal del árbol dendrítico de las neuronas piramidales con el cual establecen contacto, generalmente en una comunicación recíproca (Scheyltjens and Arckens, 2016; Urban-Ciecko and Barth, 2016). Entre las interneuronas, son especialmente importantes debido a la presencia de espinas dendríticas a lo largo de sus dendritas las cuales pueden sufrir remodelado dendrítico en respuesta a diferentes eventos. En último lugar, en esta tesis también han sido objeto de estudio las interneuronas que expresan el neuropéptido **colecistoquinina**, presentes tanto en la CPF (Tremblay et al., 2016) como el hipocampo (Booker and Vida, 2018). Del mismo modo que las células en cesto que expresan parvalbúmina, estas interneuronas también inervan la región perisomática y las dendritas proximales de las neuronas piramidales. Una característica relevante y que nos ha facilitado su estudio, es la expresión del receptor de cannabinoides 1 (CB1r) en sus terminales axónicos.

Tanto las neuronas piramidales como las interneuronas, están sujetas a procesos de **plasticidad estructural** que pueden ser modulados, entre otros, por cambios en la neurotransmisión, la expresión de estructuras relacionadas con la plasticidad y diferentes factores tróficos y hormonas. Estos cambios estructurales pueden estudiarse a diferentes niveles, desde cambios en la longitud y complejidad de los árboles dendríticos, alteraciones en la densidad y morfología de sus espinas dendríticas hasta cambios en la densidad de los botones axónicos.

Efectos de la neurotransmisión excitadora e inhibidora sobre la plasticidad

Una alteración de los sistemas glutamatérgico y GABAérgico que perturbe el balance de excitación/inhibición, puede afectar a la integridad de las neuronas, produciendo desde cambios en la expresión de moléculas hasta fenómenos de remodelación neuronal.

Respecto al **sistema glutamatérgico**, utiliza glutamato como principal neurotransmisor excitador, siendo las neuronas piramidales los miembros más numerosos de neuronas excitadoras. Para su estudio, son de gran ayuda ciertas proteínas de vesícula sináptica como el transportador vesicular de glutamato (**VGLUT**), un excelente marcador de terminales presinápticos excitadores. Se destaca también el estudio de la expresión de sinaptofisina (**SYN**), una de las proteínas de vesícula sináptica más abundante y conservada, que supone alrededor del 10% de la proteína total presente en la vesícula (Takamori et al., 2006). Dicha proteína desempeña un papel clave en la formación de sinapsis dependiente de actividad (Tarsa and Goda, 2002), por lo que, junto con su presencia exclusiva en la vesícula sináptica, su expresión es usada ampliamente como marcador presináptico de ambos terminales, glutamatérgicos y GABAérgicos. El glutamato puede ejercer su función a través de receptores ionotrópicos y metabotrópicos. Entre los receptores ionotrópicos, se destacan tres tipos: los receptores del ácido α-amino-3-hidroxi-5-metil-4-isoxazolpropiónico (**AMPA**), N-metil-D-aspartato (**NMDA**) y kainato, presentes tanto en las neuronas piramidales como en las interneuronas (Akgül and McBain, 2016). Aunque su efecto final es semejante, la despolarización de la membrana postsináptica, su modo de acción y propiedades son ligeramente diferentes. La manipulación de estos receptores tiene efectos sobre ciertos

procesos de plasticidad funcional y estructural como los que ocurren durante la memoria y el aprendizaje (Newcomer et al., 2000). Además, el uso de agonistas y antagonistas ha demostrado su implicación en la remodelación estructural de neuronas piramidales e interneuronas (McKinney, 2010; Perez-Rando et al., 2017a; Pérez-Rando et al., 2017b; Tian et al., 2007).

El **sistema GABAérgico**, utiliza el GABA como neurotransmisor principal, sintetizado y utilizado por las interneuronas para su comunicación. Para su estudio, es de gran ayuda la expresión de ciertas moléculas. Es el caso del ácido glutámico decarboxilasa (**GAD**) que cataliza la síntesis de GABA a partir de glutamato, o del transportador vesicular de GABA (**VGAT**). Ambos son excelentes marcadores de terminales presinápticos GABAérgicos. El neurotransmisor GABA puede ejercer su función, hiperpolarización de la membrana postsináptica, a través de receptores ionotrópicos y metabotrópicos localizados tanto en neuronas piramidales como interneuronas (Pettit and Augustine, 2000). Entre los receptores ionotrópicos, destaca el papel del receptor $GABA_A$. Este receptor ha sido de gran interés como diana de diferentes fármacos como es el caso de la benzodiazepina diazepam, un agonista alostérico de los receptores $GABA_A$ con propiedades ansiolíticas, sedativas, anticonvulsivas y miorelajantes. Las **benzodiazepinas** pueden actuar modulando la plasticidad sináptica. En el hipocampo, el uso del agonista diazepam aumenta la estabilización sináptica y la agrupación de receptores $GABA_A$ durante la actividad neuronal reduciendo así su difusión lateral, lo que resulta en una potenciación de las sinapsis inhibidoras (Gouzer et al., 2014; Lévi et al., 2015). La activación o inhibición de los receptores $GABA_A$ parece tener un papel adaptativo en las sinapsis GABAérgicas. Esta actividad es responsable de los rápidos efectos ansiolíticos, anticonvulsivos e hipnóticos de las benzodiazepinas. Alteraciones indirectas del nivel de neurotransmisión inhibidora a través del uso de diferentes hormonas como el estradiol y estrógenos, se han visto acompañadas de cambios en la estructura de las neuronas (Murphy et al., 1998; Tan et al., 2012).

Tipos de moléculas relacionadas con la plasticidad estructural

Existen dos tipos de moléculas relacionadas con fenómenos de plasticidad estructural de especial interés en la presente tesis: la forma polisializada de la molécula de adhesión celular neural (poliSia-NCAM) y los componentes de las redes perineuronales (PNNs).

PoliSia-NCAM se caracteriza por sus propiedades anti-adhesivas y está implicada en eventos clave durante el desarrollo embrionario donde su expresión es máxima. Durante este periodo, facilita la correcta migración y diferenciación neuronal, el crecimiento de neuritas, así como el remodelado dendrítico y sináptico (Bonfanti, 2006; Gascon et al., 2007; Rutishauser, 2008). Aunque hay un notable descenso durante la edad adulta, su expresión puede encontrarse asociada a neuronas inmaduras de la corteza piriforme y nichos neurogénicos. Además, y de ahí el interés para la presente tesis, en el cerebro adulto se encuentra asociada a una subpoblación de interneuronas corticales maduras y elementos inhibidores de la CPF y el hipocampo (Gómez-Climent et al., 2011; Nacher et al., 2013), asociada principalmente a fenómenos plásticos. La adición de poliSia a NCAM está catalizada por dos polisialiltransferasas independientes, **ST8SIA2** y **ST8SIA4**, con diferente patrón de expresión temporal y espacial (Hildebrandt et al., 2007). ST8SIA2 parece ser la principal enzima responsable durante el desarrollo embrionario, mientras que ST8SIA4 lo es en el cerebro adulto. Además, ST8SIA4 está principalmente implicada en la expresión de poliSia asociada a las interneuronas corticales maduras, mientras que ST8SIA2 es la principal enzima implicada en la síntesis de poliSia en las neuronas inmaduras de la corteza piriforme y nichos neurogénicos adultos (Nacher et al., 2010). Su íntima relación con las interneuronas hace que alteraciones en su expresión provocadas por diferentes paradigmas puedan afectar la estructura y conectividad de algunas subpoblaciones, y de manera indirecta también la de neuronas piramidales (Carceller et al., 2018; Castillo-Gómez et al., 2015, 2016a, 2017; Guirado et al., 2014a). Además, la depleción de poliSia utilizando la enzima Endo-Neuraminidase-N (Endo-N) afecta la plasticidad estructural y la conectividad de interneuronas y neuronas piramidales (Castillo-Gómez et al., 2016a, 2016b; Guirado et al., 2014b).

Por otro lado, las **PNNs** son estructuras especializadas de la matriz extracelular que se encuentran alrededor del soma y dendritas de ciertos tipos neuronales restringiendo su conectividad y plasticidad (Wang and Fawcett, 2012). Las PNNs están constituidas por diversos componentes sintetizados no solo a partir de las propias neuronas, sino también de las células gliales circundantes, como los oligodendrocitos y astrocitos (Carulli et al., 2006). Todos ellos secretan las moléculas al espacio extracelular, donde se asocian con receptores de la superficie celular para conformar agregados heterogéneos. Entre sus principales componentes destaca al ácido hialurónico, proteoglicanos condroitín sulfato, tenascinas y proteínas de unión. Su aparición supone el cierre del periodo crítico de elevada plasticidad (Pizzorusso et al., 2002), y coincide con la maduración de las interneuronas y el establecimiento del adecuado equilibrio excitador/inhibidor (Harauzov et al., 2010; Morishita and Hensch, 2008). Por ello, las PNNs son ampliamente consideradas indicadores de maduración neuronal. Las PNNs se encuentran en varias regiones del cerebro, incluyendo la CPF y el hipocampo, principalmente alrededor de interneuronas GABAérgicas que expresan parvalbúmina (Celio, 1993; Kosaka and Heizmann, 1989). Algunos tratamientos son capaces de alterar la densidad de PNNs, lo cual se ha visto acompañado de cambios en la estructura de las neuronas (Castillo-Gómez et al., 2017; Guirado et al., 2014a). Dada su íntima relación con las interneuronas parvalbúmina, las PNNs juegan un papel clave en la actividad de estas interneuronas y, por lo tanto, en el equilibrio excitador/inhibidor.

Inductores moleculares de la plasticidad estructural en cerebro adulto

Son varias las moléculas que pueden desempeñar un papel en la modulación de la plasticidad estructural de las neuronas, como son los factores tróficos y diversas hormonas. En cuanto a los factores tróficos, se trata de moléculas que promueven el crecimiento y supervivencia de un grupo específico de células. Entre ellos se encuentra el factor neurotrófico derivado del cerebro (BDNF por sus siglas en inglés). Son diferentes los tratamientos que han demostrado su efecto sobre el remodelado neurítico (Amaral and Pozzo-Miller, 2007; Chapleau et al., 2009). Por otro lado, algunas hormonas como la insulina o los glucocorticoides juegan un papel en diferentes aspectos

de la plasticidad neural, lo cual se ha visto reflejado por sus efectos sobre la neurogénesis adulta y la plasticidad estructural y sináptica (Anderson et al., 2002; Lee et al., 2011; Lucassen et al., 2014). En esta tesis, se estudiará en profundidad la molécula de **eritropoyetina** (EPO), una hormona conocida principalmente por su papel como factor estimulador de la eritropoyesis, pero con propiedades interesantes en diferentes procesos cerebrales. Se ha visto que tanto la EPO como su receptor, EPOR, son expresados en el cerebro por neuronas y células gliales. Aunque ciertamente hay un notable descenso tras el desarrollo embrionario, aún mantienen una marcada expresión en ciertas áreas cerebrales incluyendo la CPF y el hipocampo (Digicaylioglu et al., 1995; Ehrenreich et al., 2003; Ott et al., 2015). Su acción a través de su receptor EPOR promueve un amplio rango de acciones que incluyen efectos anti-apoptóticos, anti-oxidantes y anti-inflamatorios, tanto en neuronas como en células gliales. Además, promueve la supervivencia y proliferación celular, así como la neurogénesis adulta (Alnaeeli et al., 2012; Sirén et al., 2009). Durante los últimos años se ha demostrado su fuerte efecto procognitivo, no solo en pacientes y animales sanos sino también en cerebros comprometidos (Adamcio et al., 2008; Ehrenreich et al., 2007a, 2007b; El-Kordi et al., 2009; Gao et al., 2015; Miskowiak et al., 2007). Aunque tenemos alguna pista sobre las bases neurobiológicas que operan estos procesos cognitivos, poco se sabe sobre sus efectos sobre la plasticidad de las neuronas.

OBJETIVOS

El principal objetivo de esta tesis doctoral es estudiar los efectos que diferentes manipulaciones farmacológicas y genéticas producen sobre la plasticidad estructural de las neuronas excitadoras e inhibidoras en el encéfalo de ratón, su conectividad y la expresión de moléculas relacionadas con la plasticidad, tanto en edad adulta como durante la adolescencia. Para alcanzar este objetivo principal, a continuación se detallan los diferentes objetivos específicos:

1. Evaluar el impacto que puede tener un aumento directo de la neurotransmisión inhibidora, por medio de un tratamiento crónico con la

benzodiazepina diazepam, sobre la estructura de las neuronas piramidales de la corteza prefrontal.

2. Estudiar los efectos que puede tener una depleción genética de las polisialiltransferasas ST8SIA2 y ST8SIA4 sobre la estructura dendrítica y la conectividad de las interneuronas de la corteza prefrontal.

3. Estudiar el impacto de un tratamiento crónico con eritropoyetina sobre la estructura y conectividad de las neuronas inhibidoras de la región CA1 del hipocampo, sobre el balance excitación/inhibición de esta región y sobre moléculas relacionadas con la plasticidad de las interneuronas.

METODOLOGÍA Y RESULTADOS

EXPERIMENTO 1. *Efecto de un tratamiento crónico con la benzodiazepina diazepam sobre la plasticidad estructural de las neuronas piramidales de la corteza prefrontal*

Con el objetivo de ver cómo un aumento de la neurotransmisión inhibidora *per se* puede afectar a la densidad de espinas dendríticas de las neuronas piramidales de la capa V y la densidad de botones axónicos de la corteza cingulada, ratones macho adultos de 3 meses de la cepa THY1-YFP se han sometido a un tratamiento crónico con diazepam durante 21 días con una dosis ansiolítica pero no sedativa (2mg/kg, ip). En esta cepa de ratones transgénicos, un subconjunto de neuronas piramidales expresa de forma constitutiva la proteína amarilla fluorescente (YFP por sus siglas en inglés) entre las que se encuentran las neuronas piramidales ubicadas en las capas V y VI de la CPF y una gran población de neuronas piramidales del hipocampo (Feng et al., 2000; Porrero et al., 2010). El diazepam es un agonista alostérico de los receptores $GABA_A$, por lo que su administración crónica provocará un aumento de la neurotransmisión inhibidora. Aunque el objetivo principal es estudiar los efectos del diazepam sobre la morfología de las neuronas piramidales, también se han evaluado los efectos ansiolíticos del tratamiento con dos test de comportamiento relacionados con la ansiedad al inicio y 24 horas después de la última inyección.

En la presente tesis se muestra como un aumento de la neurotransmisión inhibidora a través del uso del agonista diazepam, disminuye la densidad de espinas dendríticas de las neuronas piramidales de la capa V de la corteza cingulada. Este estudio es la primera evidencia, hasta la fecha, de que un aumento en la inhibición *per se* actuando directamente sobre los receptores $GABA_A$, puede modificar la estructura de las neuronas piramidales de la CPF. Estos resultados están de acuerdo con estudios previos que muestran cambios indirectos en la neurotransmisión inhibidora acompañados de cambios en la estructura de las neuronas (Murphy et al., 1998; Tan et al., 2012). Todo ello sugiere que cambios en la inhibición parecen ocurrir antes o simultáneamente a los cambios en las conexiones excitadoras.

Este tratamiento, sin embargo, no provoca cambios en la densidad de botones axónicos de las capas I-II de la corteza cingulada. Un trabajo descriptivo de los ratones THY1-YFP indica que los axones de estas capas probablemente surjan de las neuronas principales de la región de la amígdala (Porrero et al., 2010). La amígdala se ha relacionado con algunos de los efectos ansiolíticos que las benzodiazepinas pueden producir en el cerebro. Pese a su interés, debido a la alta densidad de neuronas marcadas en la cepa THY1-YFP, ha sido imposible realizar un estudio de la densidad de espinas dendríticas en esta zona. Sin embargo, el inmunomarcaje con VGLUT2, el transportador vesicular de glutamato que prevalece en las regiones extracorticales, ha confirmado que la mayoría de los axones ubicados en la corteza cingulada entre las capas I-II son de origen extracortical.

Los datos obtenidos de los test de comportamiento muestran como el tratamiento crónico con diazepam no induce alteraciones en el nivel de ansiedad. A pesar de usar una dosis con efectos ansiolíticos reconocidos, no ha sido suficiente para inducir diferencias significativas en el nivel de ansiedad después de su administración crónica. Otros trabajos también han fallado en encontrar diferencias a este nivel o incluso apuntan hacia un aumento en el nivel de ansiedad (Prut and Belzung, 2003). Además, la cepa de ratones utilizada en el estudio muestra un alto comportamiento exploratorio incluso en condiciones normales (Bouwknecht and Paylor, 2002; Kim et al., 2002). Otras pruebas más sensibles podrían detectar cambios en el nivel de ansiedad.

EXPERIMENTO 2. *Impacto de la depleción genética de ST8SIA2 y ST8SIA4 sobre la estructura dendrítica y la conectividad de las interneuronas de la corteza prefrontal*

Con el objetivo de estudiar la contribución de cada polisialiltransferasa sobre la neuritogénesis y sinaptogénesis de las interneuronas corticales, se han usado dos cepas de ratones knock-out para cada una de ellas (ST8SIA2 y ST8SIA4), así como animales control. Estos animales poseen además una subpoblación de interneuronas que expresan la proteína verde fluorescente bajo el promotor de GAD67 (GAD67-GFP por sus siglas en inglés), lo cual facilita su estudio morfológico. Concretamente, se ha analizado la estructura y la conectividad de las interneuronas de las cortezas prelímbica e infralímbica. Al alcanzar los 3 meses de edad, todos los animales han sido sacrificados y sus cerebros procesados para los diferentes estudios.

Con el fin de conocer en qué subpoblación de interneuronas se realizan los análisis, se ha caracterizado el fenotipo neuroquímico de estas interneuronas GAD67-GFP de las cortezas prelímbica e infralímbica. Para ello, se han usado diferentes marcadores de interneuronas como parvalbúmina, calretinina y calbindina. Este estudio muestra como la mayor parte de las células GAD67-GFP coexpresan mayoritariamente los marcadores parvalbúmina y calbindina, y en menor proporción calretinina. Además, los porcentajes son similares en las tres cepas analizadas. Estos datos son consistentes con estudios previos realizados en la corteza motora de ratones GAD67-GFP (Tamamaki et al., 2003).

En el presente estudio, se muestra además que solo la depleción genética de la enzima ST8SIA4, y no la de ST8SIA2, es capaz de producir una reducción significativa en la arborización dendrítica de las interneuronas GAD67-GFP prefrontocorticales comparado con los animales control. Este dato sugiere que la síntesis y la unión de poliSia producida por ST8SIA4 es necesaria para el correcto desarrollo del árbol dendrítico de estas interneuronas. Aunque no se han podido diferenciar los diferentes subtipos de interneuronas para referir el análisis estructural a una subpoblación específica, no se han observado espinas dendríticas en las interneuronas GAD67-GFP analizadas, lo cual excluye a las células Martinotti del análisis dendrítico (Gilabert-Juan et al., 2013a).

Por otra parte, el análisis de la densidad perisomática inhibidora sobre neuronas piramidales de las cortezas prelímbica e infralímbica, muestra una reducción en la densidad total de puncta que expresan parvalbúmina en ambas cepas knock-out para ST8SIA4 y ST8SIA2. Para llevarlo a cabo, se ha analizado la densidad de puncta que expresan parvalbúmina y sinaptofisina alrededor del soma de neuronas excitadoras marcadas por inmunohistoquímica. Además, la disminución en la densidad de puncta que coexpresan parlvalbúmina y sinaptofisina indica una reducción en el número de sinapsis activas. Estos datos contrastan con estudios previos donde se analiza el efecto de la depleción de poliSia usando la enzima Endo-N (Castillo-Gómez et al., 2011, 2016b). Esto sugiere un papel diferencial de la expresión de poliSia durante el desarrollo temprano de la interneurona (como es el caso de nuestros ratones transgénicos) en comparación con su presencia durante la edad adulta (pudiendo ser alterada por depleción enzimática) cuando parece desempeñar un papel aislante (Castillo-Gómez et al., 2011; Nacher et al., 2013).

EXPERIMENTO 3. *Estudio del impacto de un tratamiento crónico con eritropoyetina sobre la estructura y conectividad de las neuronas inhibitorias de la región CA1 del hipocampo, el balance excitación/inhibición, así como moléculas relacionadas con la plasticidad de las interneuronas.*

En la presente tesis, se ha tratado de entender cómo un tratamiento crónico con la hormona eritropoyetina altera la estructura de las interneuronas somatostatina y parvalbúmina de la región CA1 del hipocampo, qué cambios ocurren con respecto a la neurotransmisión excitadora/inhibidora en esta región, su conectividad sináptica con las neuronas piramidales, así como cambios en la expresión de estructuras relacionadas con la plasticidad. Para llevarlo a cabo, ratones macho de 28 días de edad de la cepa Gin (denominados GAD-EGFP en esta tesis) han sido inyectados durante 3 semanas (5 IU/g in 0.01 ml) en días alternos, con un total de 11 administraciones con la hormona eritropoyetina. Tras 24 horas de la última inyección, los animales han sido sacrificados y sus cerebros procesados para los diferentes análisis. Estos ratones se caracterizan por expresar de forma constitutiva la proteína verde fluorescente (EGFP por sus siglas en

inglés) en una subpoblación de interneuronas mayoritariamente somatostatina positivas (Oliva et al. 2000).

En este trabajo, se muestra como el tratamiento crónico con eritropoyetina no produce cambios sobre la neurotransmisión excitadora e inhibidora en ninguna de las capas estudiadas de la región CA1. Sin embargo, alteraciones significativas pueden observarse al analizar la estructura de interneuronas somatostatina y parvalbúmina de la capa *oriens* de la región CA1 del hipocampo. Respecto a las interneuronas somatostatina de la capa *oriens*, estas interneuronas son principalmente células O-LM que inervan el árbol dendrítico distal de las neuronas piramidales y se caracterizan por la presencia de espinas dendríticas. Tras el tratamiento con EPO, se observa una disminución en la complejidad del árbol dendrítico así como una disminución en la densidad de espinas dendríticas. Esta atrofia estructural podría estar relacionada con el efecto que el tratamiento con EPO produce sobre las neuronas piramidales de CA1, es decir, un aumento en la densidad de espinas dendríticas (Curto et al., Resultados no publicados) y el aumento en el número de neuronas piramidales maduras en esta región (Hassouna et al., 2016). Estos efectos de la EPO sobre las neuronas piramidales podrían resultar en un aumento de la excitación sobre las interneuronas O-LM, y posiblemente, la reducción del árbol dendrítico y las espinas sea una respuesta protectora de estas neuronas inhibidoras.

La disminución de la arborización dendrítica y la densidad de espinas dendríticas en estas interneuronas somatostatina probablemente represente una disminución en su input sináptico, principalmente excitador (Blasco-Ibáñez and Freund, 1995). Esta disminución en la entrada de excitación se refleja en la disminución de la densidad de botones axónicos *en passant*, EGFP+, en el estrato *lacunosum-moleculare*. Esta reducción en la inhibición podría hacer que las neuronas piramidales sean más excitables y contribuir al aumento de las espinas dendríticas (Curto et al., Resultados no publicados) y la LTP detectada después de este tratamiento crónico de EPO (Dias et al. 2017).

Un escenario similar al descrito en las interneuronas O-LM debe estar ocurriendo en las interneuronas parvalbúmina del estrato *oriens*, donde también se observa una

disminución en la complejidad del árbol dendrítico. La reducción en la complejidad dendrítica puede ser, como en las células O-LM, una respuesta frente a un aumento en la entrada de excitación. Esta disminución en la entrada sináptica podría provocar a su vez una reducción en su señal inhibidora sobre las neuronas piramidales, como lo demuestra la disminución en la densidad de puncta perisomáticos PV+ alrededor de los somas de las neuronas piramidales. Se observa además una reducción en la densidad de puncta perisomáticos CB1+ en el estrato piramidal, lo que indica que las células en cesto que expresan colecistoquinina también están afectadas por el tratamiento con EPO, respondiendo de manera similar a las que expresan PV.

Por otra parte, se ha estudiado como dicho tratamiento afecta a la densidad de estructuras relacionadas con la plasticidad como son las PNNs y poliSia-NCAM. El tratamiento con eritropoyetina produce un aumento en la densidad de PNNs. Sin embargo, solo se observa un ligero aumento en la densidad de neuronas parvalbumina rodeadas por PNNs, lo que sugiere que el aumento de PNNs podría estar asociado a otro tipo celular, probablemente neuronas excitadoras. Dado que la presencia de PNNs parece restringir los cambios plásticos, principalmente los asociados a las interneuronas parvalbúmina, el ligero aumento de células parvalbúmina rodeadas de PNNs podría explicar, en parte, la disminución de la arborización dendrítica y la inervación perisomática inhibidora observadas en este estudio.

Finalmente, se muestra como el tratamiento con eritropoyetina produce un incremento en la expresión de poliSia-NCAM en las diferentes capas de la región CA1 del hipocampo. En el hipocampo, poliSia se asocia principlamente con subpoblaciones de interneuronas entre las que se incluyen las somatostatina y parvalbúmina (Gómez-Climent et al., 2011; Nacher et al., 2002a). Estudios previos han visto como aquellas interneuronas que expresan poliSia-NCAM tienen una menor densidad dendrítica y menos contactos perisomáticos en comparación con las interneuronas que carecen de esta molécula (Gómez-Climent et al. 2011). El aumento en el nivel de expresión de poliSia-NCAM observado después del tratamiento con eritropoyetina, podría explicar la reducción en las características estructurales de ambas subpoblaciones de

interneuronas estudiadas y también la disminución en la inervación perisomática inhibidora.

CONCLUSIONES

1. Un tratamiento crónico con diazepam, un agonista de los receptores $GABA_A$, disminuye la densidad de espinas dendríticas en la dendrita principal apical de las neuronas piramidales ubicadas en la capa V de la corteza cingulada de ratones adultos.

2. Un análisis neuroquímico usando una inmunohistoquímica para VGLUT2 muestra que la mayoría de los botones axónicos excitadores (YFP+) de las capas I-II de la corteza cingulada de ratones adultos tienen un origen extracortical.

3. Un tratamiento crónico con diazepam no induce cambios en la densidad de botones axónicos de las capas I-II de la corteza cingulada de ratones adultos.

4. El tratamiento crónico con diazepam, usando una dosis ansiolítica pero no sedativa, no induce cambios en el nivel de ansiedad de los ratones adultos.

5. El fenotipo de las interneuronas GAD67-GFP+ presentes en las cortezas prelímbica e infralímbica de las cepas de ratones transgénicos y control, es similar tanto en los knockouts para ST8SIA2 y ST8SIA4, como en los ratones control.

6. Las interneuronas que expresan GAD67-GFP+ en las cortezas prelímbica e infralímbica de los knockouts para las polisialiltransferasas ST8SIA2 y ST8SIA4 y de los ratones control, coexpresan principalmente parvalbúmina y calbindina y, en menor medida, calretinina.

7. La depleción genética de ST8SIA4, pero no de ST8SIA2, disminuye la complejidad del árbol dendrítico de las interneuronas GAD67-GFP+ de las cortezas prelímbica e infralímbica.

8. La depleción genética de cualquiera de las dos enzimas, ST8SIA2 o ST8SIA4, disminuye la densidad total de puncta que expresan parvalbúmina alrededor del soma de las neuronas piramidales de las cortezas prelímbica e infralímbica.

9. La densidad de puncta que coexpresan parvalbúmina y sinaptofisina alrededor del soma de las neuronas piramidales, disminuye en la corteza prelímbica de ratones knockout para ST8SIA2 y en la corteza infralímbica de ratones knockout para ST8SIA4.

10. Un tratamiento crónico con eritropoyetina no altera el equilibrio excitación/inhibición en las capas *oriens, pyramidale, radiatum* y *lacunosum-moleculare* de la región CA1 del hipocampo de ratones jóvenes.

11. Un tratamiento crónico con eritropoyetina disminuye la complejidad del árbol dendrítico de las interneuronas que expresan somatostatina de la capa *oriens* de la región CA1 del hipocampo en ratones jóvenes.

12. Un tratamiento crónico con eritropoyetina disminuye la densidad de espinas dendríticas de las interneuronas que expresan somatostatina de la capa *oriens* de la región CA1 del hipocampo en ratones jóvenes.

13. Un tratamiento crónico con eritropoyetina disminuye la complejidad del árbol dendrítico de las interneuronas que expresan parvalbúmina de la capa *oriens* de la región CA1 del hipocampo en ratones jóvenes.

14. Un tratamiento crónico con eritropoyetina disminuye la densidad de botones axónicos de las interneuronas que expresan somatostatina en la capa *lacunosum-moleculare* de la región CA1 del hipocampo en ratones jóvenes.

15. Un tratamiento crónico con eritropoyetina disminuye la densidad de puncta inhibidores que expresan parvalbúmina o CB1r alrededor del soma de las neuronas piramidales de la capa piramidal de la región CA1 del hipocampo en ratones jóvenes.

16. Un tratamiento crónico con eritropoyetina aumenta la densidad de redes perineuronales y la densidad de interneuronas que expresan parvalbúmina rodeadas por redes perineuronales en la región CA1 del hipocampo de ratones jóvenes.

17. Un tratamiento crónico con eritropoyetina aumenta la expresión de poliSia-NCAM en las capas *oriens*, *radiatum* y *lacunosum-moleculare* de la región CA1 del hipocampo de ratones jóvenes.

CHAPTER I
Introduction

Organisms are able to detect changes that occur within themselves as well as in its environment. These internal and external inputs are integrated and analyzed in order to execute answers that allow survival. As life becomes increasingly complex and veering, survival will depend on how well the organisms can respond to these changes. The nervous system is one of the organ systems in charge to maintain the internal order within the body and to react to events with adaptive changes. An aberrant functioning of the system may give rise to the different neuropsychiatric diseases that are currently known.

The nervous system can be divided into two major regions: the central nervous system (CNS), which is formed by the brain and spinal cord, and the peripheral nervous system (PNS), composed by all afferent and efferent nerves that connect every part of the body with the CNS. Although the nervous system contains a very diverse set of cells, two major groups can be highlighted: neurons and glial cells. Neurons are the main functional unit of the nervous system and were profoundly studied by Ramon y Cajal, who foresaw the functional bases of this system. Although the brain has been considered a static organ during most of the last century, nowadays it is well known that it retains a marked capacity for remodeling, not only during development but also, although at minor levels, during adulthood. This plasticity occurs in normal conditions and allows the system to deal with new experiences, to learn and to react adaptively to different intrinsic or extrinsic factors.

1. AREAS OF STUDY

The presence of plastic phenomena has been demonstrated in different regions of the cerebral cortex after different experimental paradigms. In the present thesis, I will focus the attention in two of these cortical areas, the prefrontal cortex and the hippocampus.

1.1 PREFRONTAL CORTEX

The prefrontal cortex (PFC) is an associative cortex located in the anterior part of the frontal lobe of the mammalian brain, rostral to motor and premotor areas (Fuster, 2015). This brain region is implicated in planning complex cognitive behavior, working memory, decision making, and moderating social behavior, among others (Carlson et al., 2006). Alterations of neurotransmission in this cortex and related structures lead to a number of pathological conditions with cognitive, emotional, behavioral, or affective manifestations: i.e. schizophrenia, major depression or dementia (Bicks et al., 2015; Kolb and Gibb, 2015). In the same way, different treatments acting on prefrontal circuitry, are known to produce therapeutic results to improve some of these compromised conditions.

Three major regions with distinct anatomical and functional features can be distinguished in this cortical region: the medial (mPFC), the orbitofrontal (OFC) and the lateral (lPFC) prefrontal cortices (Fuster, 2015; Seamans et al., 2008). In this thesis, I will mainly focus the studies on the mPFC. The **mPFC** is mainly involved in cognitive and autonomic functions, which include oculomotor attentional processes, visceromotor activity, decision making, goal directed behavior, and working memory (Gabbott et al., 2005; Hoover and Vertes, 2007; Uylings et al., 2003).

In rodents, the mPFC can be in turn subdivided into three different regions, which, although apparently similar, present distinctive cytoarchitectural and functional characteristics **(Figure 1A)**. The most dorsal part is integrated by the rostral portion of the **anterior cingulate cortex** (ACC), which at the same time is divided into a dorsal (ACd or Cg1, from Bregma 2.34 to Bregma -0.22 in mice) and a ventral (ACv or Cg2, from

Bregma 1.42 to Bregma -0.22 in mice) region. The most ventral region is constituted by the **infralimbic cortex** (IL, from Bregma 1.98 to Bregma 1.34 in mice). And the intermediate part is constituted by the **prelimbic cortex** (PrL, from Bregma 3.08 to Bregma 1.54 in mice) (Paxinos and Franklin, 2008). In humans and primates, these divisions correspond to the Broadman's areas 24 for the ACC, 25 for the IL and 32 for the PrL. Leaving aside that the brain of primates in general, and specifically the mPFC, is more complex than that of mice, several features, including both anatomical and functional, are shared throughout species (Seamans et al., 2008).

There appears to exist a **dorsal-ventral gradient** along the rodent mPFC (Heidbreder and Groenewegen, 2003). Dorsal regions, including the ACC and dorsal prelimbic cortex (dPrL), receive predominantly sensorimotor inputs and are implicated in motor sequencing of behaviors and control of actions. By contrast, ventral regions, including the ventral prelimbic cortex (vPrL) and IL, have been associated with diverse emotional, cognitive, and mnemonic processes, which control autonomic and emotional functions due to the primary limbic inputs that they receive. Ventral regions also establish bidirectional connections with a wide range of neuromodulatory systems, which play a key role in adaptive responses to rewarding and stressful events. While the IL cortex is mainly involved in visceral/autonomic control and specially in modulation of fear-related, stress and anxiety behavior, the PrL cortex is implicated in cognitive processes, as well as attentional and visual working memory functions (Euston et al., 2012; Gabbott et al., 2005; Heidbreder and Groenewegen, 2003; Hoover and Vertes, 2007).

In all mammalian species, the maturation of the PFC, as it occurs in the rest of neocortical regions, follows the characteristic steps of expansion, cell migration, and lamination. In rodents, the laminar **architecture** of the PFC is not complete after birth. The final architectural conformation of cells and fibers in the PFC basically keeps the structural plan prevailing throughout the neocortical regions, but lacks the characteristic internal granule cell layer (layer IV) (Uylings et al., 2003). In the present thesis, I will focus my studies mainly on the mPFC **(Figure 1B)**. In general, the different layers of the mPFC receive long-range inputs from cortical and subcortical regions and send

projections to other (limbic) structures (Gabbott et al., 2005; Hoover and Vertes, 2007). The rodent mPFC is organized in five layers that run parallel to the cortical surface and are numbered from the outer surface of the cortex (pia mater) to the white matter as follows (Fuster, 2015; Paxinos and Franklin, 2008; Van Aerde and Feldmeyer, 2015):

- Layer I (molecular or plexiform layer): It is almost devoid of neurons, apart from a few interneuronal types, which are dispersed between dendrites that arise from pyramidal neurons located deeper in the cortex and axon collaterals that run across this layer or form connections in there. These dendrites receive their input from thalamic and intracortical afferents.

- Layer II (external granule cell layer): It is the thinnest layer and contains only a few rows of densely packed small granular excitatory neurons. Despite their small size, these excitatory neurons present dense apical trees. In rodents, layer II and III are usually considered together given the indistinguishable boundary between them.

- Layer III (external pyramidal cell layer): This layer is thus designated because of the predominant cell type found in there, the pyramidal cell. Pyramidal neurons of medium-size show prominent apical dendrites that bifurcated in layer I. Pyramidal cells project within their region or to other cortical areas. Because rodents lack layer IV, in some cortical areas including the mPFC, this layer borders directly on layer V.

- Layer V (internal pyramidal cell layer): In this layer, pyramidal neurons have longer dendritic length, higher number of tuft branches and larger somata than pyramidal neurons in other layers. These neurons are more densely packed than those in layer III and present clear ascending apical dendrites with bifurcations in layer I. These neurons send projections mainly outside their local region, to other cortical areas or to subcortical structures like the basal ganglia, the thalamus, brainstem nuclei and midbrain, and to the spinal cord (Gabbott et al., 2005).

- Layer VI (polymorphic layer): It is a heterogeneous layer, which contains few pyramidal neurons of great morphological variety. These range from neurons with apical dendrites that spanned all cortical layers and terminate in layer I to small

pyramidal neurons with a dendritic tree exclusively restricted to layer VI. These cells present interconnections with thalamic neurons.

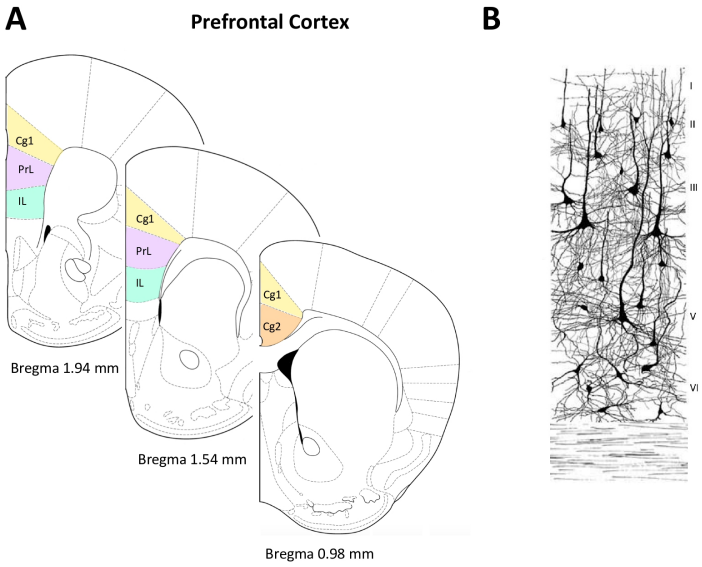

Figure 1: Subdivisions and architecture of the prefrontal cortex. A) Regions studied in the prefrontal cortex. Cg1-Cg2: cingulate cortices 1 and 2. PrL: prelimbic cortex. IL: infralimbic cortex (Modified from Paxinos and Franklin, 2008). **B)** Schematic drawing representing the different layers of the PFC (Modified from Fuster, 2015).

1.1.1 Major neuronal cells types in the cerebral cortex

The classification of the neuronal cell types has aroused great interest and problems at the same time, due to the different approaches proposed and the overlapping of some of their characteristics. In general, neurons can be classified attending to their structural features, their electrophysiological properties and their neurochemical characteristics (Purves et al., 2008). **(1) Morphologically**, neuronal features can be defined by the somatic, dendritic, or axonal shapes, which give rise to types such as pyramidal neurons, non-pyramidal neurons, interneurons and chandelier (or axo-axonic) cells. According to their **(2) electrophysiological properties**, neurons can be classified into excitatory and inhibitory neurons by the response that they evoke on the postsynaptic potentials. Excitatory synapses open sodium channels that allow the influx of Na+ ions and consequently reduce the membrane potential, referred to as excitatory postsynaptic potential (EPSP, excitatory neurons). By contrast, inhibitory synapses increase the flow of chloride (CI-) ions into postsynaptic cells, raising their membrane potential, which is called the inhibitory postsynaptic potential (IPSP, inhibitory neurons). Finally, neurons can be classified by their **(3) neurochemical characteristics,** regarding the type of neurotransmitter used to communicate with other

neurons. Glutamate and gamma-aminobutyric acid (GABA) are the most prevalent neurotransmitters used by excitatory and inhibitory neurons, respectively.

In this thesis, I will focus the studies in these two main types of neurons: excitatory/projection neurons, which use glutamate as excitatory neurotransmitter; and inhibitory/local circuit neurons (generally denominated interneurons), which use GABA as inhibitory neurotransmitter **(Figure 2)**.

1.1.1a Pyramidal neurons

Excitatory pyramidal neurons comprise about two-thirds of all neurons in the mammalian CNS and, although they present a considerable diversity in terms of morphology and connectivity, it is quite minor compared with that of interneurons (Thomson, 2007). They are also denominated projection neurons because they often display long axons that extend to distant targets, sometimes out of the CNS. Pyramidal neurons are glutamatergic (Spruston, 2008; Van Aerde and Feldmeyer, 2015).

Although their structure can vary between regions, pyramidal neurons preserve a marked stereotypical morphology characterized by a pyramidal shaped cell body, a single axon and two distinct dendritic trees: the basal and apical dendritic arbors (**Figure 2**; Spruston, 2008). Several basal dendrites emerge from the base of the pyramidal soma and branch up constituting the **basal dendritic tree**. A single apical dendrite emerges from the apex of the pyramidal soma and usually extends vertically for several hundred microns before branching to form the **apical dendritic tree**. Leaving from the principal apical dendrite, some oblique branches, which typically branch once or twice, can also be observed. The single **axon** of each pyramidal neuron normally emanates from the base of the soma (axon hillock) and branches profusely, making many glutamatergic synaptic contacts, specially in its distal segment. The high degree of branching of dendrites and axon makes a single neuron to communicate with thousands of other neurons in a network. The soma and the initial segment of the axon receive mainly inhibitory inputs, whereas most of the excitatory synaptic input arrives through the dendrites. Usually, proximal dendrites receive excitatory inputs from local circuits

whereas the distal apical tuft receives inputs from more distant locations (Spruston, 2008).

A distinctive feature of pyramidal neurons is the presence of **dendritic spines** (Hotulainen and Hoogenraad, 2010; Rochefort and Konnerth, 2012), which are quite abundant in the apical dendrites and somewhat less numerous in the basal dendritic tree. Dendritic spines are small protrusions that constitute the postsynaptic element for most excitatory glutamatergic synapses (some excitatory inputs can also contact directly the dendritic shaft). The primary function of dendritic spines is to compartmentalize local synaptic signaling pathways and restrict the diffusion of postsynaptic molecules (Rochefort and Konnerth, 2012). Although less common, the spines may also receive inputs from GABAergic neurons or other modulatory synaptic input such as the dopaminergic, serotoninergic or cholinergic systems. The dendritic spines contain the postsynaptic components of the synapse (postsynaptic density, PSD), where neurotransmitter receptors are clustered together with scaffolding and signaling molecules. The spines are commonly classified into three morphological types: thin, mushroom and stubby. Dynamic changes in their structure have been related to memory and learning processes that profoundly affect synaptic transmission (Bourne and Harris, 2007; Hotulainen and Hoogenraad, 2010). In the presynaptic element, axons display membranous thickenings called **axonal boutons,** which contain and release the synaptic vesicles that harbor the neurotransmitters (Kevenaar and Hoogenraad, 2015; Spruston, 2008). To sum up, the dendritic spines of pyramidal neurons constitute the postsynaptic structures that receive inputs from other neurons, whereas the axonal boutons represent the presynaptic element that establishes the output with other neurons.

1.1.1b Interneurons

Interneurons are characterized by a local short axon through which they establish feedforward and feedback connections. However, some cortical GABAergic neurons can also project to other brain areas. As inhibitory neurons, they all use GABA as primary neurotransmitter (Booker and Vida, 2018). This cell type comprises approximately the 10-20% of neurons within a cortical region and, contrary to excitatory neurons, which

are relatively homogeneous, they are highly diverse (Booker and Vida, 2018; Defelipe et al., 2013). Disruption of interneuronal networks resulting from different causes, may underlie the etiology of diseases such as schizophrenia, autism or intellectual disabilities (Marín, 2012). Although all GABAergic interneurons release GABA to communicate with their postsynaptic targets, the differences in subcellular targeting domain, connectivity and intrinsic membrane properties result in highly specific and precise spatiotemporal inhibitory control of pyramidal neurons and networks. Because of this, the classification of interneurons has been a topic of debate for some time. In the present thesis, I will follow the approach of Petilla Interneuron Nomenclature (Ascoli et al., 2008), which classifies interneurons regarding their morphological, molecular and physiological properties. **Anatomically**, interneurons are divided into those targeting pyramidal cells and those specifically targeting other interneurons. Interneurons targeting pyramidal cells have been further subdivided on basis of their target location: interneurons targeting the axonal initial segment (axo-axonic or chandelier cells), interneurons targeting the perisomatic region and proximal dendrites (basket cells) and interneurons targeting distal dendrites (dendritic-targeting interneurons, i.e Martinotti/Oriens-Lacunosum Moleculare (O-LM), double bouquet and bipolar cells) (Ascoli et al., 2008; Defelipe et al., 2013). **Molecularly** interneurons can be divided attending to the expression of specific molecular markers. Five main groups of interneurons can be distinguished: those expressing parvalbumin (PV), including chandelier and basket cells; those expressing somatostatin (SOM), such as Martinotti cells in the neocortex and O-LM cells in the hippocampus; those expressing neuropeptide Y (NPY) but not SOM; those expressing vasoactive intestinal peptide (VIP); and those expressing cholecystokinin (CCK) but not SOM or VIP, such as CCK-expressing basket cells (Ascoli et al., 2008; Defelipe et al., 2013). **Physiologically** the Petilla terminology identifies six main types of interneurons: fast-spiking and non-adapting spiking neurons, which include chandelier and basket interneurons expressing PV; non-adapting, non-fast spiking neurons; adapting neurons; burst-spiking neurons (including SOM-expressing interneurons); accelerating neurons; and irregular spiking neurons (Ascoli et al., 2008; Defelipe et al., 2013). Each of these classifications provides only a partial knowledge when taken individually. A combination of them results in the following interneuron subpopulations **(Figure 2)**:

- **Parvalbumin-expressing interneurons**

These interneurons express the calcium binding protein PV. They include the fast-spiking basket and chandelier cells. Both subpopulations can be observed in the neocortex, including the PFC, (Tremblay et al., 2016) and the hippocampus (Booker and Vida, 2018). **PV-chandelier cells** are also called axo-axonic, their axons are candelabrum shaped and synapse exclusively on the initial segment of the axon of pyramidal neurons (Defelipe et al., 2013). The other main group, the **PV-basket cells**, are by large the most studied type of interneurons. They operate as clockworks controlling the spike firing and the precision of pyramidal cells, probably through the high number of synapses that each PV-basket cell establishes. They target the somata and proximal dendrites of pyramidal neurons and other interneurons (mainly PV positive). This position allows them to accurately modulate the excitatory and inhibitory inputs received by the somata of their postsynaptic neurons. PV-basket cells can synchronize their firing via gap junctions, which help to produce a fast strong and precise inhibition on their target cells. Chandelier cells also show electrical coupling with each other. Their close proximity to the site of action potential generation allows both types of PV+ cells to powerfully influence the output of their target neurons.

- **Somatostatin-expressing interneurons**

These neurons typically express the neuropeptide SOM, but they also can co-express other markers. As dendrite-targeting interneurons, SOM-expressing cells strongly inhibit the distal dendritic tuft of pyramidal neurons, usually in a feedback manner, and often also the dendrites of other interneuronal subpopulations. They present a rich range of morphologies, including double-bouquet cells, bitufted cells, bipolar cells or neurogliaform cells. A key property of these interneurons is their high rate of basal firing activity, which even persists in absence of excitatory input (Scheyltjens and Arckens, 2016; Urban-Ciecko and Barth, 2016). Interestingly, they display **dendritic spines** along their dendrites. SOM-expressing interneurons are present throughout the cerebral cortex, including the PFC (Tremblay et al., 2016) and the hippocampus (Somogyi and Klausberger, 2005). In this thesis, I will focus specially on two subpopulations of SOM-

expressing interneurons: The Martinotti cells in the PFC, and the O-LM cells in the hippocampus (see Major cell types in the PFC and in the hippocampal CA1 region).

- **Neuropeptide Y-expressing interneurons**

NPY can be co-expressed with several neuropeptides and/or calcium binding proteins, which define several neurochemical subclasses of NPY-expressing neurons. To be exclusive, only interneurons expressing NPY, but not the neuropeptide SOM, are included in this group. Morphologically, they can present bipolar, bitufted, or multipolar morphology. Furthermore, physiologically they also represent a heterogeneous population, since they exhibit adapting, fast-spiking, or accelerating firing patterns. All these characteristics make them a diverse subpopulation, which to date has been poorly studied (Karagiannis et al., 2009). They can be found throughout the CNS, including the PFC and other regions of the neocortex and the hippocampus (Defelipe et al., 2013; Karagiannis et al., 2009).

- **Vasoactive intestinal peptide-expressing interneurons**

VIP-expressing interneurons can also co-express other neuropeptides and calcium binding proteins, constituting different subpopulations, but they never express PV or SOM. Interestingly, they control local microcircuits by preferentially targeting other interneurons and thereby temporally disinhibiting principal neurons (see IS cells). They are present in the neocortex, including the PFC (Markram et al., 2004) and hippocampus (Somogyi and Klausberger, 2005).

- **Cholecystokinin-expressing interneurons**

These interneurons express the neuropeptide CCK, but never SOM or VIP. Like PV-expressing basket cells, they also innervate the somata and proximal dendrites of pyramidal neurons, hence the term CCK-expressing basket cell. CCK-positive cells also express the **cannabinoid receptor 1 (CB1r)** in their axonal terminals, which gives them interesting properties. They have been studied in the neocortex, including the PFC (Tremblay et al., 2016), and the hippocampus (Booker and Vida, 2018).

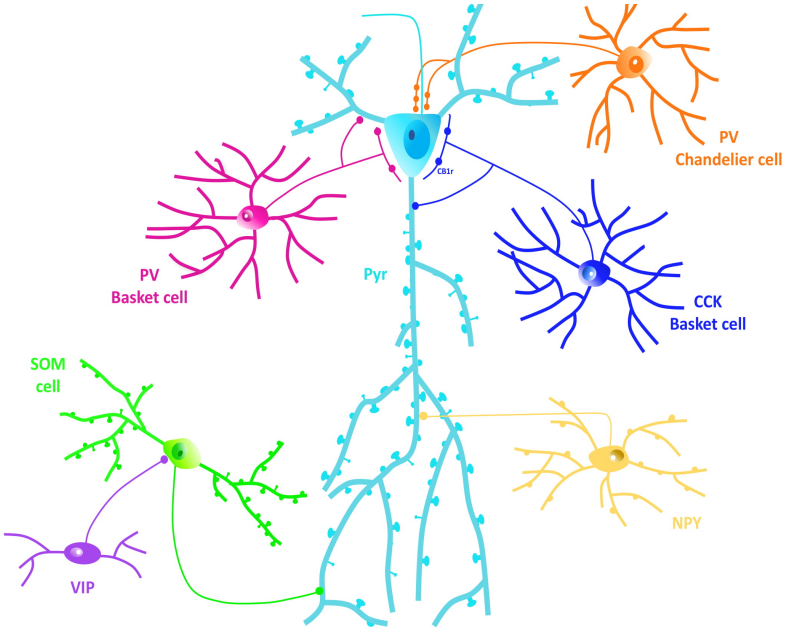

Figure 2: Scheme showing the basic connections between pyramidal neurons and the major interneuronal subtypes in the cerebral cortex. Pyr: pyramidal neuron. PV: parvalbumin-expressing interneurons, including basket and chandelier cells. SOM: somatostatin-expressing interneuron. NPY: neuropeptide Y-expressing interneuron. VIP: vasoactive intestinal peptide-expressing interneuron. CCK: cholecystokinin-expressing interneuron.

1.1.2 Major cell types in the PFC

In the PFC, the presence of **pyramidal neurons** is confined to layers III and V and they recapitulate the characteristics of principal neurons. By contrast, interneurons constitute a much more diverse population and are scattered throughout the extension of this cortical region (**Figure 3**; Kubota, 2014; Markram et al., 2004; Sultan and Shi, 2018; Tremblay et al., 2016). The main group of prefrontocortical interneurons is formed by PV-expressing cells (around 40% of the GABAergic population), with either basket or chandelier morphology. As mentioned before, **PV-expressing basket cells** establish synaptic contacts on the cell somata and proximal dendrites of principal neurons. Their axon usually extends horizontally in a layer-specific manner. However, some axon collaterals can also reach other layers; although rarely innervate layer I. These interneurons are mainly involved in cognitive functions, controlling the time spiking and the precision of cortical gamma and theta oscillations (Gonzalez-Burgos et al., 2015). Alterations in these interneurons are related to cognitive deficits, such as those observed in schizophrenic patients (Gonzalez-Burgos et al., 2015). By their side, **PV-expressing chandelier cells** target the initial segment of the axon of pyramidal cells, which places them in a key position to regulate the action potential output. Both PV-expressing basket and chandelier cells have been found in the PFC layers II–VI and are mainly in charge of synchronizing the excitatory output of pyramidal neurons (Cardin et

al., 2009). They receive excitatory inputs from the cortex and thalamus, as well as inhibitory inputs from other PV-expressing cells (Sultan and Shi, 2018).

The second large group of interneurons in the PFC corresponds to the dendrite-targeting **SOM-expressing Martinotti cells** (around 30% of PFC interneurons). They have feedback connections with pyramidal neurons, in addition to target other populations of interneurons (preferentially PV+) (Tremblay et al., 2016), which consequently disinhibit pyramidal cells. Martinotti cell somata are mainly present in layers II/III and V/VI, and they display an axonal plexus in layer I, where they directly inhibit the distal dendritic tuft of pyramidal neurons (Urban-Ciecko and Barth, 2016). They also can establish horizontal inhibitory inputs, as well as extend some collaterals to contact neurons present in the layer where their soma is located.

A second type of **basket cells, the CCK-positive**, also establishes contacts on the cell somata and proximal dendrites of pyramidal neurons. They exhibit accommodating firing patterns and express serotonin type 3 receptors (5-HT3r) postsynaptically and CB1r presynaptically (Freund, 2003; Freund and Katona, 2007). Their activity depends on subcortical inputs that carry information about the emotional and physiological state of the animal (Freund, 2003).

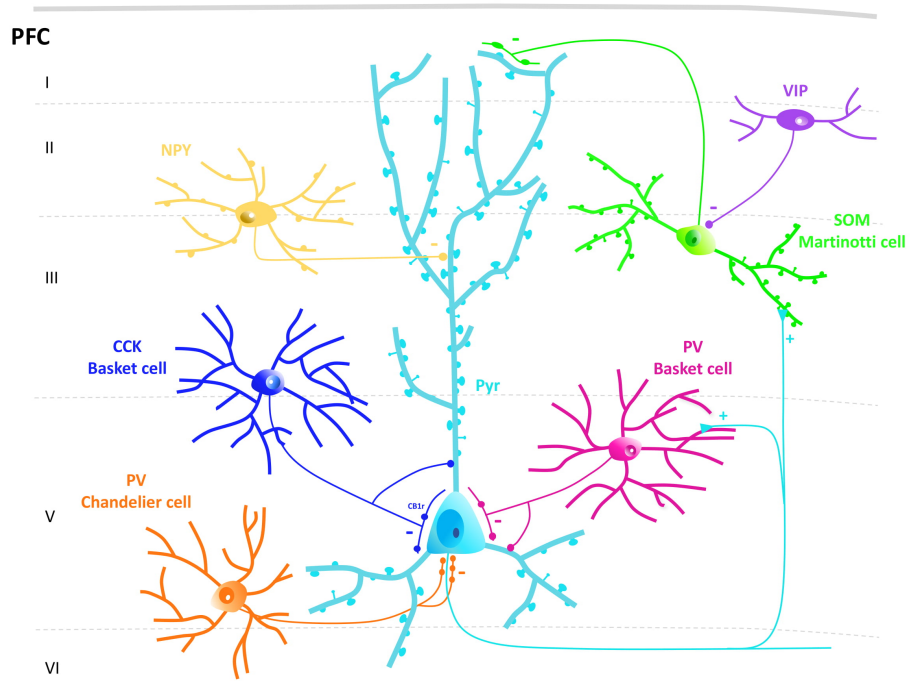

Figure 3: Schematic representation showing the basic connections between pyramidal neurons and the major interneuronal subtypes through the layers of the PFC.

Other interneuronal populations, although in minor proportions, can be found in the PFC and contribute to the regulation of pyramidal cell activity, such as the 5-HT3Ar-expressing interneurons (i.e. neurogliaform and VIP-expressing cells) or the NPY-expressing neurons, which are widely distributed throughout the depth of the cortex (Defelipe et al., 2013).

1.2 HIPPOCAMPUS

The hippocampus is a bilateral structure located deep into the temporal lobes of both hemispheres in humans and it is considered part of the archicortex, one of the oldest regions of the cerebral cortex. In mammals, the hippocampus is highly conserved across species, including humans, primates and rodents (Allen and Fortin, 2013). Anatomically, it comprises a large portion of the cerebral cortex of rodents: in mice from Bregma -0.94 to Bregma -4.16 (Paxinos and Franklin, 2008). The hippocampus is considered part of the **limbic system**, which is a complex set of structures including the amygdala, thalamus, hypothalamus, basal ganglia, cingulate gyrus, and the hippocampus properly (Rajmohan and Mohandas, 2007). These structures stablish intimate connections and are mainly involved in emotional aspects, but also in higher functions, such as learning and formation of memories. The hippocampal formation plays a key role, not only in short-term and long-term memory, but also in spatial navigation, emotional behavior and regulation of hypothalamic functions. Alterations that affect hippocampal integrity are associated with several neuropsychiatric and neurological disorders, such as Alzheimer's disease (AD), depression, schizophrenia or epilepsy (Anand and Dhikav, 2012). The hippocampal formation is constituted by the hippocampus (Cornu Ammonis; CA), dentate gyrus (DG), subiculum, and entorhinal cortex (EC). However, the term hippocampus usually refers only to the Cornu Ammonis (hippocampus properly) and the DG. Based on its histology, the hippocampus is divided into CA1, CA2, CA3, and CA4 areas and the DG. Furthermore, the hippocampus follows a striking layered structure. The CA3 region is formed by 5 strata: *lacunosum-moleculare, radiatum, lucidum, pyramidale, and oriens*. The CA2 and CA1 areas also present four of these layers although the *stratum lucidum* is absent **(Figure 4A)**. By contrast, the DG is organized in 3 layers: the molecular, the granular, and the hilus (or

polymorphic layer). Under normal conditions, adult hippocampal neurogenesis is found only in the dentate gyrus of rodents, where it generates new granule cells. The precursors of these new cells are located in the subgranular zone, the border between the granular cell layer and hilus (Amaral et al., 2007).

The basic functioning of the hippocampus follows the so called **trisynaptic circuit** (**Figure 4B**; Amaral, 1993). Briefly, afferents from the entorhinal cortex reach the granule cells in the dentate gyrus via the perforant path, with which they stablish the first synapse. Since the entorhinal cortex is the source of most of the cortical sensory information reaching the hippocampus, the dentate gyrus is considered the first step in the information processing. Axons of these granule cells, which use glutamate as their primary neurotransmitter, build the mossy fiber tract that reaches the pyramidal neurons in the CA3 region, where the second synapse is established. This axonal bundle terminates in unusually large and complex structures, the mossy fiber synapses, which are among the most powerful synapses in the brain. Some interneurons can also be found in the hilus and interspersed between the excitatory cells. The pyramidal neurons of CA3 project via the Schaffer collaterals to CA1, where the third synapse of the circuit is located. Axons from CA1 pyramidal neurons project back to the subiculum, from where an axonal projection is sent back to the entorhinal cortex, completing the trisynaptic circuit. In this thesis, my studies will be mainly focused in the CA1 region.

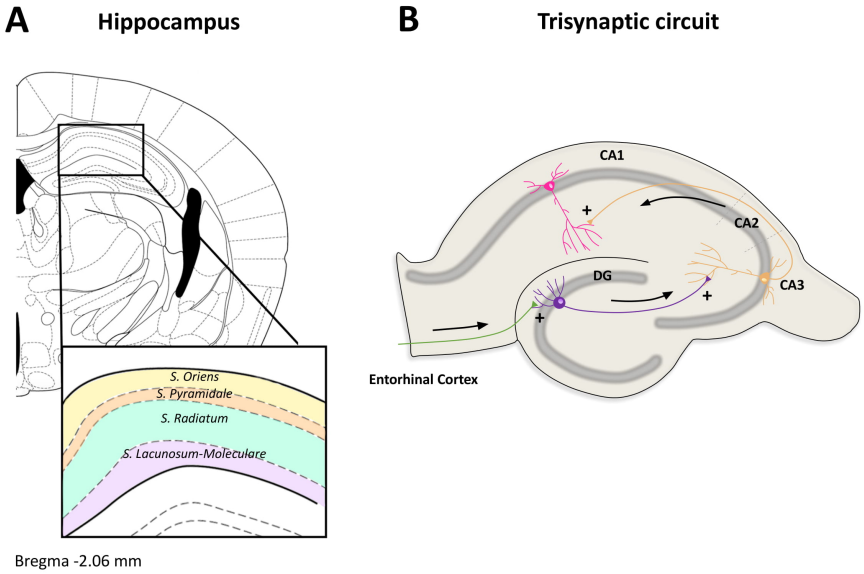

Figure 4: Hippocampal formation. A) Layers studied in the hippocampal CA1 region (Modified from Paxinos and Franklin, 2008). **B)** Drawing of the hippocampus representing the trisynaptic circuit. The main projections are shown in green (perforant path), purple (mossy fiber tract) and orange (Schaffer collaterals).

1.2.1 Major cell types in the hippocampal CA1 region

Compared to the PFC, as we have mentioned, the hippocampus is a simpler structure with more defined connections. In the CA1 region, pyramidal cells have their somata located in the *stratum pyramidale* **(Figure 5)**. These somata give rise to apical dendrites that extend into the *stratum radiatum* and form the apical dendritic tuft in the *stratum lacunosum-moleculare* (LM). Basal dendrites emerge from the soma of pyramidal neurons and extend into the *stratum oriens*. Some of the axons of pyramidal cells cross the *stratum oriens* and project along the *alveus,* while others ramify in the *stratum oriens* and establish recurrent synapses (Booker and Vida, 2018). Although pyramidal neurons generally constitute a single population located in the *stratum pyramidale*, they can be subdivided at least in three distinct types based on their connectivity. Pyramidal cells in the CA1 region receive glutamatergic inputs from five different sources: i) the CA3 pyramidal cells (numerically these neurons constitute the largest group), which innervate the apical and basal dendritic tufts; ii) the entorhinal cortex pyramidal cells; (iii) thalamic inputs that innervate the apical dendritic tufts; iv) local collaterals of CA1 pyramidal cells, which innervate the basal dendrites; v) and the amygdala (Somogyi and Klausberger, 2005).

As in the PFC, pyramidal neurons of the CA1 region are accurately timed and synchronized by a rich diversity of GABAergic interneurons (**Figure 5**; Freund and Buzsaki, 1996), which release GABA at different time points via their specific subcellular domains on pyramidal cells. This compartmentalization allows **spatio-temporal GABAergic effects** on pyramidal cells, which can change its pattern during different brain states and are the basis for network regulation (Klausberger and Somogyi, 2008).

The main group of basket interneurons in the CA1 region is constituted by fast-spiking **PV-expressing basket cells**. Their somata is located in the *stratum pyramidale* or near the *strata oriens* and *radiatum*. Their dendrites, typically aspiny, are orientated vertically, being able to reach all layers of the CA1 region. The axon of PV+ basket cells heavily ramifies within the local *stratum pyramidale*, where it stablishes synapses with the somata and proximal dendrites of pyramidal cells, as well as with other PV basket cells (preferentially in the perisomatic domain) (Booker and Vida, 2018; Somogyi and

Klausberger, 2005). In turn, PV-expressing basket cells receive more excitatory than inhibitory inputs, which makes them highly excitable elements. Their main excitatory input comes from the Schaffer collaterals, but also from pyramidal cells in CA1 and the entorhinal cortex. This connectivity makes them mainly feedforward elements, although the presence of feedback excitatory transmission is not excluded (Booker and Vida, 2018; Somogyi and Klausberger, 2005).

CCK-expressing basket cells constitute the second group of basket cells in the CA1 region. These are typically regular spiking cells with adapting trains. They include the CCK+ basket cells that co-express VIP, which have their somata in the *stratum radiatum*, and CCK+ basket cells expressing VGLUT3 in their axon terminals, which are commonly found in the *strata pyramidale* and *oriens*. The dendrites of these interneurons, also aspiny as those of PV+ cells, receive less excitatory than inhibitory inputs. Their axon usually ramifies in the *stratum pyramidale* with some collaterals in the *strata radiatum* and *oriens*. Typically, they target the somata and proximal dendrites of pyramidal cells, as well as other interneurons (including CCK+ cells). Interestingly, CCK+ basket cells can be presynaptically neuromodulated due to the high expression of CB1r in their axonal terminals, therefore active pyramidal cells can attenuate the inhibition received from CCK-expressing cells via retrograde cannabinoid receptor activation (Freund et al., 2003; Katona and Freund, 2012).

Axo-axonic interneurons, such as the **PV-expressing chandelier cells** have their aspiny dendritic tuft located in the *stratum lacunosum-moleculare*. Their axon establishes several collaterals that ramify heavily in the proximal *stratum oriens* and synapse on the initial segments of the axons of pyramidal cells. In turn, they receive strong excitatory inputs from all major inputs to CA1 (Booker and Vida, 2018).

The second larger group of interneurons in the CA1 region is represented by the dendrite-targeting interneurons, which establish synapses with the dendritic domain of pyramidal neurons and other interneurons. The main subpopulation is constituted by the **SOM-expressing oriens/lacunosum-moleculare cells (O-LM)** that express the neuropeptide SOM. Their somata and dendrites are located, horizontally oriented, in the *stratum oriens*. Their dendrites rarely cross the *stratum pyramidale* and,

interestingly, they are densely covered by dendritic spines. The axon of O-LM cells extends until the *stratum lacunosum-moleculare*, where it heavily ramifies and establishes synaptic contacts with the distal dendritic tuft of pyramidal cells and with other interneurons. Local axonal collaterals can also be found in the *stratum oriens*. O-LM cells receive mainly excitatory inputs that arise almost entirely from local CA1 pyramidal cells (Blasco-Ibáñez and Freund, 1995), which makes them typical feedback interneurons. Although the majority of SOM+ interneurons in the *stratum oriens* can be considered O-LM cells, a lower proportion of SOM-expressing interneurons can project to extra-hippocampal areas: the hippocampo-septal (HS) cells (Müller and Remy 2014). Although they will not be discussed in the present thesis, dendrite-targeting interneurons also include bistratified cells that express both PV and SOM, CCK+ cells with at least seven subtypes identified in the CA1, neurogliaform cells that express neuronal nitric oxide synthase (nNOS), Ivy cells expressing nNOS and NPY, and trilaminar cells.

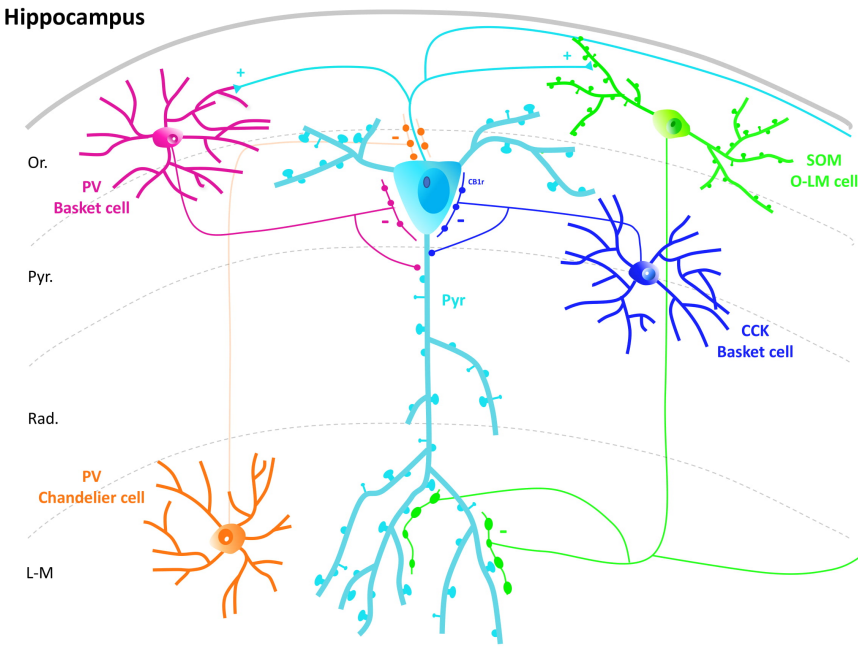

Figure 5: Schematic representation showing the basic connections between pyramidal neurons and the major interneuronal subtypes through the layers of the hippocampal CA1 region.

The last but not the least interesting group corresponds to the **interneuron-specific cells (IS cells)**. Although interneurons preferentially innervate pyramidal cells, a specific population of interneurons innervate GABAergic cells selectively. It is the case of IS cells, which target preferentially the dendritic domains of other interneurons and thereby produce a disinhibition in the local microcircuit (Tyan et al., 2014). IS cells can

be further divided into three subtypes (IS-IN type I, IS-IN type II and IS-IN type III) based on their neurochemistry and morphology.

1.2.2 The CA3 region

Similar to CA1, pyramidal neurons also comprise the main group in the CA3 region, although with some morphological differences. The main excitatory input of this area comes from the mossy fiber projection originated in the granule cells of the DG, which reaches the *stratum lucidum*, and from other CA3 pyramidal cells. Pyramidal cells establish contacts with CA1 pyramidal neurons through the Schaffer collateral pathway, as well as recurrent collateral inputs with themselves. Interneurons in the CA3 recapitulate many of the interneuronal subtypes present in CA1 (Tukker et al., 2007), although with some morphological and specific differences.

1.2.3 The dentate gyrus

The DG is the most different region of the hippocampus, taking into account neuronal populations, layering and synaptic connectivity. The dentate gyrus principal neurons, the **granule cells**, have their dendrites located in the molecular layer and their axons in the hilus. They receive afferents from the entorhinal cortex and hilar mossy cells (inner molecular layer). The output of granular cells is the **mossy fiber tract,** which synapses with CA3 pyramidal cells. The population of interneurons in the DG is quite different from that of the CA1 and CA3 regions, with at least four classes of interneurons in the DG with distinct morphology (Amaral et al., 2007; Booker and Vida, 2018).

2. THE EXCITATORY AND INHIBITORY BALANCE

Neurotransmitters are chemical messengers that carry, boost, and balance signals from neurons to a target cell across a synapse. Functionally, neurotransmitters can be classified in (1) **excitatory neurotransmitters** with excitatory effects on the postsynaptic neuron, which use L-glutamate (**glutamate**) as the main excitatory neurotransmitter, and (2) **inhibitory neurotransmitters,** which exert inhibitory effects

on the postsynaptic neuron. The main inhibitory neurotransmitter is **GABA**. Alterations in the excitatory/inhibitory (E/I) balance can induce neuronal plasticity, which includes from changes in the expression of different molecules to changes in their neurite structure. One of the objectives of the present thesis is to study how alterations in the glutamatergic and GABAergic systems can impact the structure of neurons. Some available tools can be used to study directly or indirectly alterations in this E/I balance.

2.1 GLUTAMATERGIC NEUROTRANSMISSION

Glutamate is the major excitatory neurotransmitter in the vertebrate CNS. Glutamatergic neurotransmission is mediated and regulated through diverse families of receptors and transporters. In the presynaptic element, synaptic vesicles (SV) are concentrated in the axon terminals of every neuron (Takamori et al., 2006). They store the neurotransmitters and undergo Ca^{2+}-dependent exocytosis when the action potential arrives. After exocytosis, SVs can be recaptured to be locally recycled. SVs express a high number of synaptic proteins involved in the correct functioning of neurotransmitter release. Among them, **synaptophysin (SYN)** is the most abundant and conserved synaptic vesicle protein (around 10 % of total vesicle protein) (Takamori et al., 2006). SYN plays a key role in activity-dependent synapse formation (Tarsa and Goda, 2002); thus, together with its exclusively presence in the synaptic vesicle, it is widely used as a presynaptic marker of both, glutamatergic and GABAergic terminals **(Figure 6)**. Several roles have been suggested for this protein, including exocytosis, synapse formation, biogenesis and endocytosis of the SVs (Kwon and Chapman, 2011). Another important protein located in the SV is the **vesicular glutamate transporter (VGLUT)**. The VGLUT is responsible for the accumulation of L-glutamate from the cytoplasm into synaptic vesicles in the terminal of glutamatergic neurons, which makes it an excellent marker of glutamatergic synapses. VGLUTs comprise a family of three distinct isoforms, with similar characteristics but different patterns of expression (Santos et al., 2009): VGLUT1 is the major isoform in synapses formed by neurons in the cortex, hippocampus and cerebellar cortex, whereas VGLUT2 prevails in the synapses of thalamic and brainstem neurons (extracortical regions). The third type, VGLUT3 is expressed by other neuronal populations, including cholinergic, serotoninergic and GABAergic neurons,

where it can mediate its co-release together with other neurotransmitters. The expression of these vesicular glutamate transporters can be used as a marker of specific glutamatergic terminals **(Figure 6)**.

Once the glutamate is released from synaptic vesicles into the synaptic cleft, it can bind to different glutamate receptors. In parallel, the action of excitatory amino acid transporters **(EAATs),** located in the pre- and post-synaptic terminals (Maragakis and Rothstein, 2004), as well as on surrounding glial cells including astrocytes (but also microglia and oligodendrocytes) (Eulenburg and Gomeza, 2010), efficiently removes glutamate from the synaptic cleft, which makes glutamate available for receptor binding only for a short period of time.

Glutamate can exert its action through two main groups of receptors: ionotropic and metabotropic. **Ionotropic receptors** are voltage sensitive and have fast responses: once opened, they directly mediate synaptic excitability and plasticity. They are present in both pyramidal neurons and interneurons (Akgül and McBain, 2016). Three types of ionotropic glutamate receptors can be distinguished (Traynelis et al., 2010): *N*-methyl *D*-aspartate (NMDA), α-amino-3-hydroxy-5-methyl-4-isoxazolepropionic acid (AMPA), and kainate receptors **(Figure 6)**. In addition to the ionotropic receptors, glutamate can also activate **metabotropic receptors,** which are ligand sensitive and coupled to G-protein (Swanson et al., 2005). They have slower responses and exert their effects indirectly through gene expression and protein synthesis. There are three main groups of glutamate metabotropic receptors named from I to III (Group I-III metabotropic receptors) that can be found in inhibitory and pyramidal cells, where they mediate slow excitatory postsynaptic currents (EPSCs) (Sheng et al., 2017).

2.2 GABAERGIC NEUROTRANSMISSION

Similar to excitation, alterations in the inhibitory neurotransmission may underlie some of the structural changes found in neurons. Expression of specific molecules can be used to study alterations in the GABAergic transmission. GABA is the main inhibitory neurotransmitter in the adult brain. GABA is synthesized by decarboxylation of glutamate by the **glutamic acid decarboxylase (GAD)**. GAD can exist

in two isoforms, **GAD65** and **GAD67,** encoded by independent genes with different molecular weights, properties and location (Esclapez et al., 1994; Soghomonian and Martin, 1998). GAD is only expressed in cells that use GABA as a neurotransmitter, for this reason both isoforms are excellent markers for GABAergic neurons **(Figure 6)**. Although both isoforms are present in the majority of GABAergic neurons, they are not equally distributed within the neuron. GAD67 mRNA is more concentrated in the somata and proximal dendrites of inhibitory neurons, whereas GAD65 is particularly prominent in axon terminals (Esclapez et al., 1994). After being synthetized, GABA is transported into synaptic vesicles by the **vesicular GABA transporter (VGAT).** Similar to VGLUT transporters, the main function of VGAT is to store the GABA neurotransmitter synthetized into the synaptic vesicle until its release (Edwards et al., 1997). Since VGAT is localized in the axon terminals of GABAergic neurons, it can be used as a marker of their presynaptic elements **(Figure 6)**. As in glutamatergic neurons, **SYN** is an abundant synaptic vesicle protein in the presynaptic elements of inhibitory neurons (Tarsa and Goda, 2002).

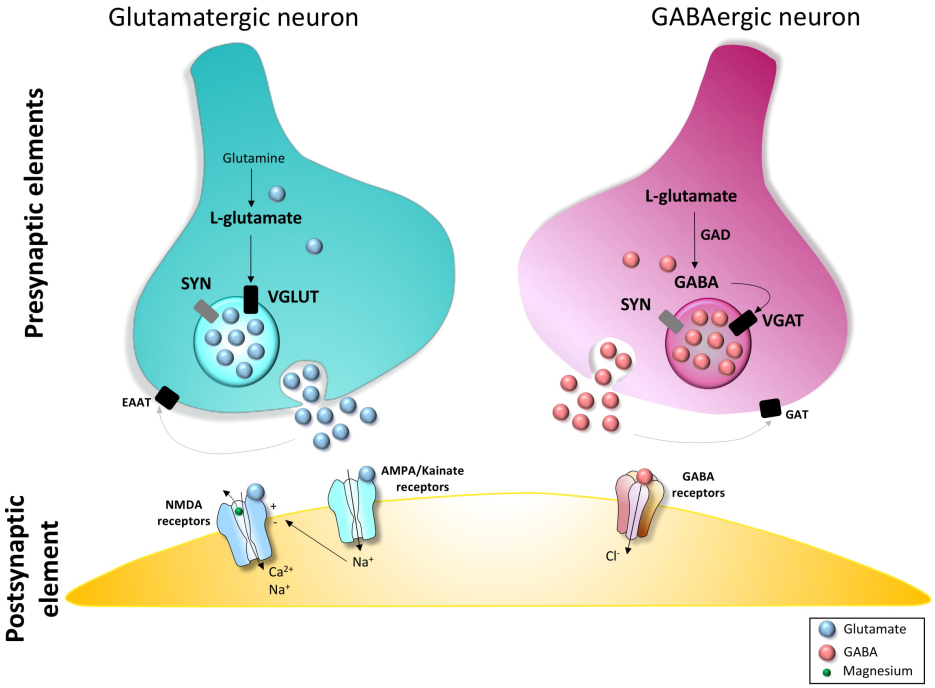

Figure 6: Scheme showing the presynaptic glutamatergic (blue) and GABAergic (pink) elements acting on the receptors of the postsynaptic element. The vesicular proteins and enzymes studied in the present thesis are represented in the scheme. VGLUT: vesicular glutamate transporter. SYN: synaptophysin. EAAT: excitatory amino acid transporters. GABA: gamma-aminobutyric acid. GAD: glutamic acid decarboxylase. VGAT: vesicular GABA transporter GAT: GABA transporters. Glutamate (NMDA and AMPA/Kainate) and GABA receptors action are depicted in the postsynaptic element.

When the presynaptic neuron is depolarized, GABA is released into the synaptic cleft by Ca^{2+}-dependent exocytosis, where it diffuses and can bind to the target postsynaptic and extra-synaptic GABA receptors (Pettit and Augustine, 2000). GABA can also be recaptured through **GABA transporters (GATs)** located in the pre- and post-synaptic terminals as well as in surrounding glial cells (Bak et al., 2006). Some scaffolding proteins, such as gephyrin, a postsynaptic GABAergic protein, play a crucial role in the accumulation and anchoring of neurotransmitter receptors (Gouzer et al., 2014). GABA can exert its function through two main types of receptors, the ionotropic $GABA_A$ receptors and the metabotropic $GABA_B$ receptors. **$GABA_A$ receptors,** which regulation will be studied in this thesis, mediate fast inhibitory neurotransmission in the vertebrate CNS. They are heteropentameric ligand-gated chloride ion channels that mainly present the α, β and γ subunit composition (**Figure 7**; Chang et al., 1996). When GABA binds to its binding site, the ion channel pore opens and Cl^- diffuses into the cell producing an hyperpolarization in the postsynaptic element. In the typical conformation, there are two binding sites for the agonist GABA, located between the extracellular interfaces of β and α subunits (Baumann et al., 2003).

$GABA_A$ receptors are specially important as drug targets. Among the different drugs that bind these receptors, **benzodiazepines** (BZs) such as diazepam (DZ) are among the most studied due their anxiolytic, sedative, muscle relaxant and anticonvulsant effects **(Figure 7)**. BZs act as allosteric agonists, increasing the binding affinity of GABA, but also facilitating the channel opening (Baur, 2005; Sigel and Ernst, 2018). The term allosteric refers to the ability of BZ to bind at a site distinct from GABA. BZs can act by modulating synaptic plasticity. In the hippocampus, DZ treatment increases synaptic stability and clustering of $GABA_A$ receptors upon neuronal activity and reduces their lateral diffusion, which results in enhanced potency of inhibitory synapses (Gouzer et al., 2014; Lévi et al., 2015). As therapeutic factors, BZs are commonly used for the treatment of anxiety and insomnia. Moreover, they are also used as adjunctive treatment to neuroleptics in patients with schizophrenia, despite their sedative effect and conflicting results (Chaudhry et al., 2015; Rudolph and Knoflach, 2011). In the light of the GABAergic hypothesis of depression, which points to a central role of the GABA system (Luscher et al., 2011), the use of BZs has been proposed in the treatment of this

disorder. In particular, α2-containing $GABA_A$ receptors seem to be a promising target for novel non-monoamine-based antidepressant drugs (Rudolph and Knoflach, 2011).

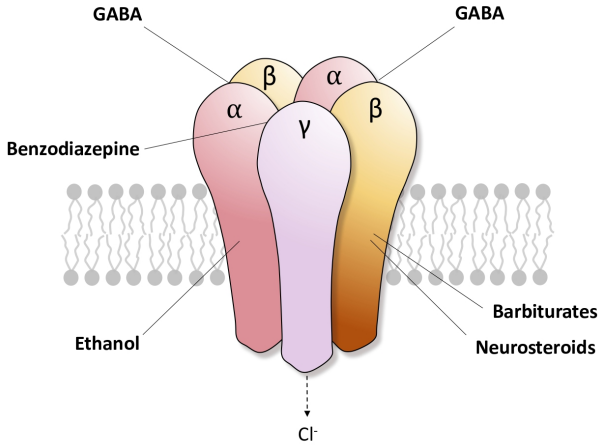

Figure 7: $GABA_A$ receptor composition. Heteropentameric structure composed by α, β and γ subunits and a ligand-gated chloride ion channel. For this thesis, are of special interest the binding sites for GABA located in the interfaces of β-α subunits, and the binding site for benzodiazepines located in the interface of α-γ subunits.

2.3 INVOLVEMENT OF ALTERATIONS IN EXCITATORY/INHIBITORY BALANCE ON PSYCHIATRIC DISORDERS

Together with the excitatory neurotransmitter glutamate, GABA modulates the proper E/I balance necessary for correct brain function (Wu and Sun, 2015). During early stages of brain development, the activation of $GABA_A$ receptors produces a membrane depolarization. Thus, in immature neurons, glutamate and GABA induce an excitatory effect, through which they play a key role in the maturation of the CNS (Ben-Ari et al., 2007). In rodents, the "**GABA switch**" starts after birth and it is complete by the end of the first and second postnatal week (Valeeva et al., 2013). The progressive increase in inhibitory transmission triggers the onset of critical periods and, at the same time, the closure of periods of elevated neuronal plasticity. Indeed, a longer duration of depolarizing effects of GABA during early postnatal development prolongs the critical period of plasticity in the visual cortex (Deidda et al., 2015). On the contrary, the use of BZs can prematurely elevate inhibitory neurotransmission and the subsequent plasticity processes before the normal onset of the critical period. Interestingly, once the natural critical period has finished and the inhibitory level is already set, BZs cannot trigger a second window of plasticity (Hensch and Fagiolini, 2000).

Impairments of this excitation/inhibition balance may underlie different neurodevelopmental brain disorders such as autism or schizophrenia (Selten et al.,

2018). In **autistic** brains, there is a reduction of the GABA synthesizing enzymes GAD65 and GAD67, as well as mutations in genes implicated in the excitatory and inhibitory ratio (Fatemi et al., 2002; Nelson and Valakh, 2015). There are also evidences linking the glutamatergic and GABAergic systems to the pathology of **schizophrenia**. The use of NMDA receptor antagonist is one of the most used models to mimick some schizophrenia-related symptoms in experimental animals (Gilabert-Juan et al., 2013b). Administration of MK-801 or ketamine, both NMDAr glutamate antagonists, can trigger some alterations similar to those observed in patients (Kerner, 2009; Stone, 2011). Furthermore, some candidate risk genes for schizophrenia are involved in glutamatergic neurotransmission (Harrison and Weinberger, 2005). As a consequence, a large number of glutamatergic compounds have been developed as novel therapeutic agents. In schizophrenia, a decrease in the expression of interneuron markers such as PV and changes in gamma oscillations are also characteristic features of this psychiatric disease (Gonzalez-Burgos et al., 2015; Lewis et al., 2005). Administration of NMDA receptor antagonist also produces a decrease in GABAergic neurotransmission and the number of PV-expressing neurons in the PFC and hippocampus (Rotaru et al., 2012). These alterations in the inhibitory neurotransmission and some genes implicated in its metabolism have been largely associated with schizophrenia (Gonzalez-Burgos et al., 2015; Harrison and Weinberger, 2005; Lewis et al., 2005). Some mood disorders are also affected by alterations in the E/I balance such as **major depression** and abnormalities in the GABAergic system also contribute to the pathophysiology of major depression and other mood disorders (Luscher et al., 2011).

3. NEURONAL PLASTICITY

Neuronal plasticity can be defined as the ability of the CNS to react with adaptive responses to changes happening in the environment or inside the organism, naturally or due to injury or disease (De Magalhães and Sandberg, 2005; Sharma et al., 2013). This brain dynamism does not occur only during development, when the precise patterns of nervous system are being established, but also throughout life. Although the levels of

neuronal plasticity decrease with age, the adult brain still maintains a marked capacity for reorganization dependent on experience, which ranges from molecular to structural plasticity (Xerri, 2008). In the present thesis, I will focus mainly in these structural changes.

3.1 STRUCTURAL PLASTICITY

Molecular mechanisms involved in neuronal plasticity are largely dependent on protein dynamics at synapses, which comprise a wide range of molecular events, such as vesicle trafficking at excitatory and inhibitory terminals, neurotransmitter receptor number/dynamics at synapses and their relation with scaffold proteins, Ca2+ influx, genes induction and regulation of proteins (Belzung, 2013; Schaefer et al., 2017). These molecular mechanisms are involved in **synaptic plasticity**, which generally refers to any change in the efficacy of a given synapse. Changes in synaptic efficiency include short-term and long-term mechanisms. At the same time, some of these molecular changes are implicated in the structural remodeling of neurons and synapses, specially those regulating the expression of neuronal cytoskeletal proteins, adhesion molecules involved in cell to cell and cell to extracellular matrix relationships and components of the extracellular matrix. Pyramidal neurons and interneurons undergo structural remodeling at different levels, which range from changes in the length and complexity of the dendritic arbors, alterations in the density and morphology of their dendritic spines to changes in the density of axonal boutons.

Pyramidal neurons have been the main focus of interest when studying neuronal structural remodeling. Many of these structural analyses have focused on the spines that these excitatory neurons display in their dendrites. The cytoskeleton of **dendritic spines** is constituted mostly by actin filaments, which extend from the base of the spine to the postsynaptic density (Zhang et al., 2010). Functionally, dendritic spines seem to be more related to the remodeling of neuronal circuits rather than to merely increase the surface for synaptic contact (Yuste, 2011). Alterations in dendritic spines have been found after brain injury, in neurological and psychiatric disease, as well as in learning and memory processes. Different changes in spine number/morphology are hallmarks of injuries and neurological disorders, such as ischemic stroke (Zhang, 2005) or

neurodegenerative disease (Spires, 2005), where the number of dendritic spines is decreased, or in Fragile X syndrome (Pan et al., 2010), where the number of spines increases. Moreover, experience-dependent spine remodeling provides a structural basis for learning and memory. A strong relationship between dendritic spines and memory has been demonstrated using different paradigms (Jedlicka et al., 2008; Moser et al., 1994). Increased dendritic spine size/number has been associated with long term potentiation (LTP), while decreases in these parameters are associated with long-term depression (LTD) (Zhang et al., 2010). Certain hormones, like estradiol or corticosterone also alter the dendritic spine density on pyramidal cells in the hippocampus and cortex (Cerqueira et al., 2007; Chen et al., 2009; Luine and Frankfurt, 2013). Indeed, increased levels of estrogens are related to higher dendritic spine density in pyramidal cells of the PFC and the hippocampus and to improved memory function (Frankfurt and Luine, 2015). Previous work in our laboratory has shown that pharmacological manipulations, such as the use of TrkB agonists (Perez-Rando et al., 2018) and dopamine D2 agonist receptors (Castillo-Gómez et al., 2016a) alter the structure and neurotransmission of excitatory neurons. In animal models of depression, including chronic stress, pyramidal neurons also experience structural remodeling (McEwen, 1999; Qiao et al., 2016).

The **dendritic arbor** of pyramidal neurons is also the focus of several studies, which have found alterations in its complexity, such as elongations/retractions or the formation of new dendrites after chronic stress (Banasr et al., 2011; Cook and Wellman, 2004; Radley et al., 2004).

Changes in morphology and connectivity in the adult brain are not only mediated by postsynaptic structures, the axonal branches and synaptic **boutons** of pyramidal neurons are also dynamic structures. Remodeling of *terminaux* and *en passant boutons* from pyramidal neurons also occurs in the adult cerebral cortex, where their appearance and disappearance provides a reliable measure for cortical plasticity (De Paola et al., 2006; Stettler et al., 2006).

Despite that **interneurons** play a key role in regulating the function of neural circuits in the CNS, studies on the structural remodeling of these inhibitory neurons are still very scarce. **Dendritic spines** were thought to be present only in pyramidal neurons,

but a subset of GABAergic interneurons, mainly those expressing SOM and NPY, in the hippocampus and PFC also display these postsynaptic specializations (Karagiannis et al., 2009; Urban-Ciecko and Barth, 2016). This has led to works focusing their efforts on the study of interneuronal remodeling. When studying the dendritic spines in interneurons, some similarities and differences have been found when comparing to pyramidal neurons. Several synapses can be established per spine in interneurons (in contrast with the one or two found in pyramidal neuron spines) although spines are usually less numerous than in pyramidal neurons (Gulyas et al., 1991; Keck et al., 2011; Scheuss and Bonhoeffer, 2014). Regarding their structure, dendritic spines in interneurons have similar head dimensions than those in pyramidal cells. However, interneuronal spines display longer necks and consequently a greater total length, thereby providing an increase in the probability of synaptic contact (Stepanyants et al., 2002). Interneuronal spines have a similar compartmentalization of biochemical signals and, compared to interneurons lacking spines, they may have the ability to support major rewiring, for example, during experience-dependent plasticity (Keck et al., 2011).

The dendrite-targeting (SOM-positive) interneurons, have been the focus of most of the research interest regarding the analysis of structural plasticity in interneurons. Several studies from our laboratory have demonstrated the remodeling of SOM-expressing interneurons, including changes in the density of dendritic spines and axonal boutons and changes in the complexity of arborization, after different experimental paradigms such as a chronic antidepressant treatment (Carceller et al., 2018; Guirado et al., 2014a), early-life stress (Castillo-Gómez et al., 2017), chronic stress during adulthood (Gilabert-Juan et al., 2013a, 2017), experimental induction of diabetes (Castillo-Gómez et al., 2015), NMDA receptor manipulation (Perez-Rando et al., 2017a) or in a murine model for schizophrenia (Gilabert-Juan et al., 2013b).

3.2 STRATEGIES USED TO STUDY THE STRUCTURAL ANALYSIS

The analysis of cell morphology is a key component to understand neuronal function and this is why the techniques used for its study have undergone different modifications in an attempt to improve the methodology used. Different strategies have been developed to study changes in the structure of principal neurons and interneurons.

Classically, the morphology of neurons was studied using the black reaction invented by Camillo Golgi in 1873, better known as the Golgi stain. It was the first technique to reveal neurons in their entirety with all their processes, providing major advances in the microscopic anatomy for over a century. Although new techniques have appeared later, the Golgi stain is still used alone or in combination with techniques like electron microscopy (Pannese, 1999). However, the technique has some inconveniences: the tissue fixation used for Golgi staining is often incompatible with other methods such as immunohistochemistry; the method has low frequency and unpredictable staining; and long processing periods are required. New methods have been developed to overcome some of the limitations of the Golgi staining, such as the use of fluorescent markers as one of the most common methods for neuronal morphology examination employed to date (Colello et al., 2012). Fluorescence immunolabeling, used commonly in immunohistochemistry, is a highly specific method that allows to study not only the cell structure but also the protein expression and interactions between cells. There is an enormous amount of commercially available dyes and fluorochrome labeled antibodies that make experiments specific and reproducible, as well as faster.

Furthermore, genetically encoded fluorescent proteins have been used in transgenic animals to drive constitutively fluorescent expression under specific promoters (Malinow et al., 2010). In particular, the green fluorescent protein (GFP) and their modifications, such as the enhanced green fluorescent protein (EGFP) or the yellow fluorescent protein (YFP) have been extensively use, which provides a great specificity of fluorescent expression unveiling even the most detailed structures, such as dendritic spines and boutons. In the present thesis, two examples of these transgenic strains have been used: the THY1-YFP line H mice and the GAD-EGFP mice. Regarding the **THY1-YFP**, this strain of mice express the YFP in a subset of pyramidal neurons (Feng et al., 2000; Porrero et al., 2010) throughout the brain, including pyramidal neurons located in layers V and VI of the mPFC and a large population of hippocampal principal neurons. By their side, the **GAD-EGFP** mice express EGFP in a subpopulation of interneurons (Oliva et al., 2000). In the line used in the present thesis, the GIN mice (GFP-expressing Inhibitory Neurons), EGFP is expressed in a subpopulation of SOM-containing GABAergic interneurons in the hippocampus and neocortex. In the mPFC, the somata of EGFP-

expressing interneurons are largely restricted to layers II-III and upper layer V. In the hippocampus, most EGFP-expressing interneurons are located in the *stratum oriens* and belong to O-LM cells. Furthermore, other two subtypes located in the *stratum pyramidale* and *stratum radiatum* have been identified (Oliva et al., 2000).

4. MOLECULAR MEDIATORS OF STRUCTURAL PLASTICITY

The structural plasticity may be mediated by changes in the expression of cytoskeletal proteins, certain cell adhesion molecules and different components of the extracellular matrix. In this regard, the polysialylated form of NCAM (polySia-NCAM) and the perineuronal nets have shown to play a key role in synaptogenesis and neurite remodeling.

4.1 POLYSIA-NCAM

NCAM is an abundant cell-surface molecule implicated in cell–cell and cell–matrix adhesion, as well as in the induction of some cytoplasmic signals. This molecule can suffer several post-translational modifications, but glycosylation by the addition of long polymeric chains of the carbohydrate polysialic acid (polySia, PSA), is by far the most important. To be consistent with the published results, I will use the term polySia in the present thesis.

4.1.1 The NCAM and polySia structure

The vast majority of the polySia is attached to NCAM (Mühlenhoff et al., 2013). NCAM belongs to the immunoglobulin superfamily of adhesion molecules and it is coded by a single copy gene composed of 26 exons. At least 20–30 distinct forms are known to be generated by alternative splicing and by post-translational modifications. However, three classes stand out depending on their weight: 180, 140 and 120 kDa isoforms (**Figure 8A**; Gascon et al., 2007). These three isoforms differ in their cytoplasmic domains (NCAM 180 and 140) or in the way of binding to the cell membrane (NCAM 120), the latter lacks the cytoplasmic segment and is attached to the cell surface through a

glycosylphosphatidylinositol (GPI) anchor (Gascon et al., 2007). **NCAM-180** and **NCAM-140** are transmembrane proteins that differ only in the exon 18 and the cytoplasmic domain, which is shorter in the NCAM-140. Both are attached to the plasma membrane through a transmembrane (TM) domain, which connects them with intracellular cytoskeleton for signal transduction. Only the two transmembrane isoforms NCAM-140 and NCAM-180 harbor the polysialylation (Gascon et al., 2007; Hildebrandt and Dityatev, 2015). By their side, the isoform **NCAM-120** is a GPI anchored protein. Its expression is scarcely detectable before birth, but there is a strong upregulation during postnatal development without polysialyation. NCAM-120 seems to be the characteristic isoform of mature oligodendrocytes and myelin sheaths, indeed its increased levels coincide with the time course of myelination and strongly differ from the expression patterns of polysialyltransferases.

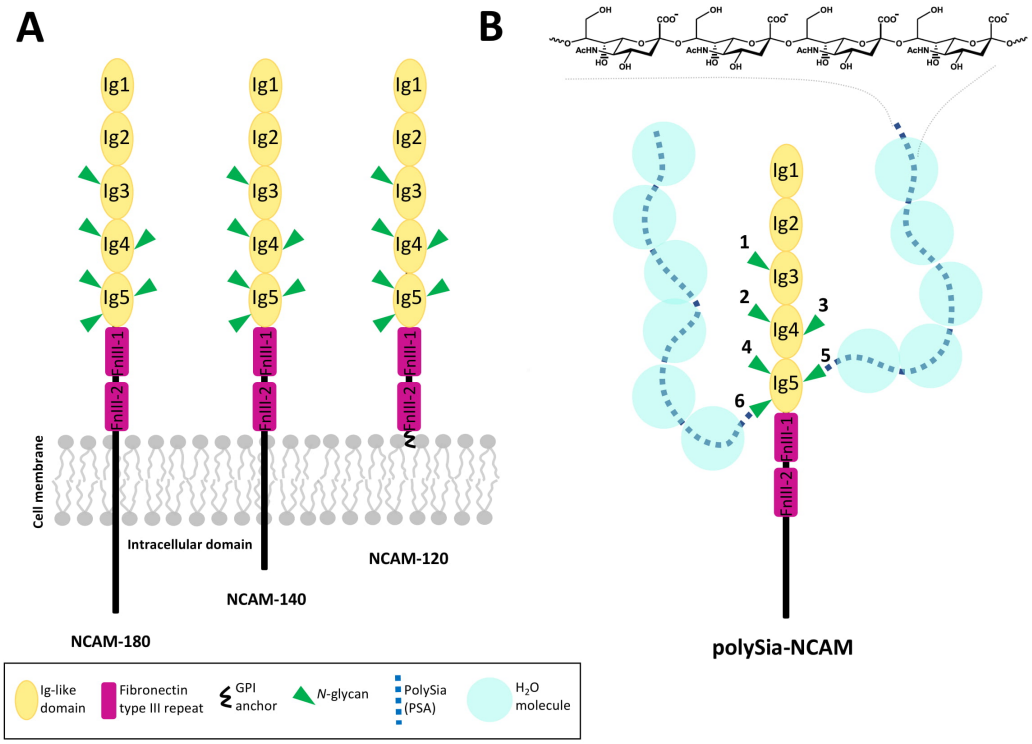

Figure 8: NCAM and polySia structure. A) Scheme of the three major NCAM isoforms with identical extracellular domain, composed by five immunoglobulin(Ig)-like domains (in yellow) and two fibronectin type III repeats (FnIII, in pink). Arrows in green represent the N-glycosylation sites. Differences can be observed in their intracellular domains (NCAM 180 and 140) or in the mode of binding to the cell membrane (NCAM 120), which is attached through a glycosylphosphatidylinositol (GPI) anchor. **B)** Polysialylated form of NCAM. Only the fifth and sixth N-glycosylation sites located in Ig5 are substrates for polySia attachment. The hydrodynamic radii of polySia are depicted as blue spheres and the structure of α-2,8-linked sialic acid polymers is detailed on the top (Modified from Hildebrandt et al., 2010).

Soluble forms of NCAM can be generated as a result of enzymatic excision of NCAM-120 from the GPI anchor or by the proteolytic cleavage of the extracellular domain of NCAM molecules (Gascon et al., 2007). **Structurally**, the three NCAM isoforms have identical extra-cellular structures, but differ in the weight and in the way they are anchored to the cell membrane. The extracellular domain presents different identifiable motifs: five immunoglobulin-like domains (Ig 1–5) where N-glycosylation sites can be found, followed by two fibronectin type III domains (FnIII). As I will discuss below, only the fifth and sixth N-glycosylation sites located in the fifth Ig-like domain (Ig5) are substrate for polySia attachment (Gascon et al., 2007; Hildebrandt et al., 2010; Hildebrandt and Dityatev, 2015).

Although NCAM is the preferred substrate for polysialyltransferases, other cell surface components can harbor detectable levels of polySia. It is the case of the alpha subunits of sodium channel (Zuber et al., 1992), the scavenger receptor CD36 in human milk (Yabe et al., 2003), and the polySia synthesizing enzymes themselves, which are able to polysialylate their own *N*-glycans in a process termed autopolysialylation (Close and Colley, 1998). The synaptic cell adhesion molecule SynCAM 1 and neuropilin-2 have been recently discovered as a targets for polysialylation in the early postnatal mouse brain (Mühlenhoff et al., 2013).

PolySia is a sugar formed by a linear homopolymer chain of negatively charged α-2,8-linked sialic acid, which allows it to incorporate H_2O molecules, creating a steric impediment that increases the intermembrane space for homo- and heterophilic cell-cell and cell-matrix adhesion, adjustment of receptor functions and membrane dynamics (**Figure 8B**; Gascon et al., 2007; Hildebrandt et al., 2010). These **anti-adhesive** properties of polySia-NCAM underlie key events, not only during brain development, such as correct migration and differentiation of postmitotic progenitor cells, neurite outgrowth, synaptogenesis and axon guidance (Bonfanti, 2006; Gascon et al., 2007; Rutishauser, 2008), but also in adulthood, associated to neurogenesis and plasticity-related events (Gómez-Climent et al., 2011; Nacher et al., 2010).

4.1.2 Polysialylation of NCAM

The addition of polySia to NCAM is catalyzed by two independent Golgi-resident polysialyltransferases (polySTs), **ST8SIA2** (STX) and **ST8SIA4** (PST) (Hildebrandt et al., 2007). These enzymes show a high sequence homology and are typical members of the mammalian sialyltransferase family, with a type II *trans*-membrane topology, a short *N*-terminal cytoplasmic tail, a stem region, and a large catalytic domain facing the Golgi lumen **(Figure 9A)**. The catalytic domain includes three sialylmotifs L, S, and VS, with highly conserved sequences between mammalian sialyltransferases that are implicated in the substrate binding. The polysialyltransferases also contain two unique polybasic motifs, the polysialyltransferase domain and the polybasic region (PD and PBR, respectively) (Hildebrandt et al., 2010; Hildebrandt and Dityatev, 2015). While PD is part of the catalytic domain and it is crucial for polyST catalytic activity, the PBR is located in the stem region and seems to be implicated in substrate recognition. Using cytidine 5-monophosphate (CMP), ST8SIA2 and ST8SIA4 catalyze the transfer of α-2,8-linked sialic acid residues to N-linked core glycan. Although NCAM has six N-glycosylation sites, the attachment of polySia is restricted to sites 5 and 6 located in the fifth Ig-like domain (Ig5) **(Figure 9B)**. FnIII domain is critical for the recognition of NCAM by polySTs (Mühlenhoff et al., 2013).

4.1.3 Time-course expression of polysialyltransferases and NCAM

During brain development, there is a widespread expression of polySia and almost all neurons seem to be positive for polySia in some stage of their development. In mice, the expression of both polySTs starts with the closure of the neural tube at embryonic day (E) 8.5 reaching maximum levels between E13.5 and E14.5 (Hildebrandt and Dityatev, 2015), which are maintained until birth. The time-course of ST8SIA2 and ST8SIA4 upregulation is almost identical to the increase in the expression of NCAM. NCAM begins to bear polySia shortly after its appearance during embryogenesis. The polysialylated form of NCAM increases and reaches its maximum expression during the perinatal phase, when it keeps up until day 9 of postnatal development; at this time almost all NCAM is polysialylated (Oltmann-Norden et al., 2008). Both enzymes are expressed with partially overlapping distribution but distinct time course (**Figure 9C**;

Hildebrandt et al., 2007, 2010). ST8SIA2 expression, prominent in embryonic and perinatal stages, drops quickly in a short period of time between postnatal day (P) 5 and P11 and remains low in young and adult animals. By contrast, the level of ST8SIA4 expression, although reduced as well, remains higher and more persistent after early postnatal development (Hildebrandt et al., 2007; Oltmann-Norden et al., 2008). Due to this, ST8SIA2 is considered the main polyST during embryonic development, while ST8SIA4 is considered the major polysialyltransferase in the adult brain. Since the expression of NCAM remains almost constant, the reduced polysialylation causes a gradual appearance of polySia-free NCAM-140 and NCAM-180. The downregulation of polySia and the increase of polySia-free NCAM concur with the end of major morphogenetic events happening during the first 3 weeks of postnatal brain development (Hildebrandt et al., 2007). However, as explained below, the expression of polysialylated NCAM persists into adulthood in connexion with neurogenic and plasticity-related events (Bonfanti, 2006).

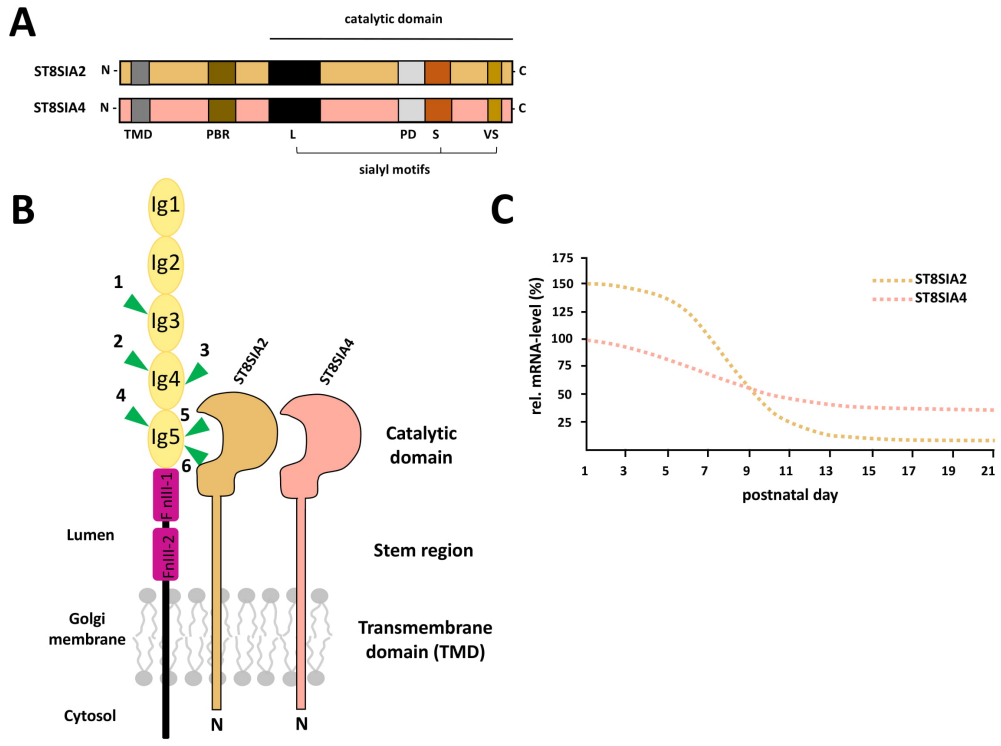

Figure 9: Schematic representation of the polysialyltransferases ST8SIA2 and ST8SIA4. A) PolySTs are formed by a short N-terminal cytoplasmatic part, a transmembrane domain (TMD), a stem region and a C-terminal catalytic domain facing the Golgi lumen. The catalytic domain includes three sialyl motifs: the large (L), short (S) and very short (VS) sialyl motifs implicated in substrate binding. PolySTs also contain two unique motifs termed polybasic region (PBR) and polyST specific domain (PD) **B)** ST8SIA2 and ST8SIA4 recognizing the fifth and sixth N-glycosylation sites located in Ig5 (Modified from Mühlenhoff et al., 2013). **C)** Expression of the two polysialyltranferases during development (Modified from Oltmann-Norden et al.,2008).

Deficient mice for each polyST have been generated (Galuska et al., 2006). Single knockout lines maintain a considerable expression of polySia and only a complete deletion of both genes produces a total ablation of polySia (Oltmann-Norden et al., 2008; Weinhold et al., 2005). ST8SIA2-deficient mice exhibit neurodevelopmental alterations with aberrant topology projections (Angata et al., 2004). By contrast, mice lacking ST8SIA4 do not show morphological defects but display impaired synaptic plasticity (Eckhardt et al., 2000). Mice with simultaneous ablation of ST8SIA2 and ST8SIA4 show marked postnatal growth retardation and premature death, a high incidence of hydrocephalus, as well as malformation of major brain axon tracts (Hildebrandt et al., 2009; Weinhold et al., 2005). Recent reports also have shown how attenuation of polySia interferes with the developmental migration of specific cortical interneurons in the mPFC. Dysregulation of polySTs by ablation of ST8SIA2, ST8SIA4 or both enzymes causes a reduction in interneuronal densities, specifically of those expressing parvalbumin or somatostatin, while densities of calretinin- and calbindin-expressing interneurons seem to be unaffected. This decline appears to be the result of an accumulation of precursors in the ganglionic eminences, as well as of the reduced entry of tangentially migrating interneurons in the pallium (Krocher et al., 2014).

4.1.4 Expression and functions of polySia in the adult brain

During brain development, polySia expression is mainly associated to neural migrating precursors and it is crucial for their correct final position and differentiation (Mühlenhoff et al., 2009). PolySia also plays a role in axon guidance reducing the fasciculative interactions between axons and allowing a better response to stimuli (Rutishauser, 2008). The expression of polySia is also important for the functional maturation of GABAergic inhibition, which determines the critical period of plasticity in the visual cortex (see critical periods) (Di Cristo et al., 2007).

Although neuronal plasticity is certainly more profound during brain development than in adulthood, high levels of polySia expression are still found in regions that retain neurogenic capacity or are associated to physiological plasticity or remodeling of neurites and synapses (Bonfanti, 2006; Gascon et al., 2007; Rutishauser, 2008). Neuroblasts from the **neurogenic niches** of the anterior subventricular zone and

early postmitotic granular cell precursors in the subgranular layer of the hippocampal dentate gyrus transiently express high levels of polySia during their migration (Bonfanti, 2006; Petridis et al., 2004). Moreover, high levels of polySia expression can be also found in a population of immature neurons located in the **paleocortex layer II**. Interestingly, despite being generated prenatally, they retain this immature neuronal phenotype into adulthood (Gómez-Climent et al., 2008).

In the adult brain, polySia is not only associated to immature neurons, a subpopulation of **mature cortical interneurons** is also characterized by the expression of polySia-NCAM (Gómez-Climent et al., 2011). These cells also co-express NeuN, the enzyme responsible for GABA synthesis (GAD67), and different calcium-binding proteins and neuropeptides. Interestingly, none of the polySia-expressing cells express the marker of principal neurons Ca(2+)/CAM-dependent protein kinase II (CaMKII-α). PolySia-positive interneurons have been detected in different cortical areas, including the PFC (Varea et al., 2005, 2007b), the septum (Foley et al., 2003), hippocampus (Nacher et al., 2002a; Seki and Arai, 1993) and the amygdala (Nacher et al., 2002b). The **neurochemical phenotype** of these mature interneurons shows certain diversity depending on the region (Nacher et al., 2013). PolySia-NCAM is mostly expressed in the somata and cell body of calbindin and SOM expressing interneurons, and it is rarely associated to the soma of those expressing calretinin, NPY, CCK or VIP. The analysis of polySia-expressing puncta in the neuropil, also demonstrates that many of these structures co-express markers of GABAergic terminals such as GAD67 or VGAT. Interestingly, although the somata of PV+ interneurons rarely co-express polySia-NCAM, many polySia-expressing puncta surrounding the somata of pyramidal are positive for PV (Castillo-Gómez et al., 2011; Gómez-Climent et al., 2011; Nacher et al., 2013). In the adult brain ST8SIA4 seems to be the solely responsible for polySia expression in mature cortical interneurons, whereas ST8SIA2 is the major polyST in the immature neurons of the paleocortex and the neurogenic niches (Nacher et al., 2010).

The expression of polySia in the adult brain is implicated in **structural plasticity,** which includes the remodeling of the structure and connectivity of neurons, especially interneurons, through its anti-adhesive and insulating properties (Nacher et al., 2013;

Rutishauser, 2008). Moreover, in many synapses of certain brain regions, polySia also modulates **synaptic plasticity** processes. In the hippocampus, ST8SIA4 plays a key role in synaptic plasticity processes associated to CA1 synapses. Mice lacking this enzyme show impaired LTP and LTD associated to the Schaffer collateral-CA1 synapses (Eckhardt et al., 2000). Moreover, polySia-NCAM is an important factor in the modulation of interneuronal structural plasticity. In different paradigms such as an antidepressant fluoxetine treatment, early-life stress, diabetic induced mice or the use of dopamine receptor agonist, changes in polySia expression are accompanied by alterations in the structure of SOM-expressing interneurons (Carceller et al., 2018; Castillo-Gómez et al., 2015, 2016a, 2017; Guirado et al., 2014a), which suggests that polySia may promote this plasticity by its anti-adhesive properties. Interestingly, interneurons expressing polySia have reduced dendritic arborization, spine density and less synaptic input than interneurons lacking polySia-NCAM (Gómez-Climent et al., 2011). Consequently, another non-excluding hypothesis implies that polySia may play an **insulating role** in the plasma membrane, restricting the possibility of establishing synaptic contacts. Direct manipulations through polySia depletion, using the enzyme Endo-Neuraminidase-N (Endo-N), affect the structure and connectivity of SOM- and PV- expressing interneurons (Castillo-Gómez et al., 2016b; Guirado et al., 2014b). This depletion also affects the structural features of pyramidal neurons, probably as an indirect effect (Castillo-Gómez et al., 2016a).

Although polySia is mainly associated to mature interneurons, certain **populations of excitatory neurons** in the hippocampus express polySia-NCAM in their axons or their terminal boutons, it is the case of the axons (mossy fibers) of many mature granule cells in the hilus and CA3 *stratum lucidum* (Seki and Arai, 1999) and the terminal boutons of the axons of CA3 pyramidal neurons (Schaffer collaterals), some of which terminate in the CA1 *stratum lacunosum-moleculare* (Schuster et al., 2001).

4.1.5 Neurological diseases

Alterations of polySia levels can be observed in different neurological and psychiatric disorders and in animal models of these diseases, including major depression, schizophrenia, Alzheimer's disease, and temporal lobe epilepsy (Castillo-

Gómez et al., 2015; Gilabert-Juan et al., 2012, 2013b; Mikkonen et al., 1999; Pham et al., 2003; Varea et al., 2012). Especially remarkable are the alterations found in **schizophrenia**. In human patients and in animal models, several studies have shown alterations in polySia expression and genetic associations of *NCAM1* and *ST8SIA2* variants with schizophrenia (Anney et al., 2010; Brennaman and Maness, 2010; Castillo-Gómez et al., 2016a, 2017; Gilabert-Juan et al., 2013c; McAuley et al., 2012; Varea et al., 2007a). Similar associations are found with autism spectrum and bipolar disorder (Anney et al., 2010; Yang et al., 2015), indicating that variations in the *ST8SIA2* gene are associated with increased risk to mental illness.

4.2 PERINEURONAL NETS

In the CNS three main types of ECM can be distinguished (Lorenzo Bozzelli et al., 2018; Sorg et al., 2016): (1) The first one includes the "loose" ECM, an homogenous, based mainly on hyaluronic acid (HA) matrix that surrounds the cell bodies, dendrites and synapses of most neurons within the brain and spinal cord. (2) The second type of ECM is composed by the extracellular part of membrane adhesion molecules. This subtype can be remodeled in response to neuronal activity or injury. (3) The last type is formed by the so-called perineuronal nets (PNNs), a relatively rigid and unique lattice-like structure enriched with chondroitin sulfate proteoglycans and hyaluronic acid that intimately interact with synaptic contacts around the soma and proximal dendrites of neurons and that are subjected to activity-dependent modulation. The last type, the PNNs, will be the object of study of this thesis.

PNNs have been largely ignored by the scientific community, being considered as possible artifacts until 1970. The improvement of histological techniques and the development of immunohistochemistry, allowed researchers to confirm the existence of PNNs in many vertebrate species including mice and humans.

4.2.1 PNNs composition

PNNs are specialized regions of the extracellular matrix, which enwrap the soma and dendrites of certain neuronal subpopulations, restricting their connectivity and plasticity-related events (Wang and Fawcett, 2012). PNNs are constituted by diverse

components synthesized not only from neurons themselves, but also from surrounding glial cells, such as oligodendrocytes and astrocytes (Carulli et al., 2006). All of these cells secrete the molecules into the extracellular space, where they associate with cell surface receptors, conforming heterogeneous aggregates. PNNs are formed by four families of ECM molecules (**Figure 10**; Lorenzo Bozzelli et al., 2018; Sorg et al., 2016): (1) A linear nonsulfated **hyaluronic acid** polymer negatively charged that forms the backbone of the structure onto which other PNNs molecules can bind. It is synthesized by the hyaluronan synthases (HASs; HAS1-HAS3). While all three enzymes are expressed in the somata of neurons, only HAS1 is located in the membranes of axons. (2) **Chondroitin sulfate proteoglycans (CSPGs)**. Among CSPGs, lectican family members, including aggrecan, versican, neurocan, and brevican, are the main constituents of PNNs. (3) **Tenascins**. Although there are four members in the tenascin family (tenascin-C, tenascin-R, tenascin-X and tenascin-W), only the tenascin-R (TN-R) and tenascin-C (TN-C) are present in the CNS and have been involved in some developmental functions. TN-R seems to be a key component in PNNs structure. (4) **Link proteins** are constituted by hyaluronan and proteoglycans (HAPLNs; HAPLN 1, 3, and 4). They bind the CSPGs to the hyaluronic acid polymer to stabilize PNNs.

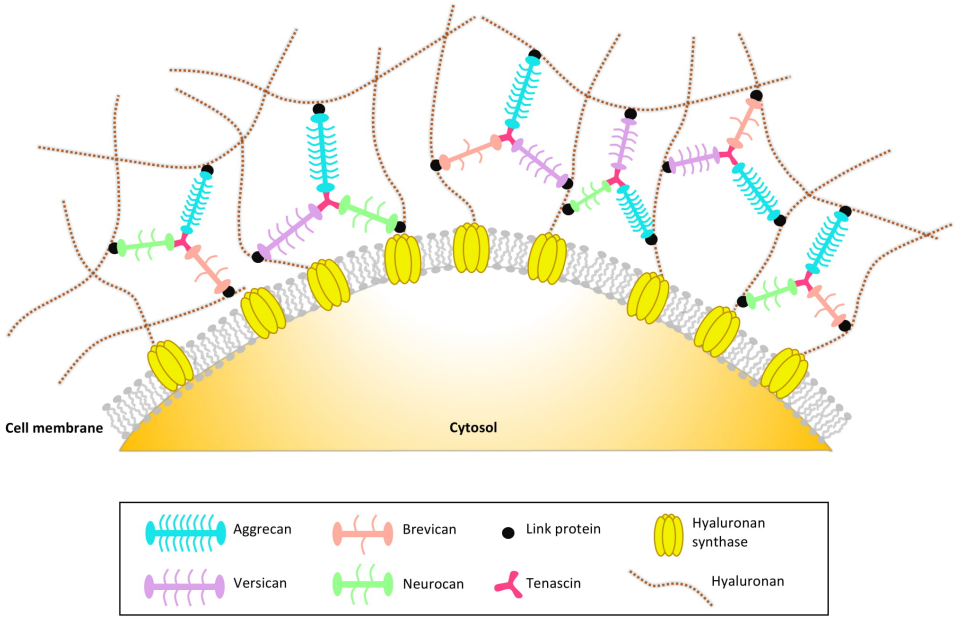

Figure 10: Composition of the perineuronal nets. PNNs are formed by four families of ECM molecules: (1) a linear polymer of hyaluronic acid negatively charged (dashed line) synthesized and anchored to the cell membrane by the hyaluronan synthases (in yellow); (2) chondroitin sulfate proteoglycans (CSPGs) from the lectican family, which include aggrecan (blue), versican (purple), brevican (orange) and neurocan (green); (3) tenascins (pink) that promote crosslinking of lecticans, and (4) link proteins (black dots) that bind the CSPGs to the hyaluronic acid polymer to stabilize PNNs (Modified from Wen et al., 2018).

PNNs can be detected using the lectin *wisteria floribunda agglutinin* (WFA), which recognizes most N-acetylgalactosamine residues present in the PNNs. The use of the bacterial enzyme chondroitinase ABC (ChABC) is also widely implemented to analyze the effects of PNNs attenuation through degradation of CSPGs. The composition and structure of PNNs is highly heterogeneous throughout regions and time. Their composition is also determined by the activity-dependent secretion of their components by surrounding neurons and glial cells, which create a continuously variable microenvironment (Sorg et al., 2016).

4.2.2 Expression pattern of PNNs components

In mice, PNNs appear at the end of **critical periods** (Pizzorusso et al., 2002), specially during postnatal development, concurring with the maturation of interneurons and the setting of the appropriate excitatory/inhibitory balance (Harauzov et al., 2010; Morishita and Hensch, 2008). It is for this reason that PNNs are widely considered indicators of neuronal maturation (Sorg et al., 2016). The maturation of PV+ inhibitory neurons has been linked to the onset of the critical period. The presence of PNNs on PV interneurons initiates its closure, reaching mature levels by its end (Testa et al., 2018). The appearance of PNNs creates an impediment that hinders the plasticity processes and consolidates the neuronal network. Interestingly, the depletion of PNNs leads to a prolonged critical period (Morishita et al., 2015; Testa et al., 2018).

PNNs can be found in several brain regions, including the neocortex, hippocampus, amygdala, hypothalamus, basal ganglia, and cerebellum. Indeed, these structures seem to have region-specific patterns and features (Ueno et al., 2017a, 2017b). PNNs are mainly found around fast-spiking, **parvalbumin-containing GABAergic interneurons** (Celio, 1993; Kosaka and Heizmann, 1989). Their presence or absence around this interneuronal subpopulation can affect the relative PV expression (Yamada et al., 2015), which suggests a role in the regulation of different functions of these PV-expressing interneurons. PNNs are deposited around neurons in an **activity dependent manner** (Dityatev et al., 2007). The somata and proximal dendrites of PV-expressing interneurons, as well as the attached presynaptic boutons and the axon initial segment, are specifically surrounded by PNNs. Excitatory and inhibitory active synapses can also

be enwrapped by PNNs, creating a specific functional microenvironment (Dityatev et al., 2007; John et al., 2006). By their side, fast-spiking interneurons express extrasynaptic molecules that stabilize the components of PNNs. It is the case of TN-R and HA, which are recognized by cell surface receptors found in the neuron (Jones and Jones, 2000; Toole, 2004). These receptors are mainly expressed in the somatodendritic domain and the axon initial segment of interneurons, although other receptors can be also observed on glial cell surfaces and presynaptic boutons. The CSPGs also interact with cell adhesion molecules of the immunoglobulin superfamily, such as Ng-CAM/L1, NCAM and TAG-1/axonin-1 (Margolis et al., 1996). Although several molecular mechanisms act to keep PNNs stable in association with the cell surface, neuronal activity continuously regulates and modifies the expression of CSPGs, tenascins, and other molecules that integrate the extracellular matrix (Dityatev and Schachner, 2003).

Although PNNs are mainly associated to PV+ interneurons, they are also found around **pyramidal cells** in the hippocampus and neocortical regions, although in a minor proportion. The presence of these PNNs on excitatory cells has been related to emotional learning and memory processes (Alpár et al., 2006; Morikawa et al., 2017; Yamada et al., 2015). Indeed, in some regions, including the piriform cortex, the lateral, basolateral and basomedial amygdala, the ventromedial hypothalamus or the entorhinal cortex, PNNs are more frequently found around excitatory neurons rather than inhibitory neurons (Morikawa et al., 2017).

4.2.3 Functions of PNNs in the adult brain

The deposition of PNNs around neurons helps to stabilize the established neuronal connections and to restrict the plastic changes. Their presence enwrapping PV-expressing cells can affect cell activity and thereby the role that these interneurons play in some processes like learning and memory, as well as in certain pathologies derived from its malfunction. PV+ interneurons regulate the firing of pyramidal cells and mainly orchestrate the generation of gamma oscillations (30–120 Hz). Gamma oscillations, which mediate communication between regions and allow information processing and cognitive flexibility, are altered after removal of PNNs (Steullet et al., 2014). Given their intimate location around fast-spiking interneurons, PNNs are in a prime position to

modify the **excitatory/inhibitory balance** and thus regulate the output of these interneurons.

PNNs are implicated in several processes. Since they have a net negative charge, PNNs can act as an **ion buffer,** creating a microenvironment around neurons that facilitates the interaction with positive ions and acts as a reservoir (Morawski et al., 2015). This is especially important in neurons with high spiking frequencies, where ions such as Ca2+ can specifically diffuse through PNNs. Interestingly, the blockade of L-type Ca2+ channels or Ca2+ permeable AMPA receptors produces a decrease in PNNs assembly, which highlights the role of Ca2+ in PNNs condensation (Dityatev et al., 2007). PNNs also have a **neuroprotective** role as it is evidenced in oxidative stress where PNNs act as a protective barrier (Cabungcal et al., 2013). Moreover, PNNs can modulate **neural plasticity** acting via different (non-exclusive) mechanisms such as hindering the formation of new neuronal contacts, acting as a scaffold for molecules that can inhibit synaptic formation, or by limiting the receptor motility at synapses (Sorg et al., 2016). Their presence around the somata and proximal dendrites decreases the lateral diffusion level of some receptors making difficult synaptic plasticity processes that can be reactivated after enzymatic degradation of PNNs (Wang and Fawcett, 2012). Indeed, removal of PNNs increases the level of receptor subunits in the neurite surface and the diffusion coefficient (Frischknecht et al., 2009). Degradation of PNNs also enhances dendritic spine turnover (De Vivo et al., 2013). Some components of PNNs can interfere with different **signaling pathways** by their union to signaling proteins such as Otx2 or Sema3A. Regarding this, the presence of PNNs facilitates the internalization of Otx2 by PV-expressing cells to maintain the closure of the critical period (Beurdeley et al., 2012). By their side, their interaction with Sema3A produces a potent inhibition of axon growth (Dick et al., 2013)**.** Given that PNNs perturb neural plasticity, they have been also related to **learning and memory** processes. In the hippocampus, PNNs are implicated in long-term memory. Indeed, the enzymatic removal of chondroitin sulfates decreases LTP at excitatory synapses in CA1 (Bukalo et al., 2001) and increases the excitability of PV+ basket cells without affecting principal neurons, which remarks the key role of PNNs in controlling their excitability (Dityatev et al., 2007). Mice deficient in CSPG also show impairments in LTP and LTD (Brakebusch et al., 2002; Bukalo et al., 2001) while short

term depression is unaffected (Bukalo et al., 2001). The loss of other PNNs components such as TN-R also results in impaired LTP but not LTD (Bukalo et al., 2001; Saghatelyan et al., 2001). In the PFC, digestion of PNNs also disrupt long-term as well as fear-conditioned memories (Hylin et al., 2013).

4.2.4 Involvement of PNNs in neurological diseases

Abnormal formation of PNNs has been associated with some neurodevelopmental diseases including schizophrenia, epilepsy, mood disorders and autism (Sorg et al., 2016). PNNs mediate a broad range of synaptic regulatory functions that affect the dendritic spine and synapse structure as well as the glutamatergic and GABAergic transmission. Since PNNs enwrap PV+ interneurons, they effectively control the excitatory/inhibitory balance. Disruption of this balance have been associated with some psychiatric disorders such as **schizophrenia**. As evidenced, the PFC of mice models and schizophrenic patients has reduced levels of PV expression and PNNs (Matuszko et al., 2017; Mauney et al., 2013; Testa et al., 2018). Abnormalities in the extracellular matrix have been also reported in mood disorders (Pantazopoulos and Berretta, 2016). Alterations in molecules that integrate PNNs have been observed in patients with major **depression** and in animal models of this disorder (Pantazopoulos and Berretta, 2016). Interestingly, the use of antidepressants also results in alterations in PNNs. A chronic treatment with the antidepressant fluoxetine, a selective serotonin reuptake inhibitor, results in a decrease in the number of PNNs in both the PFC and hippocampus of mice, together with an increase in immature neuronal markers and dendritic spine density on interneurons (Guirado et al., 2014a). Several studies have also focused their attention on PNNs in animal models of **addiction** where PNNs are found to be reduced in ventral tegmental area after several weeks of addictive behavior (Vazquez-Sanroman et al., 2017).

5. MOLECULAR INDUCTORS OF STRUCTURAL PLASTICITY IN THE ADULT BRAIN

Certain molecules, such as trophic factors and different hormones can promote neuronal structural plasticity. A **trophic factor** can be generally defined as any molecule that supports the growth and survival of specific group of cells. In the nervous system, there are many of them that operate and have effects not only during brain development, but also in the adult brain, where they are involved in proliferation, neuronal survival, differentiation and synaptic plasticity processes. Moreover, accumulating evidence suggests also a key role for these molecules in the neuronal remodeling that occurs after certain paradigms. The brain-derived neurotrophic factor (BDNF), is one of the most powerful neurotrophic factors. It is expressed in different tissues, but its role has been extensively studied in the brain, where it exerts developmental effects on neuronal differentiation and survival, and also on synaptic and structural plasticity throughout life (Cowansage et al., 2010). Its binding with the receptor TrkB can modify the structure of pyramidal neurons by promoting an increase in the number of dendritic spines (Amaral and Pozzo-Miller, 2007; Chapleau et al., 2009) and in the complexity of the dendritic arborization (Gonzalez et al., 2016), which results in improved efficiency of synaptic transmission. The use of TrkB receptor agonists also produces structural changes on neocortical pyramidal neurons and their dynamics (Perez-Rando et al., 2018). Some **hormones** such as insulin, also play a role in different aspects of neural plasticity, such as the increment of hippocampal neurogenesis (Anderson et al., 2002), the structural remodeling of neurons or the formation of new synapses (Lee et al., 2011). Steroid hormones such as corticosterone (in rodents) or cortisol (in humans) have similar pro-plastic effects (Lucassen et al., 2014).

In the present thesis, I will focus my attention in a different hormone, erythropoietin (EPO), an hormone mainly known for its role in erythropoiesis, which also has amazing properties on different levels of neuronal plasticity.

5.1 ERYTHROPOIETIN

EPO, an hypoxia-inducible factor, is a four-helix glycoprotein hormone that belongs to the cytokine superfamily, and consists of a single polypeptide of 166 amino acids and several chains of carbohydrate residues that make up around 40% of the mass of approximately 30 to 34 kDa, depending on carbohydrate content. Three *N*-glycosylation sites can each accommodate up to four sialic residues (Alnaeeli et al., 2012). In addition to the full-length EPO, splice variants have been identified, as it is the case of exon 3 deletion variant EV-3 present in humans. This variant appears to have a neuroprotective role but lacks erythropoietic activity (Bonnas et al., 2017).

EPO exerts its functions through its binding to the homodimeric **EPO receptor (EPOR)**, a member of the cytokine type I receptor family. In 1989, the EPOR was first cloned in mice and later their expression was also observed in cells with neuronal characteristics (D'Andrea et al., 1989; Masuda et al., 1993). EPOR is formed by an intracellular domain, a single transmembrane domain, and an extracellular region with two domains that provide two binding sites for EPO. The EPO binding results in a conformational change of the dimeric EPOR that initiates three major signal transduction pathways, highly conserved in vertebrates **(Figure 11)**. The main cascade, **JAK2-STAT5**, involves the phosphorylation of tyrosine residues at the intracellular domain mediated by a protein tyrosinase kinase (JAK2), a protein constitutively associated with the receptor (Witthuhn et al., 1993). The signal transduction activates the transcription of STAT factors (5A and 5B) (Klingmüller et al., 1996) that accumulate in the nucleus and mediate the transcription of genes involved in processes such as proliferation, apoptosis and cell differentiation. EPOR also activates a second pathway, which includes the phosphoinositide-3-kinase (**PI3K-AKT**), and the activation of mitogen-activated protein kinase (**Ras/MAPK**) (Alnaeeli et al., 2012; Ostrowski and Heinrich, 2018; Shi et al., 2010). Some transcription factors such as GATA1, SCL/TAL1 and EKLF and EPO itself can elevate the expression of EPOR. On the contrary, negative modulators can limit the function of EPOR signaling by acting on JAK2 and therefore preventing STAT activation (Ostrowski and Heinrich, 2018). The EPOR exists in three major isoforms generated by alternative splicing: (1) the full-length isoform described

above; (2) a soluble protein that lacks the transmembrane and intracellular domains; and (3) a truncated protein that lacks some parts of the intracellular domain. In addition to the EPOR, other receptors for EPO with neuroprotective function have been identified, such as (1) a heteromeric complex consisting of one or more EPOR together with one or more molecules of the common beta receptor chain, (2) the Ephrin B4 receptor and (3) the human orphan cytokine receptor-like factor 3 (Ostrowski and Heinrich, 2018).

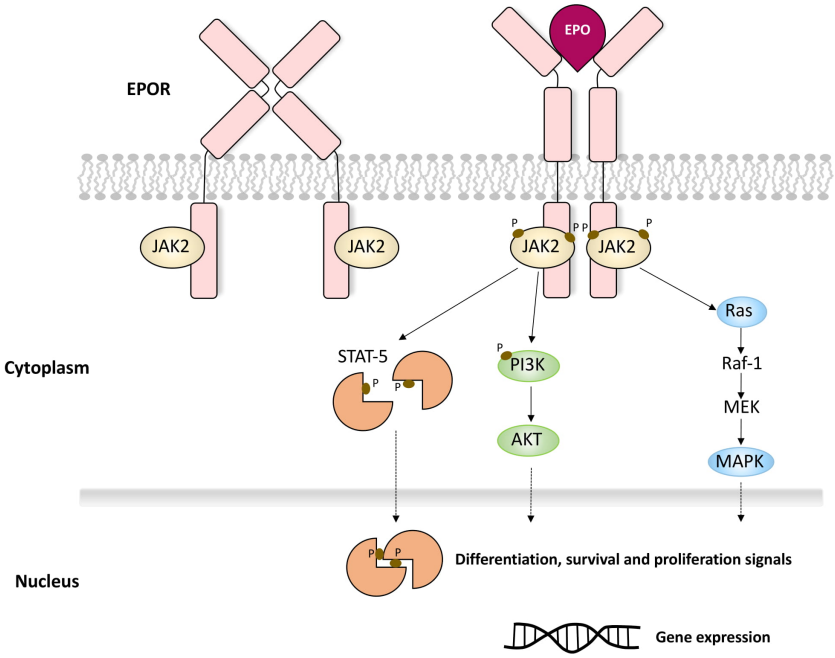

Figure 11: Erythropoietin signaling. The EPO binding to the homodimeric EPOR causes a conformational change resulting in transphosphorylation and activation of JAK2 proteins. Three major signal cascades are activated: (1) JAK2-STAT5; (2) PI3K/AKT; and (3) Ras/MAPK. As a result, there is a transcription of genes involved in processes such as differentiation, survival and proliferation (Modified from Alnaeeli et al., 2012).

EPO has been extensively used as a hematopoietic growth factor due to its stimulatory role on erythropoiesis. Its production starts in the fetal liver and continues in the adult kidney (although it can be locally produced by cells of various tissues) and it is subsequently secreted to the circulation to regulate red blood cell production in the bone marrow (Dzierzak and Philipsen, 2013). The binding to its receptor (EPOR) initiates a signaling cascade that mediates the proliferation, differentiation, and maturation of erythroid precursors, as well as preventing apoptotic effects in the erythroid progenitor cells (Kelley et al., 1993). Interestingly, the expression of EPO and EPOR are also observed in the CNS where they exert a wide range of neuroprotective actions including anti-apoptotic, anti-oxidant and anti-inflammatory effects both in neurons and in glial

cells, in addition to the stimulation of cerebral angiogenesis and neurogenesis (Sirén et al., 2009). As in the hematopoietic process, EPO is involved in the prevention of programmed cell death also in neuronal systems (Chong et al., 2002). Endogeneous EPO-EPOR signaling plays a crucial role in normal brain development, promoting cell survival and proliferation (Alnaeeli et al., 2012). Indeed, EPOR-deficient mice have an increased cell death and enhanced hypoxia sensitivity, which evidences the main functions of EPOR during developmental stages (Yu et al., 2002). In the mature brain, there is a drop in the expression of EPO and EPOR under healthy conditions. However, a notable expression of EPO and its receptor is still found in neurons, oligodendroglia, astrocytes and microglia of some areas including the prefrontal cortex and hippocampus, both in mice and humans (Digicaylioglu et al., 1995; Ehrenreich et al., 2003; Ott et al., 2015). Neurons and glial cells may release EPO as a paracrine and/or autocrine signal. Some events, such as hypoxia or metabolic stress rapidly increase the expression of EPO and EPOR (Ehrenreich et al., 2005; Ott et al., 2015; Sirén et al., 2001). In some disorders of the central nervous system, expression of EPOR is also up-regulated, as seen in the brains of schizophrenia and Alzheimer's disease patients (Assaraf et al., 2007; Ehrenreich et al., 2004).

Moreover, EPO has strong beneficial **cognitive effects**. In healthy humans and compromised brains of multiple sclerosis and schizophrenia patients, EPO enhances cognitive performance and memory retrieval (Ehrenreich et al., 2007a, 2007b; Miskowiak et al., 2007). In the same way, in healthy mice and rodent models for neuropsychiatric diseases, EPO also exerts these procognitive effects (Adamcio et al., 2008; El-Kordi et al., 2009; Gao et al., 2015). A 3-week EPO treatment in young mice, enhances LTP in the CA1 region of the hippocampus, accompanied by an improvement of hippocampal-dependent memory (Adamcio et al., 2008). At least part of these effects on cognition may be the result of an increased number of hippocampal pyramidal neurons and oligodendrocytes after EPO treatment, which remains increased after continuous cognitive challenge (Hassouna et al., 2016). Interestingly, all these effects are independent of changes in the hematocrit. Overexpression of constitutively active EPOR in pyramidal neurons of cortex and hippocampus also increases synaptic plasticity (augmented LTP), as well as spatial learning, cognitive flexibility, social memory, and

attentional capacities (Sargin et al., 2011). However, the constitutive expression of EPOR in GABAergic neurons does not alter cognitive execution (Wüstefeld et al., 2016). Despite these beneficial roles of EPO and EPOR and its impact as a therapeutic factor in the treatment of some diseases, little is known about the neurobiological bases of these effects, which would range from structural modifications of neurons to changes in the expression of plasticity-related molecules such as polySia-NCAM and PNNs.

Among the plastic processes that can occur in the adolescent and adult brain, in the present thesis I will focus mainly on the structural plasticity of neurons, both excitatory and inhibitory. This structural remodeling can be modulated, among others, through changes in neurotransmission, the expression of plasticity-related molecules, or the effect of different hormones. These studies will be performed in two brain regions that retain a marked plasticity in the adult brain: the prefrontal cortex and the hippocampus.

CHAPTER II
Objectives

The main objective of this doctoral thesis is to study the effects that different pharmacological and genetic manipulations produce on the structural plasticity of excitatory and inhibitory neurons in the mouse brain, their connectivity and the expression of plasticity-related molecules, both in adulthood and during adolescence. In order to achieve this main goal, the different specific objectives are detailed below:

1. To evaluate the impact of a direct increase in the inhibitory neurotransmission, by means of a chronic treatment with the benzodiazepine diazepam, on the structure of pyramidal neurons in the prefrontal cortex.

2. To study the effects of a genetic depletion of the polysialyltransferases ST8SIA2 and ST8SIA4 on the dendritic structure and connectivity of interneurons in the prefrontal cortex.

3. To study the impact of a chronic treatment with erythropoietin on the structure and connectivity of inhibitory neurons of the hippocampal CA1 region, on the excitatory/inhibitory balance in this region and on molecules related to interneuronal plasticity.

CHAPTER III

Material and Methods

EXPERIMENT 1. EFFECT OF A CHRONIC TREATMENT WITH DIAZEPAM ON THE STRUCTURE OF PYRAMIDAL NEURONS IN THE PREFRONTAL CORTEX.

1.1 ANIMALS

Fourteen B6.Cg-Tg THY1-YFP mice (Thy1-YFP line H) adult male mice (3 months old), were used to carry out the chronic benzodiazepine treatment. Additionally, 4 control mice were used for the study of the phenotype of *en passant boutons*. These mice express spectral variants of GFP (yellow-YFP) at high levels in motor and sensory neurons, as well as in subsets of central pyramidal neurons (Porrero et al., 2010). Animals were separated into the experimental groups (n= 7 diazepam; n= 7 saline) and housed in standard cages of three or four animals *per* cage. Animals used for the phenotype study of *en passant boutons* were housed in standard cages (n= 4). Mice were allowed to habituate to the new cages and conspecifics at least one week prior to the start of the experiments under standard conditions of temperature and humidity, with food and water *ad libitum* and normal light/dark cycle (lights on: 8:00–20:00). All animal experimentation was conducted in accordance with the Directive 2010/63/EU of the European Parliament and of the Council of 22 September 2010 on the protection of animals used for scientific purposes and was approved by the Committee on Bioethics of the Universitat de València (2014/040/UVEG/004). Every effort was made to minimize the number of animals used and their suffering.

1.2 BEHAVIORAL TESTS

Light-dark test: A light-dark test (Crawley and Goodwin, 1980) was conducted during the light phase in the day before the start of the drug treatment, in order to study the initial anxiety level of mice and to homogeneously assign them in the different experimental groups. Behavior measurements were the time spent (in seconds) in the light compartment relative to that spent in the dark compartment (Sharma et al., 2011). All procedures were studied using a video tracking system designed to automate testing in behavioral experiments (Stoelting Any-Maze, USA).

Open field test: During the light phase and 24h after the last injection of diazepam, the open field test was performed. The open field test was developed for the study of emotionality (Hall C.S., 1934) and consists in subjecting an animal to an unknown environment from which escape is prevented by surrounding walls (Walsh and Cummins, 1976). Each mouse was placed gently into the center of the enclosure for 10 min of free exploration. This test was used to study the anxiety level after chronic diazepam treatment. To assess the spatial organization of locomotor activity, the following parameters were recorded: total distance, mean speed, total mobile time, total immobile time, line crossings, immobility latency, freezing episodes, entries to periphery or center zone, latency to first entry, periphery time mobile, periphery time immobile, periphery time freezing, center time mobile, center time immobile and center time freezing. Locomotor activity and anxiety level of mice was recorded and analyzed using a video tracking system and software (Stoelting Any-Maze, USA) **(Figure 12)**.

1.3 CHRONIC TREATMENT WITH DIAZEPAM

Mice were injected intraperitoneally (i.p) daily with using an anxiolytic but not sedative dose of diazepam, 2 mg/kg (Sigma–Aldrich, St. Louis, MO) or with vehicle (saline) for 21 days at 9:30–10:00 a.m **(Figure 12)**. Compounds were prepared each day as solutions in physiological saline containing a drop of Tween 80 (0.1%) and sonicated to enhance dissolution. Mice were weighed before each injection to receive the appropriate dose (0.2 mg/ml).

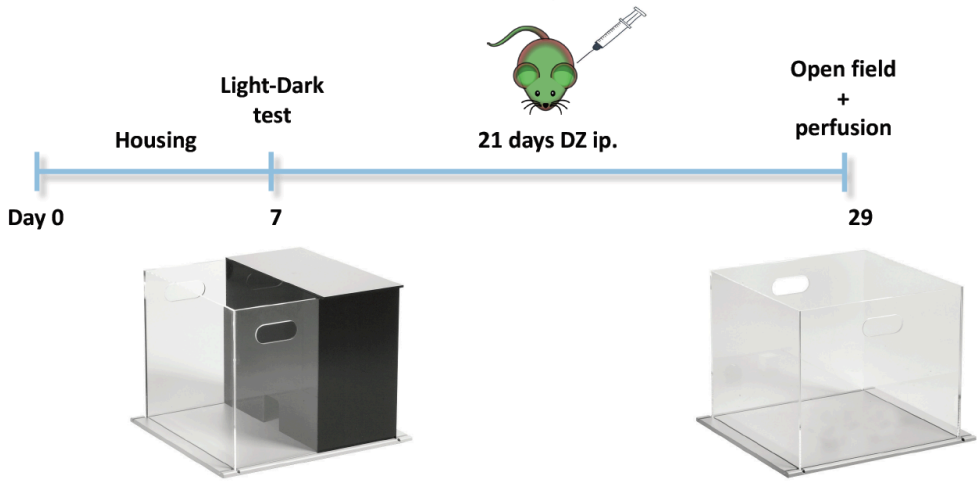

Figure 12: Schematic representation of the experimental design for Experiment 1.

1.4 PERFUSION AND MICROTOMY TECHNIQUES

After the last animal was tested in the open field, mice were perfused transcardially (in the same order as in the behavior test) under deep sodium pentobarbital anesthesia (150 mg/kg) with 0.9% saline for three minutes and then for twenty-five minutes with 4% paraformaldehyde in phosphate buffer (PB) 0.1 M, ph 7.4. Control animals destined for the phenotyping of *en passant boutons* were processed identically. After the perfusion, mice were decapitated and heads were stored for thirty minutes at 4°C. Then, brains were extracted and the two hemispheres separated. To study the density of *en passant boutons* and of dendritic spines, the right hemisphere of each animal was cut in coronal 100 μm-thick sections using a vibratome (Leica VT 1000E). Slices were collected in three subseries and stored at 4°C in PB 0.1 M with sodium azide (0.05%). To study the phenotype of *en passant boutons* the left hemisphere was frozen and cryoprotected in 30% sucrose in PB 0.1 M. Then, coronal sections, 50 μm thick, were obtained with a freezing-sliding microtome (Leica SM2000R), collected in 6 subseries and stored at −20°C in 30% glycerol, 30% ethylene glycol in PB 0.1 M until used.

1.5 CONFOCAL MICROSCOPY AND STRUCTURAL ANALYSES

For the structural study, coronal sections (100 μm-thick) were mounted on slides and coverslipped using Dako Fluorescent Mounting Medium (Dako Diagnósticos). The sections were observed under a confocal microscope (Leica TCS-SPE) using a sequential scanning mode. The area of interest was the cingulate cortex, including its dorsal and ventral regions (Bregma 1.42 to Bregma 0.02 mm, Paxinos and Franklin, 2008). To study the spine density of pyramidal neurons, apical dendrites from YFP-expressing neurons, which soma was located in the layer V of the cingulate cortex, were selected with a total of six neurons *per* animal **(Figure 13)**. Stacks of confocal images were obtained with 63x oil immersion objective and an additional 3.5x digital zoom. Confocal z-stacks covering the whole depth of the sections were taken with 0.38 μm step size. The spines were counted in four consecutive dendritic fragments (50 μm each) expanding 200 μm from the soma. The stacks obtained were processed with an image analysis package (Schindelin et al., 2012), using the Stitching plugin to reconstruct a 3D image of apical

dendrites processed (ImageJ, NIH). The multipoint tool was used to perform the counting of dendritic spines.

To analyze the density of *en passant boutons*, six axonal branches *per* animal were selected from deep layer I and superficial layer II of the cingulate region **(Figure 13)**. Stacks of confocal images were obtained with 40x objective and additional 2.5x digital zoom, using a 0.88 µm step size. Axons were examined along their lengths and the number of *en passant boutons* was counted to calculate the total density. An average of 80 microns *per* axon were analyzed. The stacks obtained were processed using FIJI (ImageJ, NIH) to measure the length of the axon and count the number of boutons.

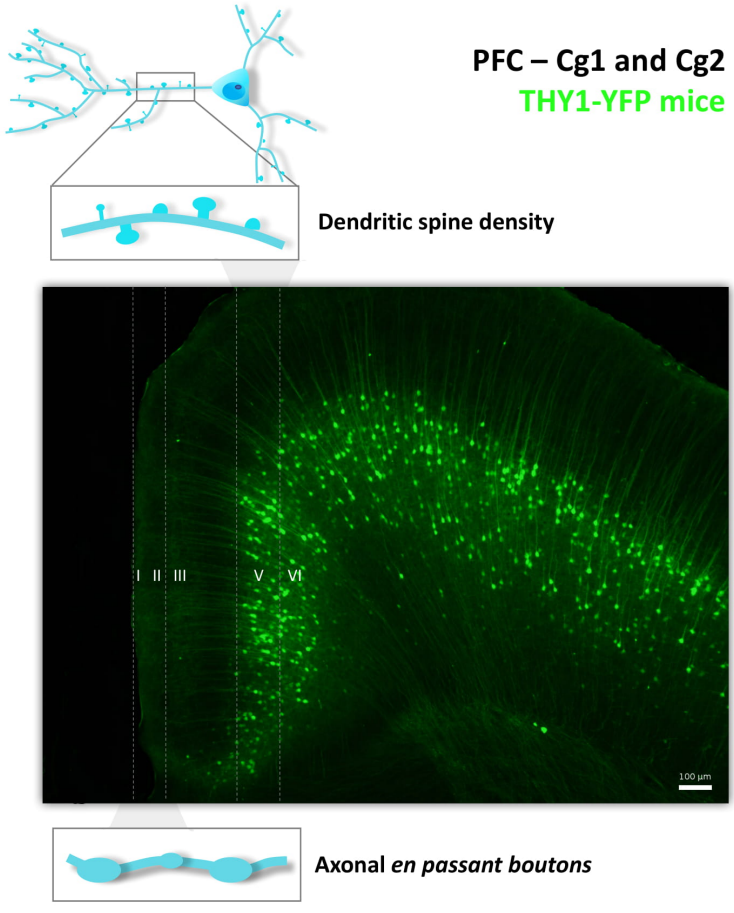

Figure 13: Panoramic microphotograph of the cingulate cortex in Thy1-YFP mice. Depicted in the image appear the layers of interest for the study (framed in dashed line) and a schematic drawing of the structures studied in pyramidal neurons: dendritic spine density (studied in layer V) and axonal *en passant boutons* (studied in layers I-II). Scale bar: 100 µm.

1.6 IMMUNOHISTOCHEMISTRY AND PHENOTYPING OF *EN PASSANT BOUTONS*

To test whether *en passant boutons* in deep layer I and superficial layer II had an extracortical origin, as suggested by Porrero et al. (Porrero et al., 2010), sections were

subjected to immunohistochemistry performed as follows: Briefly, sections were treated for 2 h with 10% normal donkey serum (NDS, Jackson ImmunoResearch Laboratories) in PBS with 0.2% Triton X-100 (PBST, Sigma–Aldrich) to block non specific binding. Then, sections were incubated overnight at room temperature in polyclonal guinea pig anti-VGLUT2 antibody (1:2000, Millipore). After washing, sections were incubated for 2 h with goat anti-guinea pig DL649 antibody (1:400, Jackson ImmunoResearch Laboratories). Primary and secondary antibodies were diluted in PBST and 5% NDS. Finally, sections were washed in PB 0.1 M and mounted on slides for confocal microscopy analysis. To study the co-localization of VGLUT2 in *en passant boutons*, nine axonal branches *per* animal were selected from deep layer I and superficial layer II of the cingulate region. Stacks of confocal images were obtained with 63x objective and additional 3.5x digital zoom. The stacks obtained were processed with the image analysis program FIJI (ImageJ, NIH) to quantify the percentage of co-localization. To perform the study, 9 axonal branches of an average of 80 microns *per* axon were randomly selected and the total *en passant boutons* present in each branch were counted. The presence of a VGLUT2 immunoreactive in close apposition to the *en passant boutons* was considered as co-localization (we established a spatial overlap equal or greater than 70% to consider the co-localization). Finally, we calculated the percentage of axons that had at least one *en passant bouton* positive for VGLUT2 to consider the extracortical origin of these branches, and the percentage of co-localization with VGLUT2 of each axon.

1.7 STATISTICAL ANALYSIS

Data were reported as mean ± SEM, and were analyzed using the IBM SPSS statistics software (version 19). The significance of differences between control and diazepam groups was determined by independent sample t-test; $p < 0.05$ was considered to be statistically significant.

EXPERIMENT 2. EFFECTS OF A GENETIC DEPLETION OF THE POLYSIALYLTRANSFERASES ST8SIA2 AND ST8SIA4 ON THE DENDRITIC STRUCTURE AND CONNECTIVITY OF INTERNEURONS IN THE PREFRONTAL CORTEX.

2.1 ANIMALS

C57BL/6J and mutant mice were bred at the central animal facility at Hannover Medical School. *St8sia2* and *St8sia4* knockout strains, backcrossed with C57BL/6J mice for six generations, were cross-bred with GAD67-GFP knock-in mice (Tamamaki et al., 2003) to obtain *St8sia2*$^{-}$/$^{-}$ or *St8sia4*$^{-}$/$^{-}$ mice heterozygous for the transgene (*St8sia2*$^{-}$/$^{-}$ GAD67-GFP and *St8sia4*$^{-}$/$^{-}$GAD67-GFP). The control group consisted of GAD67-GFP positive *St8sia2*$^{+}$/$^{+}$ and *St8sia4*$^{+}$/$^{+}$ mice derived from the same founder colonies as the knockout animals. Genotyping was performed by PCR as previously described (Tamamaki et al., 2003; Weinhold et al., 2005). Six animals *per* group were used to perform the different experiments. All animal experimentation was conducted in accordance with the Directive 2010/63/EU of the European Parliament and of the Council of 22 September 2010 on the protection of animals used for scientific purposes and was approved by the Committee on Bioethics of the Universitat de València. Every effort was made to minimize the number of animals used and their suffering.

2.2 PERFUSION AND MICROTOMY TECHNIQUES

All mice were perfused transcardially when 3 months old, first for 1 min with 0.9% saline and then for 30 min with 4% paraformaldehyde in PB 0.1 M, pH 7.4. To analyze the dendritic arborization of GFP-expressing interneurons, the right hemispheres were sectioned in coronal 100 μm-thick sections using a vibratome (Leica VT 1000E), collected in three subseries and stored at 4°C in PB 0.1 M with sodium azide (0.05%). For the immunohistochemical assays, the left hemispheres were frozen and cryoprotected in 30% sucrose in PB 0.1 M. Then, coronal sections (50 μm-thick) were obtained with a freezing-sliding microtome (Leica SM2000R), collected in six subseries and stored at −20°C in 30% glycerol, 30% ethylene glycol in PB 0.1 M until used.

2.3 IMMUNOHISTOCHEMICAL ASSAYS

2.3.1 Neurochemical phenotype of GAD67-GFP interneurons

In order to characterize neurochemically the GAD67-GFP interneurons in the mPFC, double immunostainings were performed using free-floating 50 μm sections tissue of thickness from the different strains of mice: anti-GFP primary antibody was used in combination with anti-: (a) parvalbumin (anti-PV); (b) calretinin (anti-CR); and (c) calbindin (anti-CB) primary antibodies **(Table 1)**. Briefly, sections were washed in PBS and then incubated for 1 h in 10% normal donkey serum (NDS, Jackson ImmunoResearch Laboratories) in PBS with 0.2% Triton X-100 (PBST, Sigma-Aldrich). Afterwards, sections were incubated for 48 h at 4°C with the primary antibodies diluted in PBST and 5% NDS **(Table 1)**. After washing, sections were incubated for 2 h at room temperature with the appropriate secondary antibodies diluted in PBST and 5% NDS **(Table 1)**. Finally, sections were washed in PB 0.1 M, mounted on slides, and coverslipped using fluorescence mounting medium (Dako Diagnósticos).

2.3.2 Morphological study

To perform the structural analysis, a simple fluorescent immunohistochemistry against GFP was performed using coronal sections of 100 μm microns. The immunohistochemical protocol was similar to that described above, using a polyclonal chicken IgY anti-GFP antibody to amplify the GFP fluorescent signal in interneurons destined to morphological studies **(Table 1)**.

2.3.3 Analysis of the inhibitory perisomatic puncta

In order to analyze the density of perisomatic puncta surrounding pyramidal neurons, after washing, coronal 50 μm-thick sections were first treated for 1 min with an antigen unmasking solution (0.01 M citrate buffer, pH 6) at 100°C. After cooling down sections to room temperature, they were processed for immunofluorescence as described above with a cocktail of primary antibodies **(Table 1)** including anti-CaMKII-α, anti- SYN and anti-PV (1:2000, Synaptic Systems). After being washed, sections were incubated with the appropriate fluorescent secondary antibodies **(Table 1)**. Sections

incubated with donkey anti-guinea pig biotinylated antibodies were subsequently incubated for 1 h in Streptavidin (Life Technologies). Finally, sections were mounted on slides and coverslipped using fluorescence mounting medium (Dako Diagnósticos).

All studied sections passed through all procedures simultaneously in order to minimize any difference from the immunohistochemical staining itself. To avoid any bias in the analysis, all slides were coded prior to analysis and remained coded until the experiment was completed.

Anti	Host	Isotype/Label	Dilution	Incubation	Company
Primary antibodies					
GFP	Chicken	Ig Y	1:1000	48h, 4ºC	Abcam
PV	Guinea Pig	Ig G	1:2000	48h, 4ºC	Synaptic Systems
CR	Rabbit	Ig G	1:2000	48h, 4ºC	Swant
CB	Mouse	Ig G1	1:5000	48h, 4ºC	Sigma Life Science
CaMKII-α	Mouse	Ig G1	1:500	48h, 4ºC	Abcam
SYN	Rabbit	Ig G	1:1000	48h, 4ºC	Chemicon-Millipore
Secondary antibodies					
Chicken IgY	Donkey	CF 488	1:400	2h, 25°C	Sigma Life Science
Guinea pig IgG	Goat	Alexa 555	1:400	2h, 25°C	Life Technologies
Rabbit IgG	Donkey	Alexa 555	1:400	2h, 25°C	Life Technologies
Mouse IgG1	Goat	Alexa 635	1:400	2h, 25°C	Life Technologies
Mouse IgG1	Goat	Dylight 649	1:400	2h, 25°C	Jackson ImmunoResearch
Guinea pig IgG	Donkey	Biotin	1:400	2h, 25°C	Jackson ImmunoResearch
Streptavidin		Dylight 405	1:400	1h, 25°C	Life Technologies

Table 1. Primary and secondary antibodies used in the Experiment 2.

2.4 CONFOCAL ANALYSES

2.4.1 Neurochemical phenotype of GAD67-GFP interneurons

Sections double-labeled for GFP and interneuronal subpopulation markers (PV, CB, CR) were observed under a confocal microscope (Leica TCS-SPE) using a 40x objective. Z-series of optical sections (0.2 μm apart) were obtained using sequential

scanning mode and stacks were then processed using FIJI (ImageJ, NIH). Fifty GAD67-GFP-expressing neurons within the infralimbic and 50 within the prelimbic cortex were randomly selected from each animal and for each double immunostaining to determine the co-expression of GAD67-GFP and each marker. Percentages of co-localization were determined for each animal and mean ± SEM were calculated.

2.4.2 Morphological study

Dendritic arborization was studied using confocal microscopy (Leica TCS-SPE) as previously described (Gilabert-Juan et al., 2011; Gómez-Climent et al., 2011). Z-series of optical sections (0.2 μm apart) covering the whole dendritic tree of selected interneurons were obtained using the sequential scanning mode and a 63x oil objective. Six animals of each genotype were used to perform the analysis. From each animal, six GAD67-GFP expressing neurons were selected from the prelimbic cortex and six from the infralimbic cortex with the soma located in layers II-III. In order to be analyzed, GFP-expressing cells had to fulfill the following features: (1) the cell must not show any truncated dendrites; (2) the dendritic arbor of the cell must show at least a process longer than 150 μm; and (3) the soma must be located at least 30 μm deep from the surface of the tissue. The stacks obtained were then processed using FIJI/ImageJ Software (Schindelin et al., 2012) to obtain 3D reconstructions. Neurons with highly overlapping dendritic tress were excluded from the analyses. The ‘‘Simple neurite tracer’’ tool was used to trace the dendrites of interest and to avoid dendrites from surrounding neurons. Axons were also excluded by their more reduced thickness. The degree of dendritic arborization was analyzed using a procedure for deriving the Sholl profile (Gutierrez and Davies, 2007). The Sholl analysis consists on the measure of the number of intersections of the dendrites with spheres of increasing radius centered in the soma (Sholl, 1953). For each experimental group, mean ± SEM was determined and the resulting values were analyzed by one-way analyses of variance (ANOVA), with the number of animals as the ‘‘n.’’ Previous Kolmogorov-Smirnov and Levene tests were performed to analyze the normality and homogeneity of variances, respectively. Significant differences were further analyzed by Bonferroni post-hoc test, using the IBM SPSS statistics software (version 19).

2.4.3 Analysis of the inhibitory perisomatic puncta

The density of perisomatic puncta on pyramidal neurons was analyzed in the layers III and V of the prelimbic and infralimbic cortices using a confocal microscope (Olympus Fluoview FV 10i) and a 60x oil objective. Six animals *per* group were used for the study and 12 neurons in each of the prefrontocortical regions were counted *per* animal. The analyses were performed in sections corresponding to Bregma 3.08 mm/Interneural 6.88mm and to Bregma - 0.22 mm/Interneural 3.58 mm according to a mouse brain atlas (Paxinos and Franklin, 2008). Confocal z-stacks covering the whole depth of the sections were taken with 1 μm step size and only subsets of confocal planes with the optimal penetration level for each antibody were selected. Images were processed using ImageJ software as follows (Guirado et al., 2018): the background was subtracted with rolling value of 50, converted to 8-bit deep images and binarized using a determined threshold value. This value depended on the marker and the area analyzed and was kept the same for all images with the same marker and area. Then, the images were processed with a blur filter to reduce noise and separate closely apposed puncta. Finally, values of puncta density for PV and SYN were obtained from each CaMKII-α expressing pyramidal neuron soma analyzed and expressed as number of puncta *per* micron of soma perimeter. For each experimental group, mean ± SEM was determined and the resulting values were analyzed by one-way ANOVA, with the number of animals as the ‘‘n.’’ Previous Kolmogorov-Smirnov and Levene tests were performed to analyze the normality and homogeneity of variances, respectively. Significant differences were further analyzed by Tukey HSD or Games-Howell post-hoc test depending on the results of the homogeneity test for variances.

EXPERIMENT 3. IMPACT OF A CHRONIC TREATMENT WITH ERYTHROPOIETIN ON THE STRUCTURE AND CONNECTIVITY OF INHIBITORY NEURONS OF THE HIPPOCAMPAL CA1 REGION, THE EXCITATORY/INHIBITORY BALANCE AND THE EXPRESSION OF MOLECULES RELATED TO INTERNEURONAL PLASTICITY.

3.1 ANIMALS

Twelve transgenic young (28 days old at the start of the experiment) male mice, [GIN, (GFP-expressing Inhibitory Neurons), Tg (GadGFP) 45,704Swn] (Jackson laboratories, Bar Harbor, Maine, USA) were used for all the experiments in this study. These mice express the enhanced green fluorescent protein (EGFP) under the control of the glutamic acid decarboxylase (GAD) gene in a subpopulation of interneurons (Oliva et al., 2000). Mice were housed in groups of 3-4 animals *per* cage under standard conditions of temperature and humidity, with food and water *ad libitum*, and a normal light/dark cycle. All animal experimentation was conducted in accordance with the Directive 2010/63/EU of the European Parliament and of the Council of 22 September 2010 on the protection of animals used for scientific purposes and was approved by the Committee on Bioethics of the Universitat de València. Every effort was made to minimize the number of animals used and their suffering.

3.2 CHRONIC ERYTHROPOIETIN TREATMENT

Mice were injected intraperitoneally with EPO (Recombinant human EPO, Abcam, 5 IU/g in 0.01 ml) or placebo (distilled water, 0.01 ml/g) every other day for three weeks (11 injections in total). Mice were weighed before each injection to receive the appropriate dose. During all the procedures, the experimenter was blind to group assignment.

3.3 PERFUSION AND MICROTOMY TECHNIQUES

Twenty-four hours after the last injection, mice were deeply anesthetized with sodium pentobarbital (150 mg/kg) and transcardially perfused, first with saline and then with 4% paraformaldehyde in PB 0.1 M, pH 7.4 solution during 25 minutes. Brains were

extracted from the skull and their hemispheres separated. The right hemisphere, destined to neuronal structural analysis, was cut in 100-µm-thick coronal sections with a vibratome (Leica VT 1000E), collected in three subseries and stored at 4°C in PB 0.1 M with sodium azide (0.05%). The left hemisphere, destined to immunohistochemical analyses, was cryoprotected with 30% sucrose in PB 0.1 M for 48 h and cut afterwards in 50-µm-thick coronal sections using a sliding microtome (LEICA SM2000R). Slices were collected in 6 subseries and stored at -20°C in a cryoprotective solution (30% glycerol, 30% ethylene glycol in PB 0.1 M).

3.4 IMMUNOHISTOCHEMICAL ASSAYS

3.4.1 Immunohistochemistry for conventional light microscopy

In order to analyze the expression of polySia-NCAM in the CA1 region of the hippocampus, sections were processed "free-floating" for immunohistochemistry using the avidin-biotin-peroxidase (ABC) method. After several washes with PBS, sections were first incubated for 1 min in an antigen unmasking solution (0.01 M citrate buffer, pH 6) at 100°C. After cooling down the sections to room temperature, they were incubated with 10% methanol and 3% H_2O_2 in PBS for 10 min to block endogenous peroxidase activity. After this, sections were washed and treated for 1 h with 10% NDS (Jackson ImmunoResearch Laboratories) and were incubated for 48 h at 4°C with monoclonal mouse IgM anti-polySia-NCAM antibody (1:1400, DSHB). After washing, sections were incubated for 2 h (at room temperature) with a secondary biotinylated antibody: donkey anti-mouse IgM (1:400, Jackson ImmunoResearch), followed by an avidin-biotin-peroxidase complex (ABC; Vector Laboratories) for 45 minutes. Color development was achieved by incubating with 0,05% 3,3'-diamino-benzidine tetrahydrochloride (DAB; Sigma–Aldrich) and 0.033% H_2O_2 in PBS for 4 min. PBS containing 0.2% Triton X-100 and 5% NDS was used for primary and secondary antibodies dilution. Finally, sections were mounted on slides, dried for 1 day at room temperature, dehydrated with ascending alcohols and rinsed in xylene. After this, sections were coverslipped using Eukitt mounting medium (PANREAC). All sections passed through all procedures simultaneously in order to minimize any difference from the immunohistochemical staining itself.

3.4.2 Immunohistochemistry for confocal microscopy

For fluorescence immunohistochemistry, tissue was processed as described above but omitting the endogenous peroxidase block. Sections were incubated for 48 h at 4°C with the appropriate primary antibody or antibody cocktail **(Table 2)**. After washing, sections were incubated for 2 h at room temperature with different secondary antibody cocktails **(Table 2)**. Finally, sections were washed in PB 0.1 M, mounted on slides and coverslipped using fluorescence mounting medium (Dako Diagnósticos).

Anti	Host	Isotype/Label	Dilution	Incubation	Company
Primary antibodies					
GFP	Chicken	Ig Y	1:1000	48h, 4ºC	Abcam
PV	Guinea Pig	Ig G	1:2000	48h, 4ºC	Synaptic Systems
CaMKII-α	Mouse	Ig G1	1:500	48h, 4ºC	Abcam
CB1r	Rabbit	Ig G	1:1000	48h, 4ºC	Synaptic Systems
Wisteria Floribunda Lectin Biotin			1:200	48h, 4ºC	Sigma
VGLUT1	Guinea Pig	Ig G	1:2000	48h, 4ºC	Millipore
VGAT	Rabbit	Ig G	1:1000	48h, 4ºC	Synaptic Systems
PolySia-NCAM	Mouse	Ig M	1:1400	48h, 4ºC	DSHB
Secondary antibodies					
Chicken IgY	Goat	Alexa 488	1:400	2h, 25°C	Life Technologies
Guinea pig IgG	Goat	Alexa 555	1:400	2h, 25°C	Life Technologies
Mouse IgG1	Goat	Alexa 555	1:400	2h, 25°C	Life Technologies
Guinea Pig IgG	Goat	DyLight 649	1:400	2h, 25°C	Jackson ImmunoResearch
Rabbit IgG	Donkey	Alexa 647	1:400	2h, 25°C	Molecular Probes
Avidin		Alexa 635	1:400	2h, 25°C	Invitrogen
Rabbit IgG	Goat	Alexa 635	1:400	2h, 25°C	Life Technologies
Mouse IgM	Donkey	Biotin	1:400	2h, 25°C	Jackson ImmunoResearch

Table 2. Primary and secondary antibodies used in the Experiment 3.

3.5 CONFOCAL MICROSCOPY AND STRUCTURAL ANALYSES

All the structural parameters of GAD-EGFP+ and PV+ interneurons were studied using a laser scanning confocal microscope (Leica TCS-SPE) as described before (Gómez-

Climent et al., 2011). The studies were focused in the *stratum oriens* of the hippocampal CA1 region **(Figure 14)**. The majority of GAD-EGFP+ interneurons in this area can be considered O-LM cells, although some HS cells have also their somata located in the *stratum oriens* (Perez-Rando et al., 2017a).

For the study of the dendritic arborization, 6 GAD-EGFP expressing interneurons and 6 PV expressing interneurons *per* animal were randomly selected. Z-series of optical sections (0.8 µm step size; 40x objective) covering the whole dendritic tree of selected interneurons were imaged using the sequential scanning mode. To be suitable for analysis, these interneurons had to fulfill the following features: (1) the cell must not show any truncated dendrites, (2) the dendritic arbor of the cell must show at least a process with a length > 200 µm for the GAD-EGFP interneurons and > 100 µm for the PV+ cells (due to their shorter dendrites in our immunohistochemistry), and (3) the soma must be located at least 30 µm deep from the surface of the tissue. The stacks obtained were then processed using FIJI/ImageJ Software (Schindelin et al., 2012) to obtain 3D reconstructions. Overlapping dendritic trees and axons were excluded from the analysis. Neurons were traced using the "Simple neurite tracer" plugin to analyze their Sholl profile in 3D (Longair et al., 2011). The separation among the spheres of the analysis was set at 20 µm for the GAD-EGFP interneurons and at 10 µm for the PV+ cells. For each animal, mean ± SEM was calculated and statistical analyses were performed using the number of animals as the "n".

For the analysis of dendritic spines, six dendrites from six different GAD-EGFP expressing interneurons *per* animal were randomly selected. A 63x oil immersion objective and a 3.5x additional digital zoom was used to observe the first 150 µm of the dendrite in segments of 50 µm (Z-step size of 0.38 µm). The dendrites had to keep the following criteria to be included in the study: (1) their length should be at least 150 µm, and (2) no other dendrites should be found crossing their trajectory. Data were expressed as the total number of spines in the proximal (0–50 µm), medial (50–100 µm), and distal (100–150 µm) segments of the dendrite, depending on its distance from the soma. The total density of spines (density of spines in the entire length of the segment) was also analyzed. The same analysis was performed taking into account the different

types of dendritic spines, classified manually according to the length of the protrusion and the diameters of their head and neck. Three different categories were established as described before in this hippocampal interneurons (Guirado et al., 2014b): (1) stubby, when the length of the protrusion was < 1.5 µm; (2) mushroom, when a clear head could be observed (maximum diameter of the head should be at least 1.5 times the average length of the neck) and the total length of the protrusion was < 3 µm; and (3) thin, when the length of the protrusion was > 3 µm, or when this length was between 1.5 and 3 µm and a clear head could not be distinguished. For each animal, mean ± SEM was calculated and statistics were performed using the number of animals as the "n".

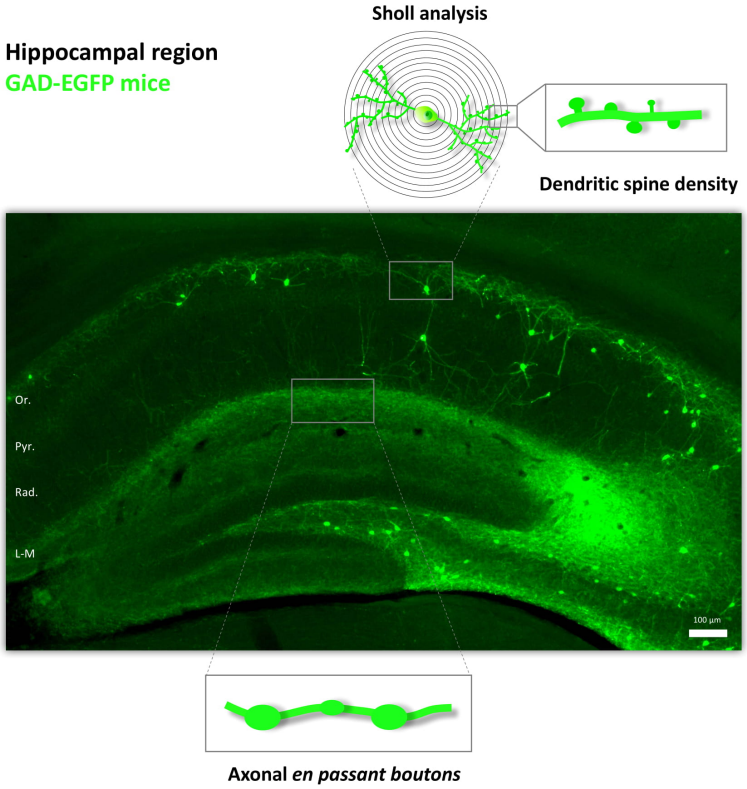

Figure 14: Panoramic microphotograph of the hippocampus in GAD-EGFP mice. The squared regions show the regions of interest for the structural analysis. Schematic drawings of the structures studied in GAD-EGFP interneurons: dendritic tree and spine density (studied in *stratum oriens*) and axonal *en passant boutons* (studied in *stratum lacunosum-moleculare*). Scale bar: 100 µm.

Since most of the EGFP+ somata located in the *stratum oriens* are O-LM interneurons, in order to study their synaptic output we also analyzed the plexus of EGFP+ axons present in the *stratum lacunosum-moleculare* of the CA1 region **(Figure 14)**. To study the density of *en passant boutons*, a 63x oil immersion objective with a 2.5x digital zoom was used. Six axonal segments, measuring at least 30 µm, were chosen randomly *per* animal. In order to avoid an overestimation, the axonal varicosities were only considered when they fulfilled three criteria: (1) they should be at least two times brighter than the axonal backbone; (2) they should be two times wider than the axonal

backbone; and (3) they should not have any crossings from other axons nearby. For each animal, mean ± SEM was calculated and statistics were performed using the number of animals as the "n".

3.6 ANALYSIS OF THE DENSITY OF VGLUT1 AND VGAT IMMUNOREACTIVE PUNCTA. CALCULATION OF THE E/I RATIO.

The images used for the analysis of the density of neuropil puncta expressing inhibitory (VGAT) or excitatory (VGLUT1) markers were obtained using a laser scanning confocal microscope (Leica TCS SPE). The regions for the analysis were the *strata oriens, pyramidale*, *radiatum* and *lacunosum-moleculare* of the hippocampal CA1 region. Confocal z-stacks covering the whole depth of the sections were taken with 0.38 µm step size (63x oil objective and 2x digital zoom magnification) and only confocal planes with the optimal penetration level for each antibody were selected. On these planes, 16 small squares of the neuropil (336 μm^2) *per* layer and animal were selected for analysis to avoid blood vessels and cell somata. Images were processed using FIJI/ImageJ software as described before (Guirado et al., 2012, 2018): the background was subtracted with rolling value of 50, converted to 8-bit deep images and binarized using a determined threshold value. This value depended on the marker and the area analyzed and was kept the same for all images with the same marker and area. Then, the images were processed with a blur filter to reduce noise and to separate closely apposed puncta. Finally, the number of the resulting dots per layer was automatically counted.

The E/I ratio was calculated as the density of VGLUT1 expressing puncta divided by the density of inhibitory VGAT expressing puncta. For each animal, mean ± SEM was calculated and statistics were performed using the number of animals as the "n".

3.7 ANALYSIS OF PERISOMATIC INHIBITORY PUNCTA ON EXCITATORY NEURONS

The density of puncta expressing PV or CB1r surrounding pyramidal neuron somata (identified by CaMKII-α expression) was analyzed following a previously described protocol (Guirado et al., 2014a). Briefly, 20 CaMKII-α expressing neurons *per* animal located in the pyramidal layer of the CA1 region, were randomly imaged in 3

different sections. Confocal z-stacks covering the whole depth of the neuron somata were taken with 0.38 µm step size using a 63x oil objective with 2x digital zoom magnification (Leica TCS-SPE). Stacks were then processed using FIJI/Image J software. Single confocal planes from each neuron, in which the penetration of each antibody was optimal, were selected. The profile of the soma of these neurons was drawn manually and the selection was enlarged 1.25 µm in order to cover the area that surrounded the somata. A puncta was defined as a structure displaying an area not smaller than 0.15 μm^2 and not larger than 2.5 μm^2 (Di Cristo et al., 2007). The density of puncta (number of puncta *per* micron of soma perimeter) was binarized and analyzed as described above (see "Analysis of the density of VGLUT1 and VGAT"). For each animal, mean ± SEM was calculated and statistics were performed using the number of animals as the "n".

3.8 QUANTIFICATION OF THE NUMBER OF PV-EXPRESSING NEURONS, PNNS, AND THEIR CO-LOCALIZATION

The total number of PV+ neurons, PNNs, and PV+ neurons surrounded by PNNs was estimated in the CA1 region. Starting at the Bregma -1.34mm level, 3 consecutive hippocampi were analyzed and all labeled cells covering the area of interest were counted. The image stacks used for the analysis were obtained with a laser scanning confocal microscope (Leica TCS SPE) and processed afterward using FIJI/ImageJ software. The results were expressed as a density using the area of the image (30485 μm^2). For each animal, mean ± SEM was calculated and statistics were performed using the number of animals as the "n".

3.9 QUANTIFICATION OF POLYSIA-NCAM IMMUNOREACTIVITY

In the CA1 region, the immunoreactivity of polySia-NCAM was analyzed in each of its different layers. One section *per* animal was selected at the Bregma -1.94 mm level (Paxinos and Franklin, 2008). Sections were examined with an Olympus CX41 microscope under bright-field illumination, homogeneously lighted and digitized using a CCD camera. Photographs of the different layers were taken at 20x magnification. Grey levels were converted to optical densities using ImageJ software (NIH). For each animal,

mean ± SEM was calculated and statistics were performed using the number of animals as the “n”.

CHAPTER IV
Results

EXPERIMENT 1. EFFECT OF A CHRONIC TREATMENT WITH DIAZEPAM ON THE STRUCTURE OF PYRAMIDAL NEURONS IN THE PREFRONTAL CORTEX.

1.1 Diazepam decreased the dendritic spine density of prefrontocortical pyramidal neurons without affecting the density of *en passant boutons*

After chronic treatment with diazepam (2 mg/kg), we observed a significant decrease (t= −4.209, p= 0.002) in the total density of dendritic spines in the apical dendrites of pyramidal neurons located in layer V of the cingulate cortex **(Figure 15A-C)**. A total of 200 μm length *per* neuron were measured, considering the distance from the soma (0–200 μm).

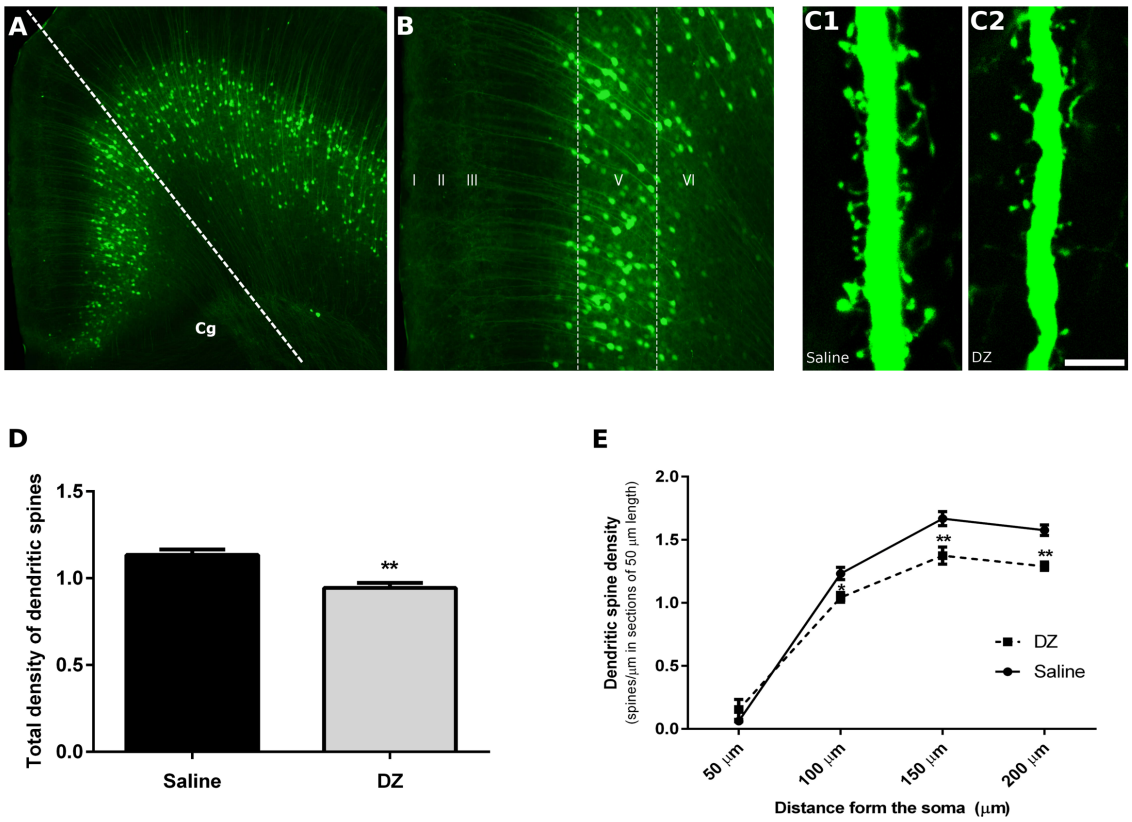

Figure 15: Confocal microscopic analysis of dendritic spine density in pyramidal neurons of the cingulate cortex of Thy1-YFP transgenic mice. A: Panoramic microphotograph of the cingulate cortex. **B:** Detailed of labeled pyramidal neurons in layer V. **C1-2:** 2D projection of 20 focal planes separated from each other by 0.38 microns showing apical dendrites from YFP-expressing pyramidal neurons bearing spines. C1 corresponds to an animal treated with saline and C2 to one treated with diazepam. **D-E:** Graphics showing changes in spine density in apical dendrites of pyramidal neurons after chronic diazepam treatment. Spine density in the total length of the measured dendrite (D) and in the different 50 μm fragments from the soma (E). Unpaired Student's t-test; * 0.05, ** 0.01, ***0.001 for statistically significant values. Scale bar: 160 μm for A, 63 μm for B and 5 μm for C.

The density of dendritic spines was also analyzed specifically in 50 μm segments. After 21 days of diazepam treatment, we did not find significant differences in the dendritic spine density of the proximal segment (0–50 μm: t= 0.586, p= 0.571). However, significant differences were observed in the second (50–100 μm: t= −2.838, p= 0.018), third (100–150 μm: t= −3.351, p= 0.007) and fourth segments (150–200 μm: t= −5.018, p= 0.001) **(Figure 15D-E)**.

We next proceeded to analyze changes in the total density of *en passant boutons* in the axons of inner half of layer I and in upper layer II of the cingulate cortex **(Figure 16A-C)**. Chronic diazepam treatment did not induce changes in the density of *en passant boutons* in the superficial axonal plexus of the cingulate cortex (**Figure 16C**, t= −1.564, p > 0.1).

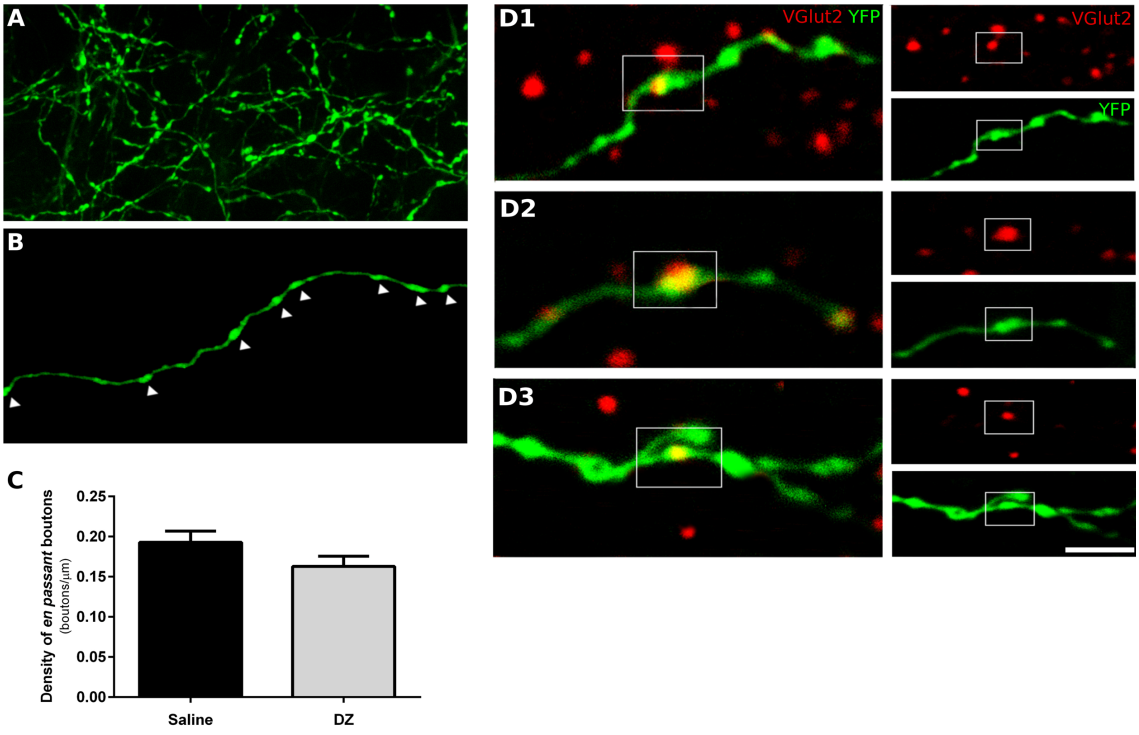

Figure 16: Confocal microscopic analysis of VGLUT2 immunoreactivity and *en passant boutons* in the cingulate cortex. A: Detailed confocal image of the field of *en passant boutons* of deep layer I and superficial layer II of the cingulate cortex. **B:** 2D reconstruction of a single axon displaying *en passant boutons* (arrowheads) in layer I. **C:** Unpaired Student t-test showed no statistically significant differences in the density of *en passant boutons* in the superficial axonal plexus of the cingulate cortex (p > 0.1). **D1-3:** VGLUT2 immunohistochemistry in the cingulate cortex layer I. Note the co-localization between the expression of the vesicular glutamate transporter and *en passant boutons*. Scale bar: 65 μm for A, 7 μm for B, 5 μm for C and D.

1.2 VGLUT2 immunolabeling confirmed the extracortical origin of axonal *en passant boutons* located in layers I-II of the cingulate cortex

Since previous work on these transgenic mice strain has indicated that these axons are likely arising from labeled principal neurons in the basolateral amygdaloid nucleus (Porrero et al., 2010), we performed a VGLUT2 immunostaining in four control animals and analyzed the presence of this vesicular glutamate transporter in the *en passant boutons* of deep layer I and superficial layer II. VGLUT2 is exclusively present in excitatory synapses from extracortical origin (Fremeau et al., 2001). Our analysis confirmed the extracortical origin of these axons and *en passant boutons*: 72% of axons analyzed displayed VGLUT2 immunoreactive boutons (at least one) and 10% of *en passant boutons* present in each axon showed co-localization with VGLUT2 **(Figure 16D)**.

1.3 Anxiety-related behaviors were unaffected after a chronic treatment with diazepam

To test the behavioral effects of the chronic BZ treatment, an open field test was performed 24 h after the last injection. However, chronic treatment with diazepam did not produce significant changes in any of the parameters studied (Total distance, mean speed, total mobile time, total immobile time, line crossings, immobility latency, freezing episodes, entries to periphery or center zone, latency to first entry, periphery time mobile, periphery time immobile, periphery time freezing, center time mobile, center time immobile or center time freezing; $p > 0.1$).

EXPERIMENT 2. EFFECT OF A GENETIC DEPLETION OF THE POLYSIALYLTRANSFERASES ST8SIA2 AND ST8SIA4 ON THE DENDRITIC STRUCTURE AND CONNECTIVITY OF INTERNEURONS IN THE PREFRONTAL CORTEX.

2.1 The neurochemical phenotype of GAD67-GFP interneuron subpopulations was not altered by polyST depletion

In order to understand in which subpopulation of interneurons we performed the analysis, the neurochemical phenotype of GFP-expressing interneurons was studied in the prelimbic and infralimbic cortices. In all transgenic and wildtype mice used in this study GFP expressing neurons were mostly located in layers II, III and upper V, similar to what has been found in a previous study of the frontal motor cortex of GAD67-GFP knock-in mice (Tamamaki et al., 2003). Most of these neurons had multipolar or bipolar morphology. After careful observation of these GFP expressing interneurons in the mPFC of all the mice strains, we have found that none of them displayed degenerative symptoms such as swollen dendrites or axons, or the presence of abnormal nuclei. Interestingly, we could not observe dendritic spines in any of the dendritic arbors of the interneurons analyzed.

The GAD67-GFP expressing neurons in the prelimbic and infralimbic cortices mainly co-expressed PV and CB (44% ± 3.5 and 48.67% ± 3.56, respectively) and at a minor level CR (11.55% ± 1.08; **Figure 17A-D**). Moreover, all the strains of mice analyzed had similar percentages of GAD67-GFP neurons co-expressing the different markers (**Figure 17E**; PV: $F_{(2,3)} = 0.700$, p= 0.563; CR: $F_{(2,3)} = 1.170$, p= 0.424; CB: $F_{(2,3)} = 0.533$, p= 0.634).

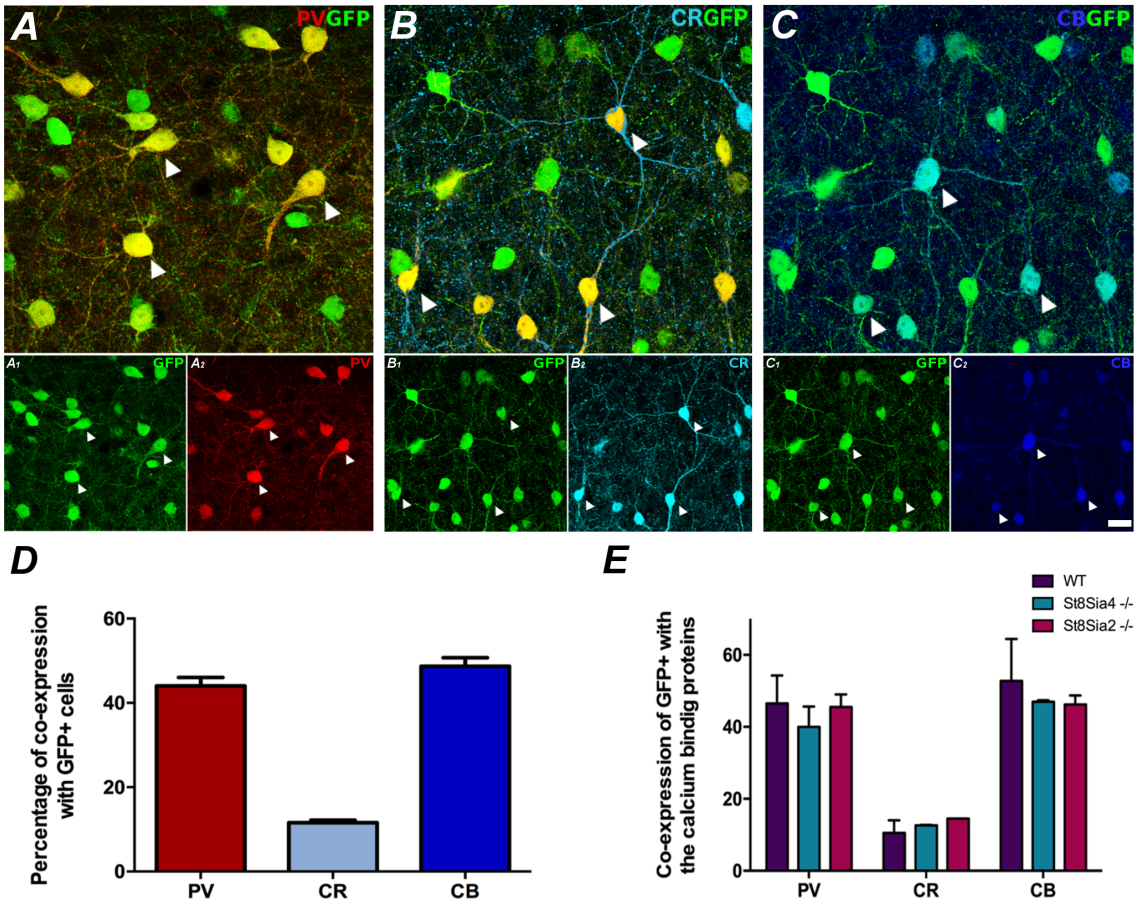

Figure 17: Neurochemical characterization of GAD67-GFP expressing neurons in the mPFC; Co-expression with the different calcium binding proteins. A: Single confocal plane showing the expression of GAD67-GFP with parvalbumin (PV), **(B)** calretinin (CR) and **(C)** calbindin (CB). Arrowheads point to cells co-expressing GAD67-GFP and the different calcium binding proteins. **D:** Graph showing the percentages of GAD67-GFP positive cells expressing these interneuronal markers. **E:** Graph showing the similarity of these percentages of co-localization in the different strains of mice analyzed. Scale bar: 15 μm.

2.2 The genetic depletion of ST8SIA4 affected the dendritic structure of prefrontocortical interneurons

The analysis of dendritic arbor complexity of GAD67-GFP expressing interneurons **(Figures 18A, B_{1-2}, C_{1-3})** revealed a significant decrease in the total number of dendrite intersections in the prelimbic and infralimbic cortex of *St8Sia4*$^{-}$/$^{-}$ mice when compared with their wildtype littermates (**Figures 18D_1, E_1**; $F_{(2,14)}$ = 3.941, p= 0.044 and $F_{(2,17)}$ = 4.312, p= 0.040, respectively). Evaluation of the individual Sholl spheres indicated for the prelimbic cortex a non-significant trend towards a decrease in the 70

μm-radius (**Figure 18D$_2$**; $F_{(2,17)}$ = 3.344, p= 0.069) and for the infralimbic cortex, significant differences in the first 40 microns (**Figure 18E$_2$**; 10 μm-radius, $F_{(2,17)}$ = 5.991, p= 0.009; 20 μm-radius, $F_{(2,17)}$ = 6.862, p= 0.012; 30 μm-radius, $F_{(2,17)}$ = 5.284, p= 0.022; 40 μm-radius, $F_{(2,17)}$ = 5.886, p= 0.014). Compared to *St8Sia2*$^{-}$/$^{-}$, *St8Sia4*$^{-}$/$^{-}$ mice displayed significantly less intersections in the 20 μm-radius of interneurons in the infralimbic cortex ($F_{(2,17)}$ = 6.862, p= 0.031) and a non-significant trend towards a decrease in the 30 and 40 radii ($F_{(2,17)}$ = 5.284, p= 0.093 and $F_{(2,17)}$ = 5.886, p= 0.088, respectively). There were no differences between *St8Sia2*$^{-}$/$^{-}$ and wildtype mice.

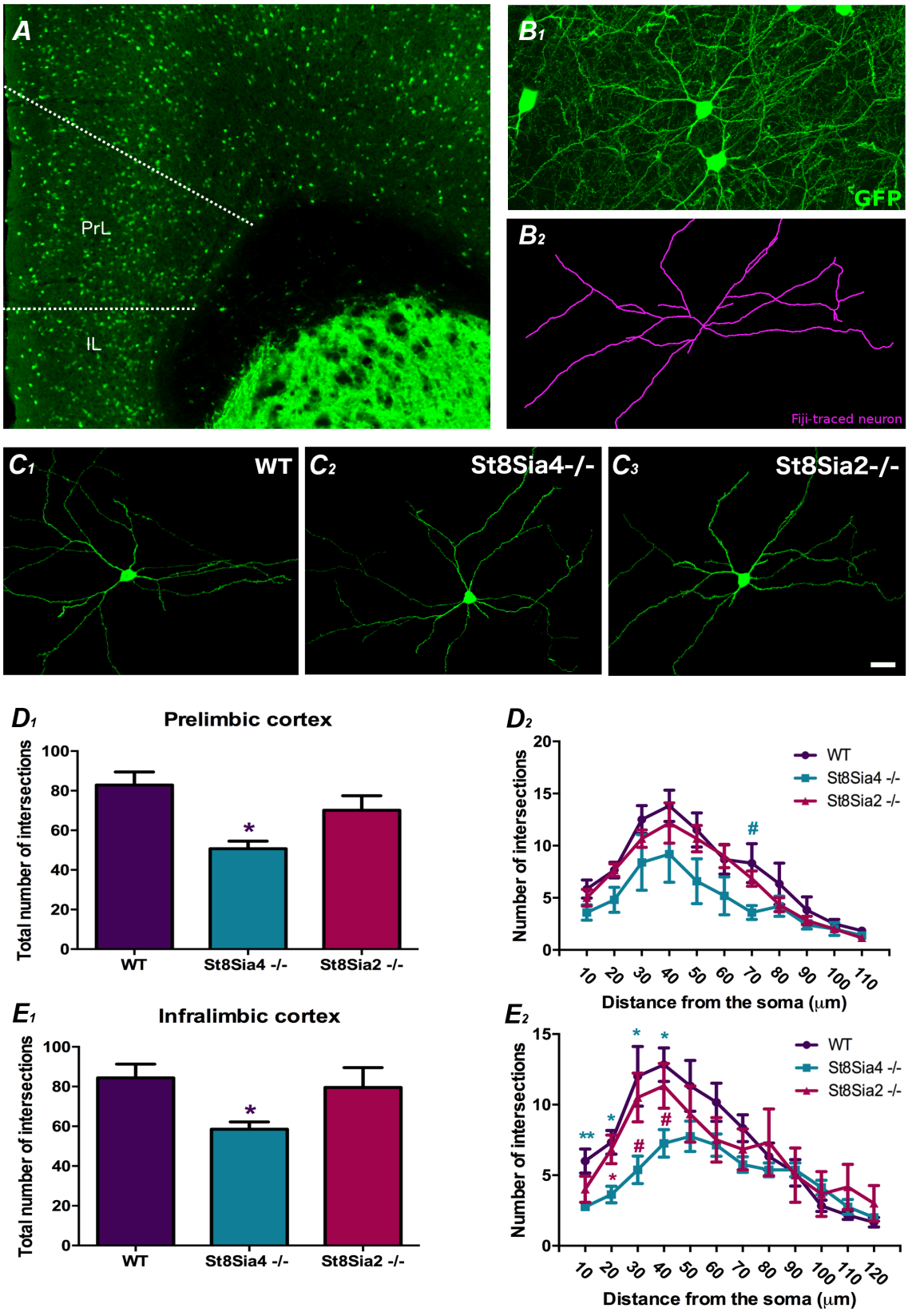
A
PrL
IL
B1
GFP
B2
Fiji-traced neuron
C1
WT
C2
St8Sia4-/-
C3
St8Sia2-/-
D1
Prelimbic cortex
Total number of intersections
WT
St8Sia4 -/-
St8Sia2 -/-
D2
Number of intersections
Distance from the soma (μm)
E1
Infralimbic cortex
E2

Figure 18: Analysis of dendritic arborization complexity in GAD67-GFP expressing interneurons in the mPFC. A: Panoramic view of the prelimbic and infralimbic cortices showing the distribution of the GAD67-GFP labeled interneurons. **B:** Higher magnification view of a GAD67-GFP expressing interneuron in green (B1) traced with FIJI software in purple (B2) for the study dendritic arborization (automated Sholl analysis). **C1–3:** 3D reconstructions of GAD67-GFP expressing interneurons from wildtype, *St8Sia4*$^{-}$/$^{-}$ and *St8Sia2*$^{-}$/$^{-}$ mice. **D1,E1:** Graphs showing statistically significant decreases in the total number of intersections in the *St8Sia4*$^{-}$/$^{-}$ strain compared with wildtypes in the prelimbic and infralimbic cortices. **D2,E2:** Graphs indicating that in the infralimbic cortex, the *St8Sia4*$^{-}$/$^{-}$ group also exhibits a significant decrease in the number of dendrite intersections analyzed with concentric spheres of 10 μm compared with both wildtypes and *St8Sia2*$^{-}$/$^{-}$ mice. No significant differences can be found in this parameter in the prelimbic cortex. One-way analyses of variance (ANOVA); #0.1 > p > 0.05 for non-significant trends and * 0.05, ** 0.01, ***0.001 for statistically significant values. Scale bar: 100 μm for A and 15 μm for B and C

2.3 The genetic depletion of either ST8SIA2 or ST8SIA4 altered the density of perisomatic inhibitory puncta on pyramidal neurons of the mPFC

The study of the PV+ puncta on the perisomatic region of prefrontocortical pyramidal neurons revealed significant decreases in both knockout strains when compared to wildtype mice **(Figures 19A$_{1–5}$, B$_{1–5}$, C$_{1–5}$)**. In the prelimbic cortex of *St8Sia2*$^{-}$/$^{-}$ mice, the density of PV+ puncta was significantly lower (**Figure 19D**; $F_{(2,15)}$ = 2.309, p= 0.033) and that of puncta co-expressing PV and SYN showed a non-significant trend towards a decrease ($F_{(2,15)}$ = 1.722, p= 0.061). There was also a non-significant trend towards a decrease in the density of PV+/SYN- ($F_{(2,15)}$ = 4.177, p= 0.086). In the infralimbic cortex of *St8Sia4*$^{-}$/$^{-}$ mice we observed significantly lower densities of PV+ (**Figure 19E**; $F_{(2,16)}$ = 9.634, p= 0.004) and PV+/SYN+ ($F_{(2,15)}$ = 6.369, p= 0.007) puncta. Additionally, in this region *St8Sia2*$^{-}$/$^{-}$ mice showed a non-significant trend towards a decrease in PV+ puncta ($F_{(2,16)}$ = 9.634, p= 0.088).

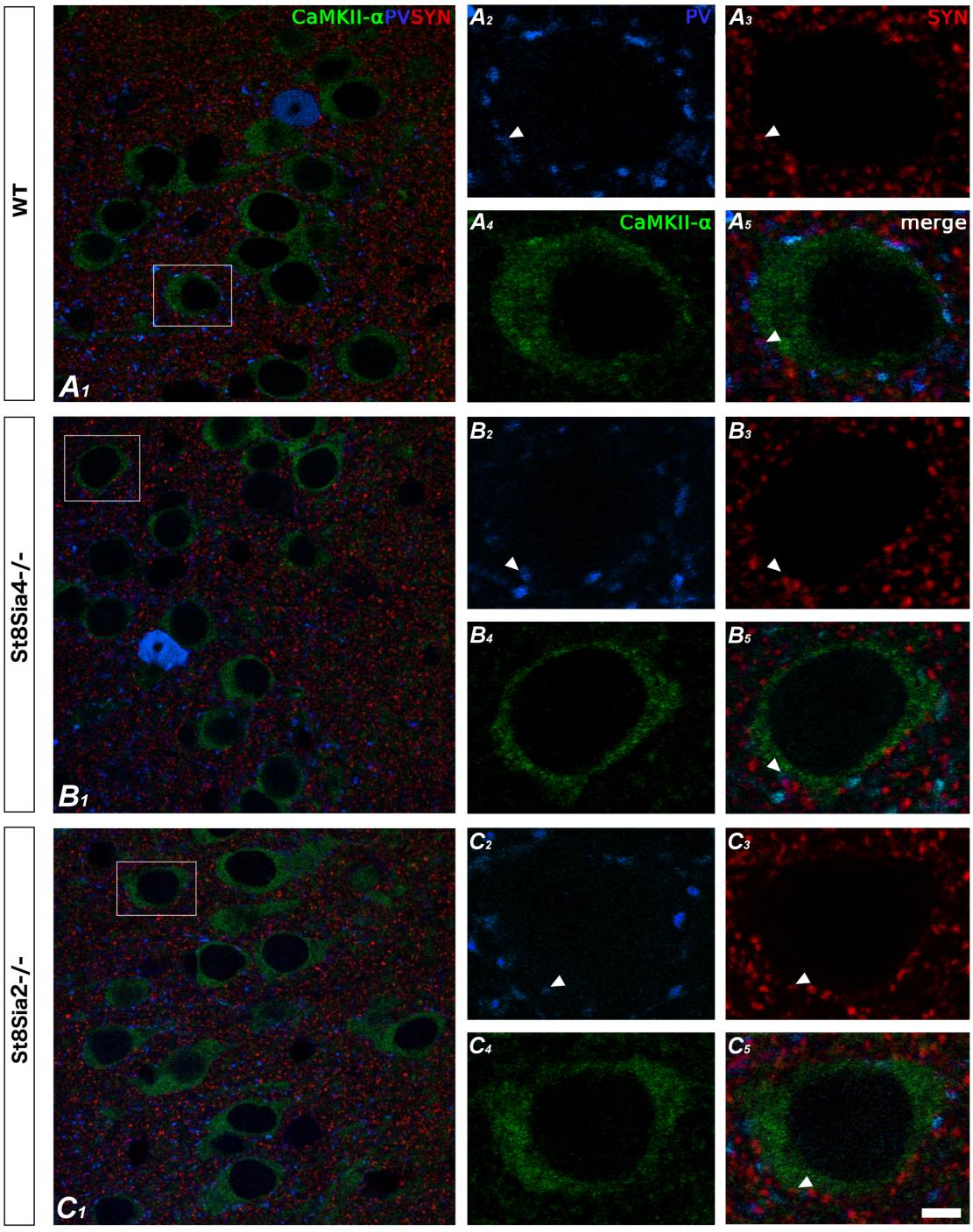
WT
St8Sia4-/-
St8Sia2-/-
CaMKII-αPVSYN
A1
A2 PV
A3 SYN
A4 CaMKII-α
A5 merge
B1
B2
B3
B4
B5
C1
C2
C3
C4
C5

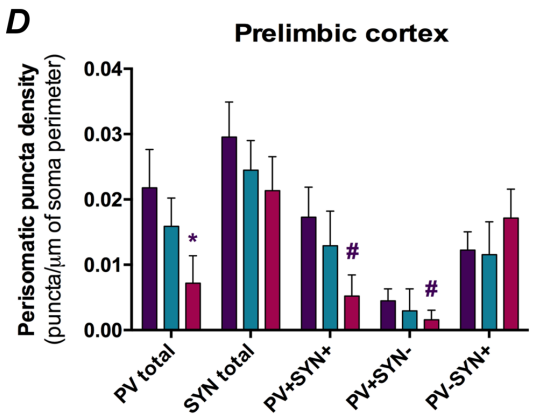
D
Prelimbic cortex
Perisomatic puncta density
(puncta/μm of soma perimeter)
0.04
0.03
0.02
0.01
0.00
*
#
#
PV total
SYN total
PV+SYN+
PV+SYN-
PV-SYN+

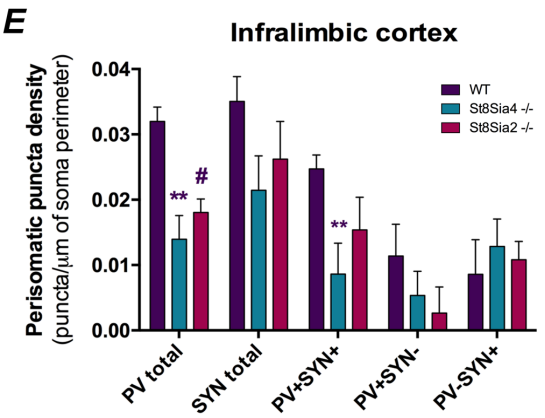
E
Infralimbic cortex
Perisomatic puncta density
(puncta/μm of soma perimeter)
0.04
0.03
0.02
0.01
0.00
WT
St8Sia4 -/-
St8Sia2 -/-
**
#
**
PV total
SYN total
PV+SYN+
PV+SYN-
PV-SYN+

Figure 19: Confocal microscopic analysis of PV and SYN immunoreactive puncta surrounding CaMKII-α excitatory cell somata in the prelimbic and infralimbic cortices. **$A_{1–5}$, $B_{1–5}$, $C_{1–5}$:** Single confocal planes of pyramidal neurons somata (immunolabeled for CaMKII-α, green) showing changes in the perisomatic density of PV (blue) and SYN (red) immunoreactive puncta in the different strains of mice analyzed. Arrowheads indicate the co-localization between PV and SYN. **D:** In the prelimbic cortex, graph shows a significant decrease in the density of PV expressing puncta in the *St8Sia2*$^{-}$/$^{-}$ mice when compared with wildtypes. **E:** In the infralimbic cortex, the graph shows that *St8Sia4*$^{-}$/$^{-}$ mice have a decrease in the density of puncta expressing PV and of that co-expressing with PV and SYN. One-way analyses of variance (ANOVA); #0.1 > p > 0.05 for non-significant trends and * 0.05, ** 0.01, ***0.001 for statistically significant values. Scale bar: 10 μm for A1, B1 and C1 and 5 μm for A2–5, B2–5 and C2–5.

EXPERIMENT 3. IMPACT OF A CHRONIC TREATMENT WITH ERYTHROPOIETIN ON THE STRUCTURE AND CONNECTIVITY OF INHIBITORY NEURONS OF THE HIPPOCAMPAL CA1 REGION, THE EXCITATORY/INHIBITORY BALANCE AND THE EXPRESSION OF MOLECULES RELATED TO INTERNEURONAL PLASTICITY.

3.1 Chronic EPO treatment decreased the dendritic complexity and spine density of hippocampal interneurons

We evaluated structural changes in two subpopulations of inhibitory neurons in the *stratum oriens* of the CA1 after chronic treatment with EPO: i) the GAD-EGFP positive interneurons, which mainly correspond to somatostatin expressing O-LM cells (Perez-Rando et al., 2017a) and ii) PV expressing cells. Automated Sholl analysis revealed a reduction in dendritic arborization in both subpopulations after chronic treatment with EPO **(Figure 20)**. Regarding the GAD-EGFP subpopulation **(Figure 20A$_{1-2}$)**, these interneurons exhibit a trend towards a decrease in the total number of dendritic intersections after EPO treatment (**Figure 20C**; t= 2.197; p= 0.053). Considering the number of intersections in the different Sholl spheres, we found statistically significant decreases in the first 80 µm of dendrite length **(Figure 20D)**: 40 µm-radius (t= 2.595; p= 0.027), 60 µm-radius (t= 2.580; p= 0.027) and 80 µm-radius (t= 3.131; p= 0.011). The Sholl analysis in the PV expressing interneurons **(Figure 20B$_{1-2}$)** revealed a significant reduction in the total number of intersections in EPO treated mice (**Figure 20E**; t= 2.458; p= 0.34) and specific reductions of intersections in Sholl spheres in the first 80 µm **(Figure 20F)**: 40 µm-radius (t= 1.910; p= 0.085), 60 µm-radius (t= 2.721; p= 0.026), 70 µm-radius (t= 2.728; p= 0.021) and 80 µm-radius (t= 2.383; p= 0.038).

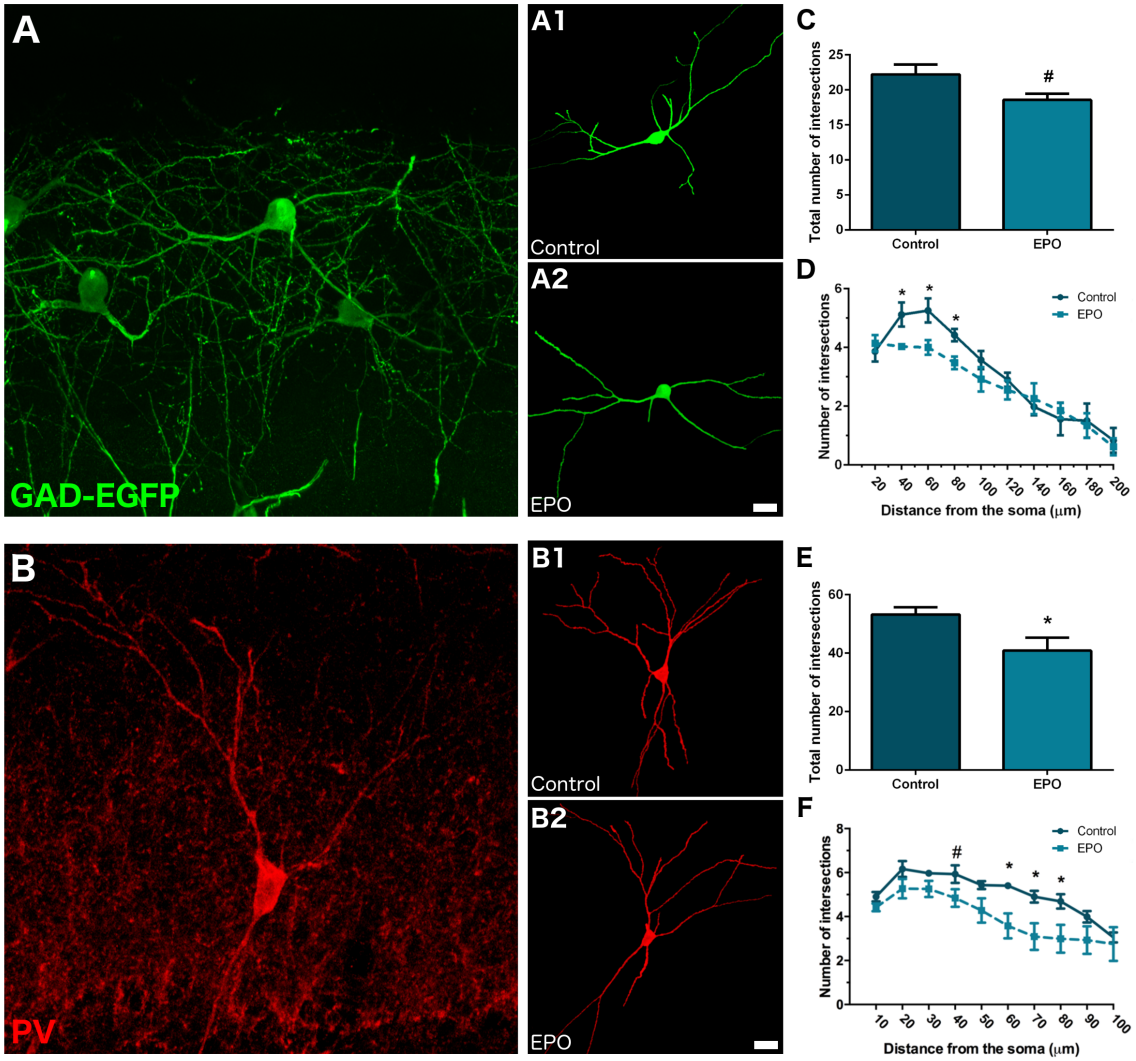

Figure 20: Structural Sholl analysis of GAD-EGFP and PV expressing interneurons in the CA1 region of hippocampus after chronic treatment with EPO. A: Z-stack confocal view showing the presence of GAD-EGFP positive interneurons located in the *stratum oriens* of the CA1 region. **$A_{1\text{-}2}$:** Representative 3D reconstructions of the dendritic arbor of GAD-EGFP interneurons in the control (A1) and EPO group (A2). **B:** Z-stack confocal view showing the presence of PV positive interneurons located in the *stratum oriens* of the CA1 region. **$B_{1\text{-}2}$:** 3D reconstructions of the dendritic arborization of PV interneurons in the control (B1) and EPO treated mice (B2). **C-D:** Graphs corresponding to GAD-EGFP positive cells, show the total number of intersections in the first 200 µm (C) and the number of intersections as a function of distance from the soma with concentric spheres of 20 µm radius increments (D). **E-F:** Graphs show the total number of intersections in the first 100 µm (E) and the number of intersections as a function of distance from the soma with concentric spheres of 10 µm radius increments (F) for the PV expressing interneurons. Unpaired Student's t-test; #0.1 > p > 0.05 for non-significant trends and * 0.05, ** 0.01, ***0.001 for statistically significant values. Scale bar: 6.5 µm for A and B, 20 µm for A1-A2 and B1-B2.

Next, we performed an analysis of dendritic spine density. Due to parvalbumin neurons do not exhibit dendritic spines, the analysis was only performed in GAD-EGFP subpopulation, which were characterized by presenting these protrusions in their dendrites (Gómez-Climent et al., 2011) **(Figure 21A-C)**. The results showed a significant

decrease when considering the whole length of the dendrites (**Figure 21D**; t= 2.565; p= 0.028). When analyzing the different segments of 50 µm, we found that this decrease was significant in the most distal segment of the dendrite, at 150 µm (**Figure 21E**; t= 3.991; p= 0.003). An analysis of dendritic spine morphology was performed taking into account three spine types **(Figure 22)**: mushroom, stubby and thin. The results showed that the decrease in the dendritic spine density was mainly due to a decrease in the density of mushroom spines in the total length of the dendrites (t= 3.055; p= 0.012) and in the more distal segments: 100 µm (t= 2.024; p= 0.070) and 150 µm (t= 3.085; p= 0.012). A significant decrease was also found in the density of stubby spines in the distal segment: 150 µm (t= 2.914; p= 0.015).

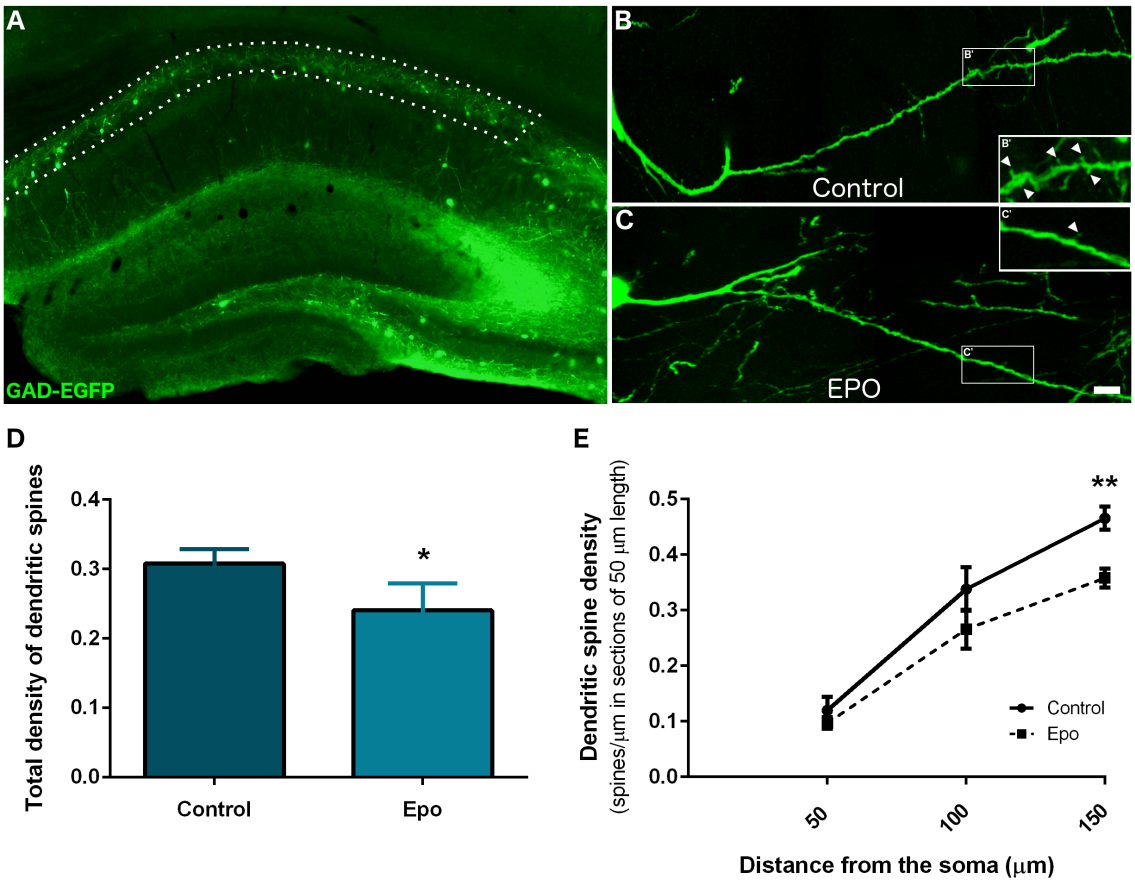

Figure 21: Analysis of the dendritic spine density in GAD-EGFP-expressing interneurons of the CA1 region after chronic treatment with EPO. A: Panoramic confocal view of the hippocampus showing the distribution of GAD-EGFP neurons with a detailed area of interest, the *oriens* layer. **B-C:** Representative sections of spiny dendrites corresponding to control (B) and EPO treated mice (C). In the amplifications (B' and C'), dendritic spines are pointed by arrowheads. **D-E:** Graphs showing the total density of dendritic spines corresponding to the first 150 µm from the soma (D) and the density of dendritic spines in the three segments stablished (50 µm, 100 µm and 150 µm), (E). Unpaired Student's t-test; * 0.05, ** 0.01, ***0.001 for statistically significant values. Scale bar: 75 µm for A, 5 µm for B and C.

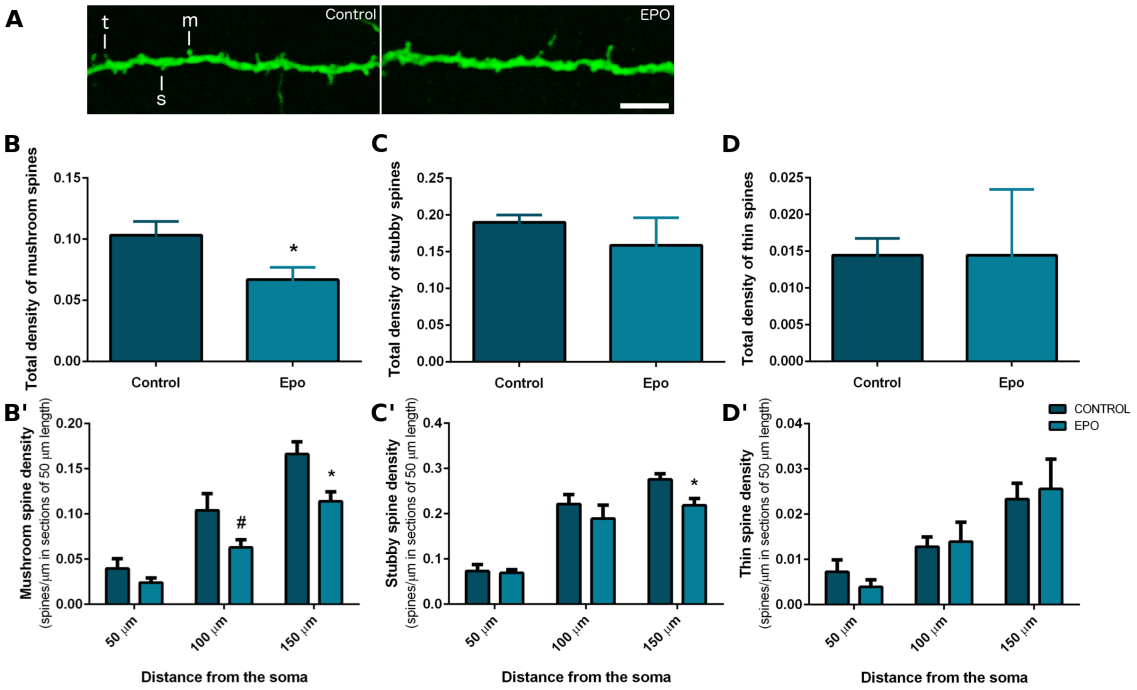

Figure 22: Analysis of the different types of dendritic spines corresponding to GAD-EGFP-expressing interneurons after chronic treatment with EPO. A: Segments of different spinous dendrites of EGFP-expressing cells from control and EPO treated mice. Lines indicate the different types of spines considered: mushroom (m), stubby (s) and thin (t). **B-D:** Graphs showing the total spine density in the first 150 µm from the soma for the mushroom (B), stubby (C), and thin spine type (D). **B'-D':** Graphs showing the differences in dendritic spine density in segments of 50 µm from the soma corresponding to mushroom (B'), stubby (C') and thin spine type (D'). Unpaired Student's t-test; #0.1 > p > 0.05 for non-significant trends and * 0.05, ** 0.01, ***0.001 for statistically significant values. Scale bar: 5 µm.

As mentioned before, the axon of somatostatin-expressing O-LM cells extends until the *stratum lacunosum-moleculare*, where it heavily ramifies and establishes synaptic contacts with the distal dendritic tuft of pyramidal cells. Thus, in order to see whether EPO treatment induced changes in the axonal projection of O-LM cells, we studied the density of GAD-EGFP positive *en passant* boutons (*EPB*) in the *stratum lacunosum-moleculare* **(Figures 23A-B)**. After a chronic treatment with EPO, we found a tendency towards a decrease (**Figures 23C-D**; t= 1.955; p= 0.079) in the density of these presynaptic specializations.

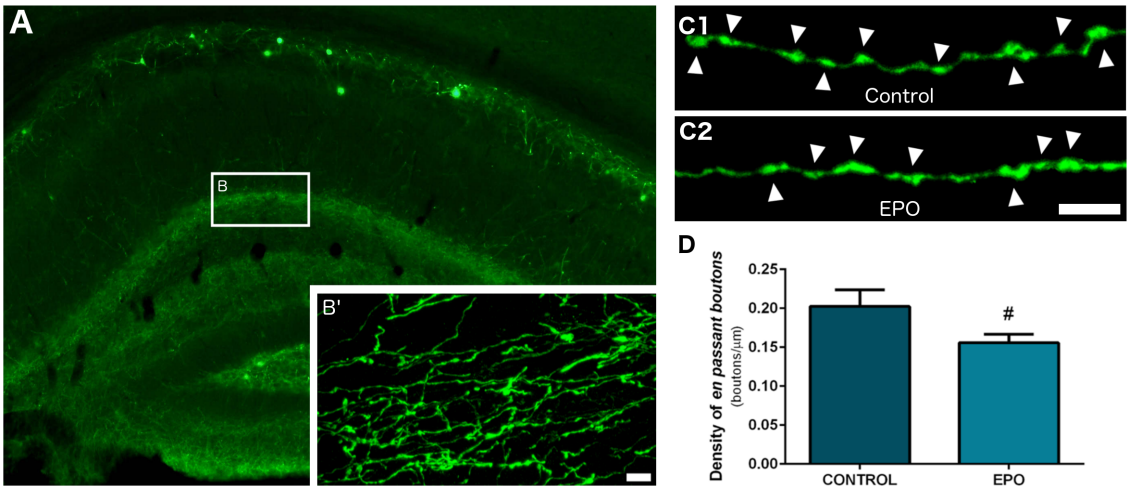

Figure 23: Structural analysis of *en passant boutons* in the CA1 region of the hippocampus after chronic treatment with EPO. A: Panoramic confocal view of the hippocampus showing the distribution of EGFP-expressing interneurons in green. **B:** The squared region was magnified to show more detailed the *en passant boutons (EPB)* located in the *stratum lacunosum-moleculare* (B'). **C1-C2:** Segments of axon somatostatin-expressing interneurons in the *stratum lacunosum-moleculare* showing *en passant boutons* (arrowheads) in the control (C1) and EPO group (C2). **D:** Graph representing the density of *EPBs* (expressed as a boutons *per* micron) in the *stratum lacunosum-moleculare* after the chronic treatment with EPO. Unpaired Student's t-test; #0.1 > p > 0.05 for non-significant trends. Scale bar: 100 µm for A, 50 µm for B and 5 µm for C1-C2.

3.2 The excitatory/inhibitory ratio was not affected by the EPO treatment

To have another readout of the putative alterations in inhibitory networks and the balance of excitatory versus inhibitory neurotransmission, we have studied with immunohistochemistry the expression of the GABA and glutamate vesicular transporters (VGAT and VGLUT1) in the *strata oriens*, *pyramidale*, *radiatum and lacunosum-moleculare* of the hippocampal CA1 **(Figure 24A-D)**. After a chronic treatment with EPO, we did not find significant differences neither in the density of VGLUT1+ and VGAT+ puncta **(Figures 24E$_{1-4}$)** nor in the E/I ratio **(Figures 24F$_{1-4}$)**. Only a tendency towards an increase was found in the density of VGAT+ puncta in the *stratum radiatum* (t= 2.178; p= 0.057).

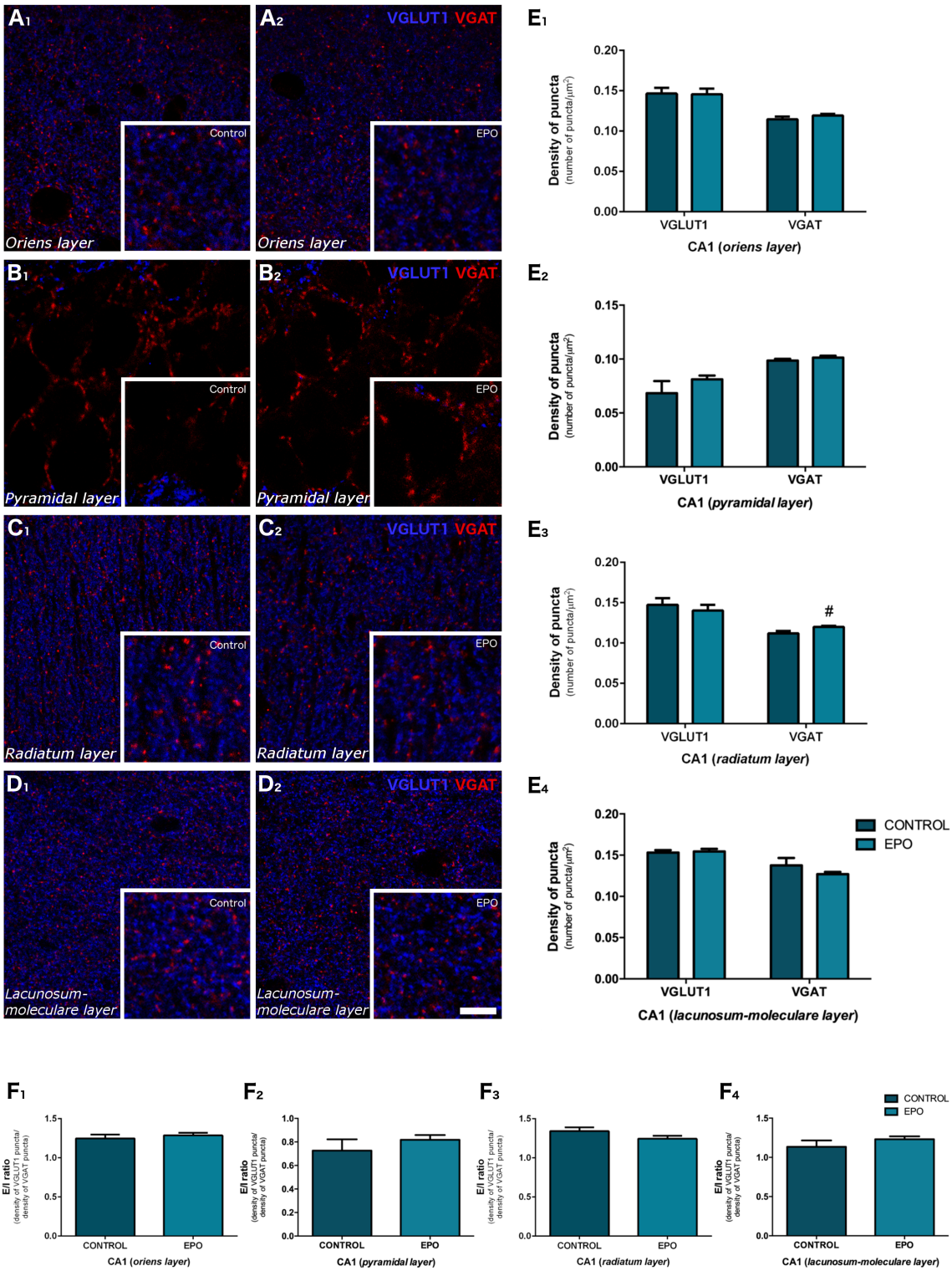

Figure 24: Analysis of the excitatory and inhibitory neurotransmission in the CA1 region of the hippocampus after chronic treatment with EPO. A-D: Single confocal planes showing the expression of VGLUT1 (blue) and VGAT (red) in the different layers of the hippocampal CA1 region: *strata oriens* (A1-A2), *pyramidale* (B1-B2), *radiatum* (C1-C2) and *lacunosum-moleculare* (D1-D2). The squared regions were magnified to show the VGLUT1 and VGAT immunoreactive puncta in the control (A1-D1) and EPO groups (A2-D2). **E:** Graphs showing the density of puncta expressed as the number of puncta *per* micron. **F:** Graphs showing the E/I ration in the different layers of the CA1 region. Scale bar: 5 µm

3.3 Chronic treatment with EPO decreased the number of inhibitory perisomatic puncta on excitatory neurons

In order to analyze changes in the perisomatic inhibitory input that pyramidal neurons (immunolabeled with CaMKII-α) receive from basket cells we analyzed the density of PV and CB1r immunoreactive puncta around individual principal cells in the *stratum pyramidale* of CA1 **(Figure 25A-D)**. We observed a significant decrease in the density of both types of inhibitory puncta after chronic EPO treatment (**Figure 25E-F**; PV+ puncta: t= 2.367; p= 0.039. CB1r+ puncta: t= 2.243; p= 0.049).

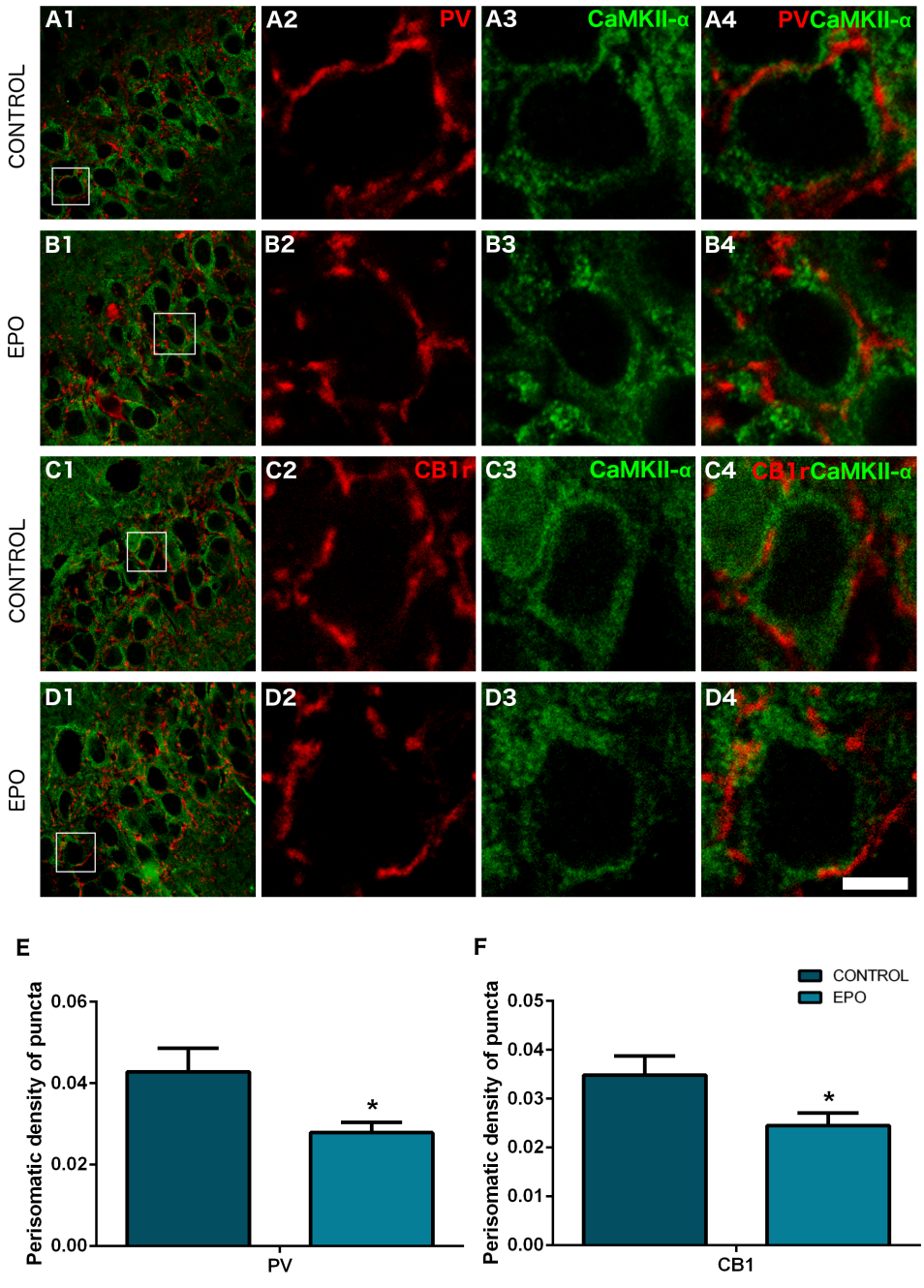

Figure 25: Analysis of the perisomatic inhibitory innervation of excitatory neurons after chronic treatment with EPO. A1-B1: Panoramic confocal view of the CA1 *stratum pyramidale* of the hippocampus showing pyramidal neurons somata, immunolabeled for CaMKII-α (green) and the PV immunoreactive expression (red) in the control (A1) and EPO group (B1). **A2-A4 and B2-B4:** Single confocal planes showing the PV-expressing puncta innervating a CaMKII-α excitatory cell in the control (A2-A4) and EPO group (B2-B4). **C1-D1:** Panoramic confocal views of the pyramidal layer in the CA1 region showing CaMKIIα-expressing pyramidal neuron somata (green) and the perisomatic puncta-expressing CB1r (red) after chronic treatment with EPO. **C2-C4 and D2-D4:** Single confocal planes showing the CB1r-expressing puncta surrounding the somata of CaMKII-α excitatory cells in the control (C2-C4) and EPO group (D2-D4). **E-F:** Graphs showing the perisomatic density of puncta expressing two of the main populations of basket cell, PV (E) and CB1r (F) that surround the somata of pyramidal neurons in the CA1 region of the hippocampus. Unpaired Student's t-test; * 0.05, ** 0.01, ***0.001 for statistically significant values. Scale bar: 25 µm for A1-D1 and 5 µm for the single amplifications.

3.4 Chronic EPO treatment altered the expression of plasticity-related structures in interneurons of the hippocampus

Different components of the extracellular matrix can play a role in the remodeling of inhibitory networks observed in our study. Of particular interest are the PNNs, which are abundant around PV-expressing interneurons. In the present experiment, we analyzed the density of PV+ interneurons, PNNs and their co-localization in the CA1 region **(Figure 26A-C)**. Animals treated with EPO displayed a significant increase in the number of PNNs when compared with control mice (**Figure 26D**; t= 2.530; p= 0.030). A trend towards an increase was found in the density of PV expressing interneurons surrounded by PNNs (t= 1.921; p= 0.084).

Another structure involved in different plasticity-related processes, mainly those associated to interneurons, is polySia. Densitometric analysis of polySia-NCAM expression was performed in the different layers of the CA1 region **(Figure 27)**. Significant increases were found in the *strata oriens* (t= 2.602; p= 0.032), *radiatum* (t= 2.782; p= 0.024) and *lacunosum-moleculare* (t= 2.818; p= 0.023) in the EPO group.

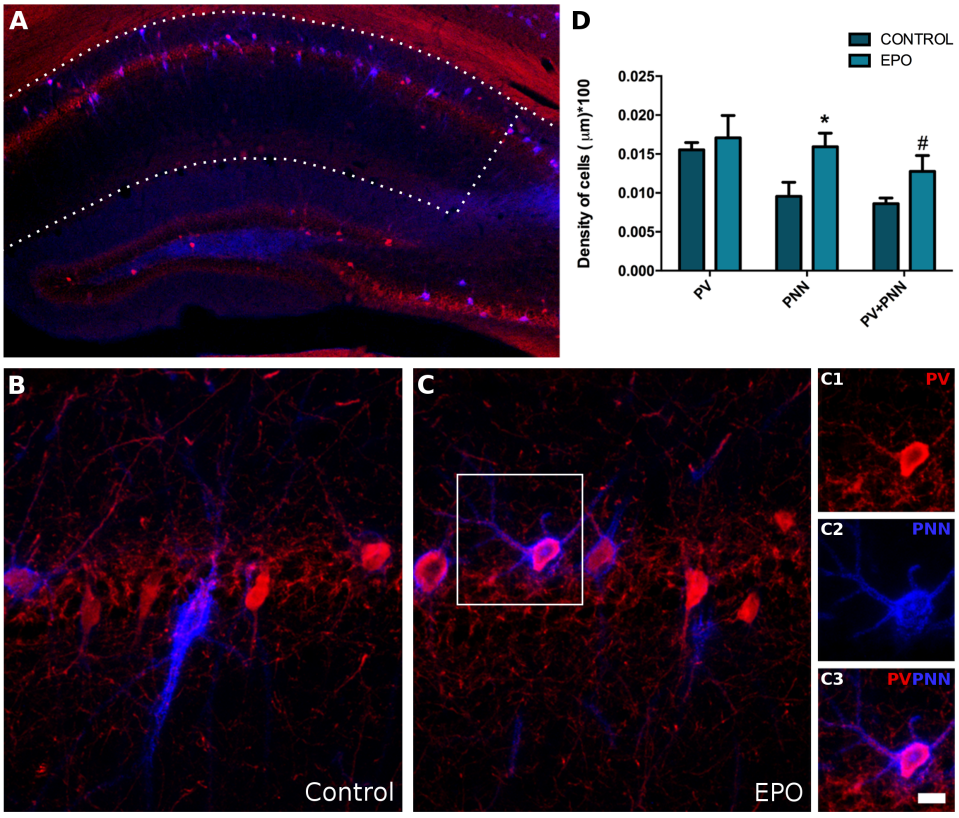

Figure 26: Expression of PV, PNNs and their co-localization after chronic treatment with EPO. A: Panoramic confocal plane showing the distribution of PV (red) and PNNs (blue) in the CA1 region of the hippocampus. **B-C**: Amplified confocal planes, centered in the pyramidal layer, showing the differences in the density of cells expressing both markers and their co-localization between the control (B) and EPO group (C). The squared section was magnified to show a single PV-immunoreactive neuron expressing PNNs (**C1-C3**). **D:** Graph shows the changes in density of PV and PNNs, and in the density of PV-expressing neurons surrounded by PNNs. Unpaired Student's t-test; #0.1 > p > 0.05 for non-significant trends and * 0.05, ** 0.01, ***0.001 for statistically significant values. Scale bar: 100 µm for A, 12.5 µm for B and C, 9 µm for C1-C3.

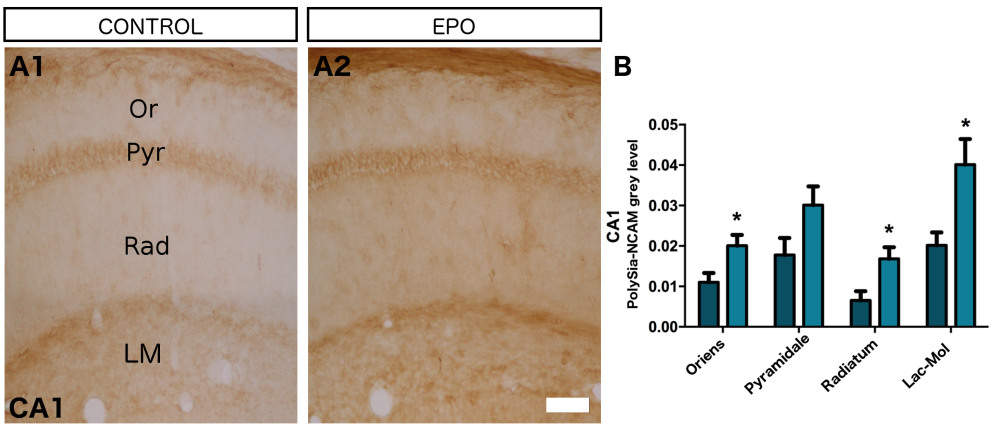

Figure 27: Densitometric analysis of polySia-NCAM expression in the CA1 of the hippocampus after a chronic treatment with EPO. **A:** Microphotographs from conventional light microscope comparing the expression of polySia-NCAM in the different layers of the CA1 region (*strata oriens, pyramidale, radiatum* and *lacunosum-moleculare*) in the control (A1) and EPO group (A2). **B:** Graph representing the changes in the grey level of polySia-NCAM immunoreactivity in the different layers of the CA1. Unpaired Student's t-test; * 0.05, ** 0.01, ***0.001 for statistically significant values. Scale bar: 62.5 µm for A1-A2 images.

CHAPTER V
Discussion

EXPERIMENT 1. EFFECT OF A CHRONIC TREATMENT WITH DIAZEPAM ON THE STRUCTURE OF PYRAMIDAL NEURONS IN THE PREFRONTAL CORTEX.

The present study demonstrates that a chronic treatment of 21 days with diazepam, a BZ that acts as an agonist of $GABA_A$ receptors, affects the dendritic spine density of pyramidal neurons in the cingulate cortex. These changes contrast with the lack of differences regarding changes in the anxiety levels or in the density of YFP-expressing *en passant boutons* in the upper layers of the cingulate cortex. These results indicate that the chronic potentiation of GABAergic synapses can induce the structural remodeling of postsynaptic elements in pyramidal neurons.

1.1. Diazepam decreases the dendritic spine density of prefrontocortical pyramidal neurons without affecting the density of *en passant boutons*

It is well stablished that dendritic spines of excitatory neurons display a baseline level of turnover in normal conditions over a period of days modulated by experience-dependent plasticity (Holtmaat et al., 2005; Tjia et al., 2017). In the present work, we have found that after 21 days of chronic treatment with diazepam, pyramidal neurons from layer V of the cingulate cortex show a marked decrease in the density of dendritic spines in their apical dendrites. Our study is the first evidence, till the date, that an increase in inhibition *per se* acting directly through $GABA_A$ receptors, can also modify the structure of pyramidal neurons of the mPFC. This finding is in accordance with previous reports that have suggested a similar influence of inhibitory neurotransmission, specially in response to estrogens. Estradiol increases pyramidal dendritic spine density by reducing GABA neurotransmission in hippocampal organotypic cultures (Murphy et al., 1998). Similarly, by using an estrogen receptor β ligand, it produces a reduction of dendritic spines on cortical and hippocampal neurons accompanied by an increase of the GABAergic signaling (Tan et al., 2012). More recent studies using transgenic approaches also support an important influence of inhibitory neurotransmission on the structure of pyramidal neurons. Mice with a missense mutation in the $GABA_A$ receptor subunit GABAR1 display a notable increase of spine density in cortical pyramidal cells (Lachance-Touchette et al., 2014). Moreover, mice

lacking GAD67 primarily in PV neurons, which exhibit reduced inhibitory synaptic transmission, display increased spine density in hippocampal CA1 apical dendrites (Fujihara et al., 2015). These data and our present results suggest that changes in inhibition seem to occur before or simultaneously to changes in excitatory connections. In fact, studies of sensory deprivation have found that a removal of visual input correlates with a rapid and lasting reduction in the number of inhibitory cell spines and boutons, which may precede structural changes in excitatory circuitry (Keck et al., 2011).

Further experiments will be necessary to unravel the molecular bases of the paths leading from the action of BZs leading to the structural remodeling of dendritic spines. They may include changes in the structure, composition or physiology of $GABA_A$ receptors, which may in turn affect the response of pyramidal neurons to excitatory input, reflected in changes in the density of dendritic spines.

The structural changes observed in our study are probably not restricted to the prefrontal cortex, since the effect of the BZs should take place in every region displaying $GABA_A$ receptors and deserves further studies, specially in regions involved in the regulation of anxiety. The amygdala has been largely associated with some of the anxiolytic effects that benzodiazepines can produce in the brain (Killcross et al., 1997). Unfortunately, it is impossible to evaluate changes in spine density in the amygdala of this strain of mice, due to the high number of labeled cells in this region (Porrero et al., 2010). However, this area has direct reciprocal connections with the prefrontal cortex, which have been implicated in the control of emotional events (Gold et al., 2016). Previous work on this transgenic mouse strain has indicated that the axons in the inner half of layer I and in upper layer II in the prelimbic and rostral cingulate cortices are likely arising from labeled principal neurons in the basolateral amygdaloid nucleus (Porrero et al., 2010). Our phenotypic analysis has confirmed that most of these axons are from extracortical origin. However, we have not been able to detect changes in their density of *en passant boutons*.

1.2 Anxiety-related behaviors are unaffected after a chronic treatment with diazepam

Although the primary objective of our study was to examine whether BZs affect the morphology of pyramidal neurons, independently of anxiolytic effects, a study of the anxiolytic effects was also performed using two anxiety-related test at the beginning and at the end of the treatment. We have found that the chronic diazepam treatment does not induce significant alterations in the level of anxiety. Although we have used a dose that has anxiolytic rather than sedative effects when administered acutely, it did not induce significant differences in the open field test after chronic administration. These data are in accordance with a previous report that describes the effects of some anxiolytic drugs (including diazepam), which have also failed to find differences or have even found increased anxiety (Prut and Belzung, 2003). It is however possible that other measures of anxiety detected by other tests would have changed with treatment. Moreover, the strain of mice used in our study displayed relatively low levels of anxiety-related behavior (Bouwknecht and Paylor, 2002; Kim et al., 2002). Additionally, the apparent lack of behavioral effects could be due to a "floor" effect, since the treatment was applied to control animals. It is also possible that the open field test by itself had also an impact on the dendritic spine density, which could mask some of the effects of BZ treatment.

Benzodiazepines have been used in clinical practice for over 50 years and they are among the most prescribed drugs due to their anxiolytic, sedative-hypnotic, anticonvulsant and muscle relaxant effects, but little is known about the impact of their chronic administration on neuronal structure. Our study has demonstrated that the chronic intake of benzodiazepines can cause structural alterations, but whether these changes are permanent, whether they can occur after a shorter exposure to BZ or whether they can be reversed after the end of the treatment will be the subject of future studies.

EXPERIMENT 2. EFFECTS OF A GENETIC DEPLETION OF THE POLYSIALYLTRANSFERASES ST8SIA2 AND ST8SIA4 ON THE DENDRITIC STRUCTURE AND CONNECTIVITY OF INTERNEURONS IN THE PREFRONTAL CORTEX.

This study demonstrates that the genetic depletion of ST8SIA4 affects the dendritic structure of prefrontocortical interneurons, whereas loss of either ST8SIA2 or ST8SIA4 causes reductions in the density of the perisomatic inhibitory puncta that a fraction of these cells establishes on pyramidal neurons. These data add to previous experiments demonstrating the impact of these enzymes on developmental migration and final densities of interneurons in the PFC (Kröcher et al., 2014).

2.1 The neurochemical phenotype of interneuron subpopulations is not altered by polyST depletion

A neurochemical phenotype of GAD67-GFP-labeled interneurons in the mPFC was performed in the wildtype and polyST knock-out mice. The phenotype of the GFP+ interneurons analyzed in the mPFC in the present study is consistent with previous data for the motor cortex of GAD67-GFP mice (Tamamaki et al., 2003). Although we have not performed a detailed analysis of the different layers over the whole depth of the cortex, the percentages of GAD67-GFP positive cells expressing PV or CR are similar between the two studies. Despite the high levels of co-localization with CB+ (similar to PV+ cells), a comparison was not possible since this marker was not used in the previous study.

An interesting finding of our study is that the percentages of the different subpopulations of interneurons, based on the expression of calcium binding proteins, were not altered by polyST depletion. This data seems to be in contrast with the reduction in the density of PV+ and GFP+ cells found in the mPFC of adult *St8Sia2* $^{-/-}$ *and* *St8Sia4* $^{-/-}$ mice of a previous study (Krocher et al., 2014). However, a simultaneous reduction of GFP+ and PV+ cells suggests a general reduction of interneuron densities in both polyST knockouts and it can explain the lack of differences in the percentage of the PV+ subpopulation of GFP+ interneurons in wildtype controls and *St8Sia2* $^{-/-}$ or *St8Sia4* $^{-/-}$ mice.

2.2 The genetic depletion of ST8SIA4 alters the dendritic structure of prefrontocortical interneurons

Experimental manipulations affecting the expression of polySia show its involvement in some structural changes associated with interneurons (Carceller et al., 2018; Castillo-Gómez et al., 2015, 2016b, 2017; Guirado et al., 2014b). In our study, we have demonstrated that only the genetic ablation of ST8SIA4 and not the ST8SIA2 is able to produce a significant reduction in the dendritic arborization of the prefrontocortical GAD67-GFP-labeled interneurons. The 100 μm sections are thick enough to obtain a reasonable number of neurons that fulfill our requirements for inclusion in our analyses. However, the use of thicker sections would allow the quantification of wider dendritic arborizations and thus increase the precision of the analyses. This result from Sholl analysis suggests that the synthesis and attachment of polySia by ST8SIA4 is required for the correct development of the dendritic arbor of prefrontocortical interneurons. Further analyses need to be done to establish whether the reduction in dendritic arborization affects the excitatory or the inhibitory input that these cells receive or whether it has a similar impact on both types of afferences. Unfortunately, we were unable to differentiate between different subtypes of interneurons in our structural analysis. However, it has to be noted that we have not observed dendritic spines in the GFP+ interneurons analyzed, excluding that these were Martinotti cells (Gilabert-Juan et al., 2013a).

Considering that ST8SIA4 becomes predominant during postnatal maturation and seems to be the only polyST to produce polySia in the adult cortex (Nacher et al., 2010; Oltmann-Norden et al., 2008), it is possible that the reduced dendritic arborization observed in prefrontocortical interneurons of *St8Sia4*$^{-/-}$ mice is caused by the lack of this enzyme during neuritogenesis. Interestingly, similar effects on dendritic structure have been found in motor neurons of polySia-deficient *NCAM* $^{-/-}$ mice, which exhibit a reduction in their dendritic field (Franz, 2005). Conversely, the enhancement of polySia expression increases neurite outgrowth in motoneurons derived from mouse embryonic stem cells (ESCs) (El Maarouf et al., 2015). Future experiments should explore this putative effect of polySia on neuritogenesis by studying the structure of the dendritic

arbor of interneurons during early postnatal development. Another, non-excluding, explanation is that the structural changes observed were due to the absence of polySia in cortical interneurons after postnatal development. In fact, ST8SIA4 is the sole polyST responsible for the presence of polySia in adult cortical interneurons (Nacher et al., 2010). However, this possibility seems unlikely, because polySia is only present in the somata and dendrites of a small subpopulation of cortical interneurons (around 8% in the PFC). Moreover, a previous study from our laboratory showed that in the adult cerebral cortex polySia expressing interneurons have a reduced dendritic arborization when compared with interneurons lacking this molecule (Gómez-Climent et al., 2011). Nevertheless, it has to be noted that this study focused only on a subfraction of interneurons: those expressing somatostatin, which, as we have discussed above, are probably not included in the present analysis.

2.3 The genetic depletion of either ST8SIA2 or ST8SIA4 alters the density of perisomatic inhibitory puncta on pyramidal neurons of the mPFC

Despite the fact that the structural changes mentioned above were exclusively triggered by the genetic depletion of ST8SIA4, both knockout strains show a reduction in the perisomatic inhibitory puncta surrounding prefrontocortical pyramidal neurons. Our data suggest that this reduction affects mainly PV immunoreactive puncta, which most likely belong to fast-spiking basket cells. The decrease in the density of puncta immunoreactive for PV and SYN indicates that this is a reduction in active synapses. However, there is also a strong tendency towards a decrease in the density of PV+SYN- puncta, especially in *St8Sia2* $^{-/-}$ mice. It should be noted that, unlike *St8Sia4* $^{-/-}$, adult *St8Sia2*$^{-/-}$ mice still express polySia in cortical interneurons (Nacher et al., 2010). In PV+ basket interneurons polySia can be found in some of the perisomatic puncta that these cells form around pyramidal neurons (Castillo-Gómez et al., 2008). Previous research in our lab showed that in the rat prefrontal cortex around 70% of polySia+ puncta lacked SYN expression suggesting that these might be silent synapses. In any case, the decreases in perisomatic puncta observed in the present study contrast with the increased densities observed in response to an acute enzymatic depletion of polySia using the Endo-N in the prefrontal cortex *in vivo* during adulthood (Castillo-Gómez et

al., 2011) or in organotypic cultures derived from early postnatal brain (Castillo-Gómez et al., 2016b). Our data also contrast with the inverse correlation between polySia expression and the establishment of inhibitory perisomatic input during maturation of the visual cortex (Di Cristo et al., 2007). Together, this points towards a differential role for the expression of polySia during early interneuron development (as is the case with our transgenic mice) as compared to their presence during postnatal maturation and adulthood (that can be altered by enzymatic depletion) when the presence of this molecule appears to play an insulating role, restricting the connectivity of the polySia positive interneuron population (Castillo-Gómez et al., 2011; Nacher et al., 2013). Hence, the deficits in embryonic interneuron migration and the resulting decrease of interneuron densities in the mPFC (Krocher et al., 2014) could be the underlying cause why *St8sia2*$^{-/-}$ and *St8sia4*$^{-/-}$ mice form less PV+ synaptic boutons on prefrontocortical pyramidal neurons.

In conclusion, the present study reveals an important impact of polySTs on the structure and connectivity of cortical interneurons. This is particularly relevant considering that genetic variation in both NCAM and these enzymes (especially ST8SIA2) has been associated with schizophrenia (Gilabert-Juan et al., 2013c; Sullivan et al., 2007; Tao et al., 2007), that ST8SIA2 knockout mice show schizophrenia-like phenotypes (Bacq et al., 2018; Kröcher et al., 2013), and that reductions in polySia-NCAM expression as well as alterations in inhibitory neurotransmission were detected in the PFC and hippocampus of schizophrenic patients (Barbeau et al., 1995; Gilabert-Juan et al., 2012) and in animal models of this disorder (Castillo-Gómez et al., 2017; Gilabert-Juan et al., 2013b).

EXPERIMENT 3. IMPACT OF A CHRONIC TREATMENT WITH ERYTHROPOIETIN ON THE STRUCTURE AND CONNECTIVITY OF INHIBITORY NEURONS OF THE HIPPOCAMPAL CA1 REGION, THE EXCITATORY/INHIBITORY BALANCE AND THE EXPRESSION OF MOLECULES RELATED TO INTERNEURONAL PLASTICITY.

In the present study, we report the effects of a chronic treatment with EPO on the structural features and connectivity of interneurons in the CA1 region of the hippocampus. EPO decreases the structural complexity of certain interneuronal subpopulations and the density of inhibitory perisomatic puncta that surround pyramidal cells. Furthermore, these changes are accompanied by alterations in the expression of the polysialylated form of the neural cell adhesion molecule (polySia-NCAM) and the density of perineuronal nets (PNNs), which play a key role in plasticity-related processes and are mainly associated to interneurons in the hippocampal CA1.

The expression of EPOR has been demonstrated in the adult rodent hippocampus by RT-PCR and by immunohistochemistry (Nadam et al., 2007). Immunohistochemical analysis has shown its expression in CA1 neurons, both in the pyramidal layer and in the *strata oriens, radiatum and lacunosum-moleculare*, strongly suggesting its presence in interneurons (Nadam et al., 2007). Although there is still no direct evidence of EPOR in hippocampal interneurons, previous experiments have shown that the overexpression of EPOR in GABAergic neurons alters hippocampal gamma oscillations and enhances long-term potentiation associated to the hippocampus (Wüstefeld et al., 2016). Despite these evidences supporting the expression of EPOR in hippocampal interneurons it is possible that some, or even all, the effects of EPO treatment that we have observed on CA1 interneurons were indirect, mediated by EPOR located in pyramidal neurons (Wüstefeld et al., 2016).

3.1 Chronic EPO treatment decreases the dendritic complexity and spine density of hippocampal interneurons

We have observed a marked reduction in the complexity of the dendritic arbor and the density of mature dendritic spines of EGFP+ interneurons in the *stratum oriens*

of CA1. These cells have their somata in the *stratum oriens* and extend their axonal arbor in the *stratum lacunosum-moleculare* (hence their name) (Freund and Buzsaki, 1996). In the hippocampus of the strain of mice used in our study, the majority of EGFP+ interneurons in the *stratum oriens* of the CA1 region are considered O-LM cells that innervate the distal dendritic tuft of pyramidal neurons, although a small percentage of EGFP+ cells belong to the HS type and have also their somata among these fluorescent interneurons (Perez-Rando et al., 2017a). These interneurons are of special interest when studying structural plasticity because they display dendritic spines which mainly receive excitatory glutamatergic input from local pyramidal cells in a feedback manner (Blasco-Ibáñez and Freund, 1995; Müller and Remy, 2014). We think that the loss of dendritic complexity and spines from their dendritic arbor induced by EPO may be related to the effect that the treatment produces on CA1 pyramidal neurons, namely an increase in their dendritic spine density (Curto et al., unpublished results) and an increase in the number of mature pyramidal neurons in this region (Hassouna et al., 2016). These effects of EPO on pyramidal neurons may result in an increase of excitation on O-LM interneurons and it is possible that the reduction in the dendritic arbor and spines could be a protective response of these inhibitory neurons. A similar structural response of somatostatin-expressing interneurons has been detected in the basolateral amygdala after chronic stress. In this limbic region stress induces hypertrophy and increases spine density in the dendrites of excitatory neurons, but reduces dendritic arborization in somatostatin-expressing interneurons (Gilabert-Juan et al., 2011). Moreover, the manipulation of glutamate NMDA receptors cells induces changes in the dynamic of the dendritic spines of these interneurons and of their axonal projections in the *stratum lacunosum-moleculare* (Perez-Rando et al., 2017a, 2017b).

The decrease in the dendritic arborization and spine density in these dendrite-targeting interneurons may probably represent a decrease in their synaptic input, which is mainly excitatory (Blasco-Ibáñez and Freund, 1995). This decrease in the excitatory input is probably reflected in the decrease in the density of axonal *en passant boutons* that the O-LM cells establish in the *stratum lacunosum-moleculare.* This reduction in inhibition may render the pyramidal neurons more excitable and contribute to the

increase in dendritic spines (Curto et al., unpublished results) and LTP detected after this chronic EPO treatment (Adamcio et al., 2008; Dias et al. 2017).

A similar scenario to that described in O-LM interneurons must be occurring in the parvalbumin-expressing interneurons of the *stratum oriens*, where we also observe a decrease in dendritic complexity. The reduction in dendritic complexity may be, as in O-LM cells, a response against an increase in excitatory input.

3.2 Chronic treatment with EPO decreases the number of inhibitory perisomatic puncta on excitatory neurons

The decrease in the synaptic input that receives EGFP+ and PV-expressing interneurons may lead also to reduction in their input onto pyramidal neurons, as demonstrated by the decrease in the density of PV+ perisomatic puncta around pyramidal neurons. This EPO-induced reduction in perisomatic inhibition is consistent with the reported impairment in gamma oscillations in mice with selective activation of EPOR signaling in GABAergic neurons (Wüstefeld et al., 2016). PV+ basket cells regulate gamma oscillations generated around *stratum pyramidale* through their perisomatic innervation of pyramidal neurons (Lasztóczi and Klausberger, 2014). We have also observed a reduction in the density of CB1+ perisomatic puncta on the *stratum pyramidale*, indicating that cholecystokinin expressing basket cells, which also regulate hippocampal gamma oscillations (Hájos et al., 2000), are also the target of EPO treatment, responding similarly to those expressing PV.

It is possible, however, that the response of interneurons, both O-LM and parvalbumin+, precedes that of excitatory neurons and that the increase in spine density in pyramidal neurons or the differentiation of new pyramidal neurons might be induced by the effects of EPO on interneurons. In fact, a decrease in the dendritic structure of interneurons and a reduction in the synapses that they make onto pyramidal neurons should decrease the inhibition on pyramidal neurons. It is known that glutamate, through NMDA receptors can increase the formation of dendritic spines and that the stimulation of GABAergic neurotransmission has the opposite effect (Curto et al., 2016; Tian et al., 2007; Ultanir et al., 2007). It has to be noted that despite all the effects that

we have detected on the structure and connectivity of SOM and PV expressing interneurons after EPO treatment, we have failed to observe significant changes in the excitatory/inhibitory balance. It is possible that compensatory mechanisms have operated, counteracting the alterations that we have described in these interneuronal subpopulations. These may include changes in the connectivity of other interneuronal subpopulations, such as chandelier cells or IS cells, or changes in excitatory input coming from extrahippocampal sources.

3.3 Chronic EPO treatment alters the expression of plasticity-related structures in interneurons of the hippocampus

The treatment with EPO produces an increase in the density of PNNs. In the CA1 region, this specialized extracellular matrix can be found enveloping mainly parvalbumin positive interneurons (Yamada et al., 2015). PNNs are widely considered a marker of the maturational degree of PV-expressing interneurons and appear to be involved in the closure and reopening of critical periods and the regulation of synaptic plasticity (Pizzorusso et al., 2002; Sorg et al., 2016). PNNs contribute to this process by promoting synapse stabilization and restricting plasticity processes (Lorenzo Bozzelli et al., 2018). EPO has been shown to improve memory and cognition dependent on the hippocampus (Adamcio et al., 2008; Hassouna et al., 2016). Considering that the neuronal circuits implicated in cognition are mainly present in the dorsal part of this region, the increase in PNNs may help to stabilize the neuronal connections implicated in such cognitive improvement, similar to the cognitive maturation that occurs during development (Yamada and Jinno, 2013). However, we only fond a slight increase in the density of PV+ neurons surrounded by PNNs, which suggest that the increase in PNNs that we observe may be due to increases in PNNs associated to other cell types, more likely excitatory neurons. Similar to the closure of the critical period, the presence of PNNs seems to restrict the plastic changes, mainly those associated to PV+ interneurons. Therefore, the slight increase in PNNs enwrapping PV+ cells may partly explain the decreased dendritic arborization and perisomatic innervation of PV+ interneurons observed in our study.

Apart from the above discussed effects of EPO treatment on the structure and connectivity of hippocampal CA1 interneurons, we also found a remarkable increase in

the expression of polySia-NCAM. In the CA1 region, this plasticity-related molecule is mainly associated with a subpopulation of mature interneurons, which includes PV+ basket cells and O-LM interneurons (Gómez-Climent et al., 2011; Nacher et al., 2002a). In fact, hippocampal interneurons expressing polySia-NCAM have reduced dendritic arborization, density of spines and less perisomatic synaptic contacts when compared to interneurons lacking this molecule (Gómez-Climent et al. 2011). This has been interpreted as an insulating role for polySia-NCAM in these mature interneurons. In fact, the enzymatic depletion of polySia-NCAM produces opposite effects to those that we have observed after EPO treatment, i.e. an increase in the density of the perisomatic puncta that PV+ basket interneurons establish on pyramidal neurons (Castillo-Gómez et al., 2011, 2016a) and a transitory increase in the density of the dendritic spines of O-LM cells (Guirado et al., 2014b).

The present results suggest an important impact of EPO treatment, both at the structural and connectivity levels, on certain hippocampal interneuron subpopulations, probably through alterations in the expression of plasticity-related molecules, such as polySia-NCAM and those constituting the PNNs, which are particularly associated to these inhibitory cells. These changes may contribute to revert many of the interneuronal changes associated to early aversive experiences or chronic stress (Castillo-Gómez et al., 2017; Gilabert-Juan et al., 2013a). Interestingly, one of the subpopulations of interneurons studied in the present thesis, which mainly express somatostatin, shows an increased density of dendritic spines in the PFC of a double hit model of schizophrenia in mice consisting in a perinatal injection of MK-801 and postweaning social isolation (Castillo-Gómez et al., 2017). Interestingly, the social isolation by itself is also able to produce these changes. In other brain regions such as the amygdala, an increased complexity of the dendritic tree of these cells can be observed in double-hit mice (Castillo-Gómez et al., 2017). Moreover, a similar dendritic hypertrophy is found in young adult mice subjected to chronic stress (Gilabert-Juan et al., 2011, 2013a). Consequently, new therapeutic approaches, such as the EPO treatment, able to modulate interneuronal structure and connectivity, as well as PNNs or polySia-NCAM expression, may be considered as promising candidates for innovative strategies.

CHAPTER VI
Conclusions

1. A chronic treatment with diazepam, a $GABA_A$ receptor agonist, decreases the density of dendritic spines in the principal apical dendrite of pyramidal neurons located in layer V of the cingulate cortex of adult mice.

2. A neurochemical analysis using VGLUT2 immunohistochemistry shows that most of the excitatory (YFP+) axonal boutons in layers I-II of the cingulate cortex of adult mice have an extracortical origin.

3. A chronic treatment with diazepam does not induce changes in the density of axonal boutons in the layers I-II of the cingulate cortex of adult mice.

4. A chronic treatment with diazepam, using an anxiolytic but non sedative dose, does not induce changes in the anxiety level of adult mice.

5. The phenotype of GAD67-GFP+ interneurons present in the prelimbic and infralimbic cortices of transgenic and control mice, is similar in both the knockouts for ST8SIA2 and ST8SIA4 polysialyltransferases, and in the control mice.

6. The interneurons expressing GAD67-GFP+ in the prelimbic and infralimic cortices of the knockouts for ST8SIA2 and ST8SIA4 polysialyltransferases and of control mice, mainly co-express parvalbumin and calbindin and, to a lesser extent, calretinin.

7. The genetic depletion of ST8SIA4, but not of ST8SIA2, decreases the complexity of the dendritic tree of the GAD67-GFP+ interneurons in the prelimbic and infralimbic cortices.

8. The genetic depletion of either of the two enzymes, ST8SIA2 or ST8SIA4, decreases the total density of parvalbumin expressing puncta surrounding the somata of pyramidal neurons in the prelimbic and infralimbic cortices.

9. The density of puncta that co-express parvalbumin and synaptophysin surrounding the somata of pyramidal neurons, decreases in the prelimbic cortex of ST8SIA2 knockout mice and in the infralimbic cortex of ST8SIA4 knockout mice.

10. A chronic treatment with erythropoietin does not alter the excitatory/inhibitory balance in the *strata oriens, pyramidale, radiatum* and *lacunosum-moleculare* of the CA1 region of the hippocampus of young mice.

11. A chronic treatment with erythropoietin decreases the complexity of the dendritic tree of somatostatin-expressing interneurons located in the *stratum oriens* of the CA1 region of the hippocampus in young mice.

12. A chronic treatment with erythropoietin decreases the density of dendritic spines of somatostatin-expressing interneurons located in the *stratum oriens* of the CA1 region of the hippocampus in young mice.

13. A chronic treatment with erythropoietin decreases the complexity of the dendritic tree of the parvalbumin-expressing interneurons located in *stratum oriens* of the CA1 region of the hippocampus in young mice.

14. A chronic treatment with erythropoietin decreases the density of axonal *en passant boutons* of somatostatin-expressing interneurons in the *stratum lacunosum-moleculare* of the CA1 region of the hippocampus in young mice.

15. A chronic treatment with erythropoietin decreases the density of inhibitory puncta that express parvalbumin or CB1r surrounding the somata of pyramidal neurons located in *stratum pyramidale* of the CA1 region of the hippocampus of young mice.

16. A chronic treatment with erythropoietin increases the density of perineuronal nets and the density of parvalbumin-expressing interneurons surrounded by perineuronal nets in the CA1 region of the hippocampus of young mice.

17. A chronic treatment with erythropoietin increases the expression of polySia-NCAM in the strata *oriens, radiatum* and *lacunosum-moleculare* of the CA1 region of the hippocampus of young mice.

CHAPTER VII
References

Adamcio, B., Sargin, D., Stradomska, A., Medrihan, L., Gertler, C., Theis, F., et al. (2008). Erythropoietin enhances hippocampal long-term potentiation and memory. BMC Biol. 6, 1–16.

Akgül, G., and McBain, C. J. (2016). Diverse roles for ionotropic glutamate receptors on inhibitory interneurons in developing and adult brain. J. Physiol. 594, 5471–5490.

Allen, T. A., and Fortin, N. J. (2013). The evolution of episodic memory. Proc. Natl. Acad. Sci. 110, 10379 LP-10386.

Alnaeeli, M., Wang, L., Piknova, B., Rogers, H., Li, X., and Noguchi, C. T. (2012). Erythropoietin in brain development and beyond. Anat. Res. Int. 2012, 1–15.

Alpár, A., Gärtner, U., Härtig, W., and Brückner, G. (2006). Distribution of pyramidal cells associated with perineuronal nets in the neocortex of rat. Brain Res. 1120, 13–22.

Amaral, D. G., Scharfman, H. E., and Lavenex, P. (2007). The dentate gyrus: fundamental neuroanatomical organization (dentate gyrus for dummies). Prog. Brain Res. 163, 3–22.

Amaral, M. D., and Pozzo-Miller, L. (2007). TRPC3 Channels are necessary for brain-derived neurotrophic factor to activate a nonselective cationic current and to induce dendritic spine formation. J. Neurosci. 27, 5179–5189.

Amaral, D. G. (1993). Emerging principles of intrinsic hippocampal organization. Curr. Opin. Neurobiol. 3, 225–229.

Anand, K. S., and Dhikav, V. (2012). Hippocampus in health and disease: An overview. Ann. Indian Acad. Neurol. 15, 239–246.

Anderson, M. F., Aberg, M. A., Nilsson, M., and Eriksson, P. S. (2002). Insulin-like growth factor-I and neurogenesis in the adult mammalian brain. Dev. Brain Res. 134, 115–122.

Angata, K., Long, J. M., Bukalo, O., Lee, W., Dityatev, A., Wynshaw-Boris, A., et al. (2004). Sialyltransferase ST8Sia-II assembles a subset of polysialic acid that directs hippocampal axonal targeting and promotes fear behavior. J. Biol. Chem. 279, 32603–32613.

Anney, R., Klei, L., Pinto, D., Regan, R., Conroy, J., Magalhaes, T. R., et al. (2010). A genome-wide scan for common alleles affecting risk for autism. Hum. Mol. Genet. 19, 4072–4082.

Ascoli, G. A., Alonso-Nanclares, L., Anderson, S. A., Barrionuevo, G., Benavides-Piccione,

R., et al. (2008). Petilla terminology: nomenclature of features of GABAergic interneurons of the cerebral cortex. Nat. Rev. Neurosci. 9, 557.

Assaraf, M. I., Diaz, Z., Liberman, A., Miller, W. H., Arvanitakis, Z., Li, Y., et al. (2007). Brain erythropoietin receptor expression in Alzheimer disease and mild cognitive impairment. J. Neuropathol. Exp. Neurol. 66, 389–398.

Bacq, A., Astori, S., Gebara, E., Tang, W., Silva, B. A., Sanchez-Mut, J., et al. (2018). Amygdala GluN2B-NMDAR dysfunction is critical in abnormal aggression of neurodevelopmental origin induced by St8sia2 deficiency. Mol. Psychiatry.

Bak, L. K., Schousboe, A., and Waagepetersen, H. S. (2006). The glutamate/GABA-glutamine cycle: Aspects of transport, neurotransmitter homeostasis and ammonia transfer. J. Neurochem. 98, 641–653.

Banasr, M., Dwyer, J. M., and Duman, R. S. (2011). Cell atrophy and loss in depression: reversal by antidepressant treatment. Curr. Opin. Cell Biol. 23, 730–737.

Barbeau, D., Liang, J. J., Robitalille, Y., Quirion, R., and Srivastava, L. K. (1995). Decreased expression of the embryonic form of the neural cell adhesion molecule in schizophrenic brains. Proc. Natl. Acad. Sci. U. S. A. 92, 2785–9.

Baumann, S. W., Baur, R., and Sigel, E. (2003). Individual properties of the two functional agonist sites in GABA(A) receptors. J. Neurosci. 23, 11158–66.

Baur, R. (2005). Benzodiazepines affect channel opening of GABAA receptors induced by either agonist binding site. Mol. Pharmacol. 67, 1005–1008.

Belzung, C. (2013). Current topics in behavioral neurosciences. In: Neurogenesis and Neural Plasticity, volume 15. Springer, Berlin, Heidelberg.

Ben-Ari, Y., Gaiarsa, J. L., Tyzio, R., and Khazipov, R. (2007). GABA: A pioneer transmitter that excites immature neurons and generates primitive oscillations. Physiol. Rev. 87, 1215–1284.

Beurdeley, M., Spatazza, J., Lee, H. H. C., Sugiyama, S., Bernard, C., Di Nardo, A. A., et al. (2012). Otx2 binding to perineuronal nets persistently regulates plasticity in the mature visual cortex. J. Neurosci. 32, 9429–9437.

Bicks, L. K., Koike, H., Akbarian, S., and Morishita, H. (2015). Prefrontal cortex and social cognition in mouse and man. Front. Psychol. 6, 1–15.

Blasco-Ibáñez, J. M., and Freund, T. F. (1995). Synaptic Input of Horizontal Interneurons in Stratum Oriens of the Hippocampal CA1 Subfield: Structural Basis of Feed-back

Activation. Eur. J. Neurosci. 7, 2170–2180.

Bonfanti, L. (2006). PSA-NCAM in mammalian structural plasticity and neurogenesis. Prog. Neurobiol. 80, 129–164.

Bonnas, C., Wüstefeld, L., Winkler, D., Kronstein-Wiedemann, R., Dere, E., Specht, K., et al. (2017). EV-3, an endogenous human erythropoietin isoform with distinct functional relevance. Sci. Rep. 7, 1–15.

Booker, S. A., and Vida, I. (2018). Morphological diversity and connectivity of hippocampal interneurons. Cell Tissue Res. 373, 619–641.

Bourne, J., and Harris, K. M. (2007). Do thin spines learn to be mushroom spines that remember? Curr. Opin. Neurobiol. 17, 381–386.

Bouwknecht, J. A., and Paylor, R. (2002). Behavioral and physiological mouse assays for anxiety: a survey in nine mouse strains. Behav. Brain Res. 136, 489–501.

Brakebusch, C., Seidenbecher, C. I., Asztely, F., Rauch, U., Matthies, H., Meyer, H., et al. (2002). Brevican-deficient mice display impaired hippocampal CA1 long-term potentiation but show no obvious deficits in learning and memory. Mol. And Cel. Biol 22, 7417–7427.

Brennaman, L. H., and Maness, P. F. (2010). NCAM in neuropsychiatric and neurodegenerative disorders. Adv. Exp. Med. Biol. 663, 299–317.

Bukalo, O., Schachner, M., and Dityatev, A. (2001). Modification of extracellular matrix by enzymatic removal of chondroitin sulfate and by lack of tenascin-R differentially affects several forms of synaptic plasticity in the hippocampus. Neuroscience 104, 359–369.

Cabungcal, J. H., Steullet, P., Morishita, H., Kraftsik, R., Cuenod, M., Hensch, T. K., et al. (2013). Perineuronal nets protect fast-spiking interneurons against oxidative stress. Proc. Natl. Acad. Sci. 110, 9130–9135.

Carceller, H., Perez-Rando, M., Castren, E., Nacher, J., and Guirado, R. (2018). Effects of the Antidepressant Fluoxetine on the Somatostatin Interneurons in the Basolateral Amygdala. Neuroscience 386, 205–213.

Cardin, J. A., Carlén, M., Meletis, K., Knoblich, U., Zhang, F., Deisseroth, K., et al. (2009). Driving fast-spiking cells induces gamma rhythm and controls sensory responses. Nature 459, 663–667.

Carlson, P. J., Singh, J. B., Zarate, C. A., Drevets, W. C., and Manji, H. K. (2006). Neural

circuitry and neuroplasticity in mood disorders: Insights for novel therapeutic targets. NeuroRx 3, 22–41.

Carulli, D., Rhodes, K. E., Brown, D. J., Bonnert, T. P., Pollack, S. J., Oliver, K., et al. (2006). Composition of perineuronal nets in the adult rat cerebellum and the cellular origin of their components. J. Comp. Neurol. 494, 559–577.

Castillo-Gómez, E., Pérez-Rando, M., Bellés, M., Gilabert-Juan, J., Llorens, J. V., Carceller, H., et al. (2017). Early social isolation stress and perinatal NMDA receptor antagonist treatment induce changes in the structure and neurochemistry of inhibitory neurons of the adult amygdala and prefrontal cortex. ENEURO 4, ENEURO.0034-17.2017.

Castillo-Gómez, E., Varea, E., Blasco-Ibáñez, J. M., Crespo, C., and Nacher, J. (2016a). Effects of chronic dopamine D2R agonist treatment and polysialic acid depletion on dendritic spine density and excitatory neurotransmission in the mPFC of adult rats. Neural Plast. 2016.

Castillo-Gómez, E., Pérez-Rando, M., Vidueira, S., and Nacher, J. (2016b). Polysialic acid acute depletion induces structural plasticity in interneurons and impairs the excitation/inhibition balance in medial prefrontal cortex organotypic cultures. Front. Cell. Neurosci. 10.

Castillo-Gómez, E., Coviello, S., Perez-Rando, M., Curto, Y., Carceller, H., Salvador, A., et al. (2015). Streptozotocin diabetic mice display depressive-like behavior and alterations in the structure, neurotransmission and plasticity of medial prefrontal cortex interneurons. Brain Res. Bull. 116, 45–56.

Castillo-Gómez, E., Varea, E., Blasco-Ibáñez, J. M., Crespo, C., and Nacher, J. (2011). Polysialic acid is required for dopamine D2 receptor-mediated plasticity involving inhibitory circuits of the rat medial prefrontal cortex. PLoS One 6.

Castillo-Gómez, E., Gómez-Climent, M. Á., Varea, E., Guirado, R., Blasco-Ibáñez, J. M., Crespo, C., et al. (2008). Dopamine acting through D2 receptors modulates the expression of PSA-NCAM, a molecule related to neuronal structural plasticity, in the medial prefrontal cortex of adult rats. Exp. Neurol. 214.

Celio, M. R. (1993). Perineuronal nets of extracellular matrix around parvalbumin-containing neurons of the hippocampus. Hippocampus 3, 55–60.

Cerqueira, J. J., Taipa, R., Uylings, H. B. M., Almeida, O. F. X., and Sousa, N. (2007).

Specific configuration of dendritic degeneration in pyramidal neurons of the medial prefrontal cortex induced by differing corticosteroid regimens. Cereb. Cortex 17, 1998–2006.

Chang, Y., Wang, R., Barot, S., and Weiss, D. S. (1996). Stoichiometry of a Recombinant GABA A Receptor. The Journal of Neurosc. 16, 5415–5424.

Chapleau, C. A., Larimore, J. L., Theibert, A., and Pozzo-Miller, L. (2009). Modulation of dendritic spine development and plasticity by BDNF and vesicular trafficking: Fundamental roles in neurodevelopmental disorders associated with mental retardation and autism. J. Neurodev. Disord. 1, 185–196.

Chaudhry, S. K., Broderick, L., Penzner, J. B., and Avery, J. (2015). Benzodiazepine maintenance treatment in schizophrenia. Prim. care companion CNS Disord. 17, 10.4088/PCC.15l01818.

Chen, J. R., Yan, Y. T., Wang, T. J., Chen, L. J., Wang, Y. J., and Tseng, G. F. (2009). Gonadal hormones modulate the dendritic spine densities of primary cortical pyramidal neurons in adult female rat. Cereb. Cortex 19, 2719–2727.

Chong, Z. Z., Kang, J. Q., and Maiese, K. (2002). Hematopoietic factor erythropoietin fosters neuroprotection through novel signal transduction cascades. J. Cereb. Blood Flow Metab. 22, 503–514.

Close, B. E., and Colley, K. J. (1998). In vivo autopolysialylation and localization of the polysialyltransferases PST and STX. J. Biol. Chem. 273, 34586–34593.

Colello, R. J., Tozer, J., and Henderson, S. C. (2012). Confocal laser scanning microscopic photoconversion: A new method to stabilize fluorescently labeled cellular elements for electron microscopic analysis. Curr. Protoc. Neurosci. 58, 2.15.1-2.15.12.

Cook, S. C., and Wellman, C. L. (2004). Chronic stress alters dendritic morphology in rat medial prefrontal cortex. J. Neurobiol. 60, 236–248.

Cowansage, K. K., LeDoux, J. E., and Monfils, M. H. (2010). Brain-derived neurotrophic factor: a dynamic gatekeeper of neural plasticity. Curr. Mol. Pharmacol. 3, 12–29.

Crawley, J., and Goodwin, F. K. (1980). Preliminary report of a simple animal behavior model for the anxiolytic effects of benzodiazepines. Pharmacol. Biochem. Behav. 13, 167–170.

Curto, Y., Garcia-Mompo, C., Bueno-Fernandez, C., and Nacher, J. (2016). Chronic benzodiazepine treatment decreases spine density in cortical pyramidal neurons.

Neurosci. Lett. 613, 41–46.

D'Andrea, A. D., Lodish, H. F., and Wong, G. G. (1989). Expression cloning of the murine erythropoietin receptor. Cell 57, 277–285.

De Magalhães, J. P., and Sandberg, A. (2005). Cognitive aging as an extension of brain development: A model linking learning, brain plasticity, and neurodegeneration. Mech. Ageing Dev. 126, 1026–1033.

De Paola, V., Holtmaat, A., Knott, G., Song, S., Wilbrecht, L., Caroni, P., et al. (2006). Cell type-specific structural plasticity of axonal branches and boutons in the adult neocortex. Neuron 49, 861–875.

De Vivo, L., Landi, S., Panniello, M., Baroncelli, L., Chierzi, S., Mariotti, L., et al. (2013). Extracellular matrix inhibits structural and functional plasticity of dendritic spines in the adult visual cortex. Nat. Commun. 4, 1410–1484.

Defelipe, J., López-Cruz, P. L., Benavides-Piccione, R., Bielza, C., Larrañaga, P., Anderson, S., et al. (2013). New insights into the classification and nomenclature of cortical GABAergic interneurons. Nat. Rev. Neurosci. 14, 202–216.

Deidda, G., Allegra, M., Cerri, C., Naskar, S., Bony, G., Zunino, G., et al. (2015). Early depolarizing GABA controls critical-period plasticity in the rat visual cortex. Nat. Neurosci. 18, 87–96.

Di Cristo, G., Chattopadhyaya, B., Kuhlman, S. J., Fu, Y., Bélanger, M.-C., Wu, C. Z., et al. (2007). Activity-dependent PSA expression regulates inhibitory maturation and onset of critical period plasticity. Nat. Neurosci. 10, 1569.

Dias, R. B., Rodrigues, T. M., Rombo, D. M., Ribeiro, F. F., Rodrigues, J., McGarvey, J., et al. (2017). Erythropoietin Induces Homeostatic Plasticity at Hippocampal Synapses. Cereb. Cortex, 1–15.

Dick, G., Liktan, C., Alves, J. N., Ehlert, E. M. E., Miller, G. M., Hsieh-Wilson, L. C., et al. (2013). Semaphorin 3A binds to the perineuronal nets via chondroitin sulfate type E motifs in rodent brains. J. Biol. Chem. 288, 27384–27395.

Digicaylioglu, M., Bichet, S., Marti, H. H., Wenger, R. H., Rivas, L. A., Bauer, C., et al. (1995). Localization of specific erythropoietin binding sites in defined areas of the mouse brain. Proc Natl Acad Sci U S A 92, 3717–3720.

Dityatev, A., Brückner, G., Dityateva, G., Grosche, J., Kleene, R., and Schachner, M. (2007). Activity-dependent formation and functions of chondroitin sulfate-rich

extracellular matrix of perineuronal nets. Dev. Neurobiol. 67, 570–588.

Dityatev, A., and Schachner, M. (2003). Extracellular matrix molecules and synaptic plasticity. Nat. Rev. Neurosci. 4, 456–468.

Dzierzak, E., and Philipsen, S. (2013). Erythropoiesis: Development and differentiation. Cold Spring Harb. Perspect. Med. 3.

Eckhardt, M., Bukalo, O., Chazal, G., Wang, L., Goridis, C., Schachner, M., et al. (2000). Mice deficient in the polysialyltransferase ST8SiaIV/PST-1 allow discrimination of the roles of neural cell adhesion molecule protein and polysialic acid in neural development and synaptic plasticity. J. Neurosci. 20, 5234–5244.

Edwards, R. H., Jorgensen, E. M., McIntire, S. L., Reimer, R. J., and Schuske, K. (1997). Identification and characterization of the vesicular GABA transporter. Nature 389, 870–876.

Ehrenreich, H., Fischer, B., Norra, C., Schellenberger, F., Stender, N., Stiefel, M., et al. (2007a). Exploring recombinant human erythropoietin in chronic progressive multiple sclerosis. Brain 130, 2577–2588.

Ehrenreich, H., Hinze-Selch, D., Stawicki, S., Aust, C., Knolle-Veentjer, S., Wilms, S., et al. (2007b). Improvement of cognitive functions in chronic schizophrenic patients by recombinant human erythropoietin. Mol. Psychiatry 12, 206–220.

Ehrenreich, H., Hasselblatt, M., Knerlich, F., von Ahsen, N., Jacob, S., Sperling, S., et al. (2005). A hematopoietic growth factor, thrombopoietin, has a proapoptotic role in the brain. Proc. Natl. Acad. Sci. U. S. A. 102, 862–867.

Ehrenreich, H., Degner, D., Meller, J., Brines, M., Béhé, M., Hasselblatt, M., et al. (2004). Erythropoietin: A candidate compound for neuroprotection in schizophrenia. Mol. Psychiatry 9, 42–54.

Ehrenreich, H., Degner, D., Meller, J., Brines, M., Béhé, M., Hasselblatt, M., et al. (2003). Erythropoietin: a candidate compound for neuroprotection in schizophrenia. Mol. Psychiatry, 42–54.

El-Kordi, A., Radyushkin, K., and Enhrenreich, H. (2009). Erythropoietin improves operant conditioning and stability of cognitive performance in mice. BMC Biol. 7, 1–8.

El Maarouf, A., Moyo-Lee Yaw, D., and Rutishauser, U. (2015). Improved stem cell-derived motoneuron survival, migration, sprouting, and innervation with enhanced

expression of polysialic acid. Cell Transplant. 24, 797–809.

Esclapez, M., Tillakaratne, N. J., Kaufman, D. L., Tobin, A. J., and Houser, C. R. (1994). Comparative localization of two forms of glutamic acid decarboxylase and their mRNAs in rat brain supports the concept of functional differences between the forms. J. Neurosci. 14, 1834–55.

Eulenburg, V., and Gomeza, J. (2010). Neurotransmitter transporters expressed in glial cells as regulators of synapse function. Brain Res. Rev. 63, 103–112.

Euston, D. R., Gruber, A. J., and McNaughton, B. L. (2012). The role of medial prefrontal cortex in memory and decision making. Neuron 76, 1057–1070.

Fatemi, S. H., Halt, A. R., Stary, J. M., Kanodia, R., Schulz, S. C., and Realmuto, G. R. (2002). Glutamic acid decarboxylase 65 and 67 kDa proteins are reduced in autistic parietal and cerebellar cortices. Biol. Psychiatry 54, 805-810.

Feng, G., Mellor, R. H., Bernstein, M., Keller-Peck, C., Nguyen, Q. T., Wallace, M., et al. (2000). Imaging neuronal subsets in transgenic mice expressing multiple spectral variants of GFP. Neuron 28, 41–51.

Foley, A. G., Rønn, L. C. B., Murphy, K. J., and Regan, C. M. (2003). Distribution of polysialylated neural cell adhesion molecule in rat septal nuclei and septohippocampal pathway: Transient increase of polysialylated interneurons in the subtriangular septal zone during memory consolidation. J. Neurosci. Res. 74, 807–817.

Frankfurt, M., and Luine, V. (2015). The evolving role of dendritic spines and memory: Interaction(s) with estradiol. Horm. Behav. 74, 28–36.

Franz, C. K. (2005). Polysialylated neural cell adhesion molecule is necessary for selective targeting of regenerating motor neurons. J. Neurosci. 25, 2081–2091.

Fremeau, R. T., Troyer, M. D., Pahner, I., Nygaard, G. O., Tran, C. H., Reimer, R. J., et al. (2001). The expression of vesicular glutamate transporters defines two classes of excitatory synapse. Neuron 31, 247–260.

Freund, T. F. (2003). Interneuron diversity series: Rhythm and mood in perisomatic inhibition. Trends Neurosci. 26, 489–495.

Freund, T. F., and Buzsaki, G. (1996). Interneurons of the hippocampus. Hippocampus 6, 347–470.

Freund, T. F., and Katona, I. (2007). Perisomatic Inhibition. Neuron 56, 33–42.

Freund, T. F., Katona, I., and Piomelli, D. (2003). Role of endogenous cannabinoids in synaptic signaling. Physiol. Rev. 83, 1017–1066.

Frischknecht, R., Heine, M., Perrais, D., Seidenbecher, C. I., Choquet, D., and Gundelfinger, E. D. (2009). Brain extracellular matrix affects AMPA receptor lateral mobility and short-term synaptic plasticity. Nat. Neurosci. 12, 897–904.

Fujihara, K., Miwa, H., Kakizaki, T., Kaneko, R., Mikuni, M., Tanahira, C., et al. (2015). Glutamate decarboxylase 67 deficiency in a subset of GABAergic neurons induces schizophrenia-related phenotypes. Neuropsychopharmacology 40, 2475–2486.

Fuster, J. M. (2015). The Prefrontal Cortex (5th. Edition). Academic Press

Gabbott, P. L. A., Warner, T. A., Jays, P. R. L., Salway, P., and Busby, S. J. (2005). Prefrontal cortex in the rat: Projections to subcortical autonomic, motor, and limbic centers. J. Comp. Neurol. 492, 145–177.

Galuska, S. P., Oltmann-Norden, I., Geyer, H., Weinhold, B., Kuchelmeister, K., Hildebrandt, H., et al. (2006). Polysialic acid profiles of mice expressing variant allelic combinations of the polysialyltransferases ST8SiaII and ST8SiaIV. J. Biol. Chem. 281, 31605–31615.

Gao, R., Tang, Y. H., Tong, J. H., Yang, J. J., Ji, M. H., and Zhu, S. H. (2015). Systemic lipopolysaccharide administration-induced cognitive impairments are reversed by erythropoietin treatment in mice. Inflammation 38.

Gascon, E., Vutskits, L., and Kiss, J. Z. (2007). Polysialic acid-neural cell adhesion molecule in brain plasticity: From synapses to integration of new neurons. Brain Res. Rev. 56, 101–118.

Gilabert-Juan, J., Bueno-Fernandez, C., Castillo-Gomez, E., and Nacher, J. (2017). Reduced interneuronal dendritic arborization in CA1 but not in CA3 region of mice subjected to chronic mild stress. Brain Behav. 7, 1–7.

Gilabert-Juan, J., Castillo-Gomez, E., Guirado, R., Moltó, M. D., and Nacher, J. (2013a). Chronic stress alters inhibitory networks in the medial prefrontal cortex of adult mice. Brain Struct. Funct. 218, 1591–1605.

Gilabert-Juan, J., Belles, M., Saez, A. R., Carceller, H., Zamarbide-Fores, S., Moltó, M. D., et al. (2013b). A “double hit” murine model for schizophrenia shows alterations in the structure and neurochemistry of the medial prefrontal cortex and the hippocampus. Neurobiol. Dis. 59.

Gilabert-Juan, J., Nacher, J., Sanjuán, J., and Moltó, M. D. (2013c). Sex-specific association of the ST8SIAII gene with schizophrenia in a Spanish population. Psychiatry Res. 210, 1293–5.

Gilabert-Juan, J., Varea, E., Guirado, R., Blasco-Ibáñez, J. M., Crespo, C., and Nácher, J. (2012). Alterations in the expression of PSA-NCAM and synaptic proteins in the dorsolateral prefrontal cortex of psychiatric disorder patients. Neurosci. Lett. 530.

Gilabert-Juan, J., Castillo-Gomez, E., Pérez-Rando, M., Moltó, M. D., and Nacher, J. (2011). Chronic stress induces changes in the structure of interneurons and in the expression of molecules related to neuronal structural plasticity and inhibitory neurotransmission in the amygdala of adult mice. Exp. Neurol. 232, 33–40.

Gold, A. L., Shechner, T., Farber, M. J., Spiro, C. N., Leibenluft, E., Pine, D. S., et al. (2016). Amygdala-cortical connectivity: Associations with anxiety, development, and threat. Depress. Anxiety 33, 917–926.

Gómez-Climent, M. Á., Guirado, R., Castillo-Gómez, E., Varea, E., Gutierrez-Mecinas, M., Gilabert-Juan, J., et al. (2011). The polysialylated form of the neural cell adhesion molecule (PSA-NCAM) is expressed in a subpopulation of mature cortical interneurons characterized by reduced structural features and connectivity. Cereb. Cortex 21, 1028–1041.

Gómez-Climent, M. Á., Castillo-Gómez, E., Varea, E., Guirado, R., Blasco-Ibáñez, J. M., Crespo, C., et al. (2008). A population of prenatally generated cells in the rat paleocortex maintains an immature neuronal phenotype into adulthood. Cereb. Cortex 18, 2229–2240.

Gonzalez-Burgos, G., Cho, R. Y., and Lewis, D. A. (2015). Alterations in cortical network oscillations and parvalbumin neurons in schizophrenia. Biol. Psychiatry 77, 1031–1040.

Gonzalez, A., Moya-Alvarado, G., Gonzalez-Billaut, C., and Bronfman, F. C. (2016). Cellular and molecular mechanisms regulating neuronal growth by brain-derived neurotrophic factor. Cytoskeleton 73, 612–628.

Gouzer, G., Specht, C. G., Allain, L., Shinoe, T., and Triller, A. (2014). Benzodiazepine-dependent stabilization of GABAA receptors at synapses. Mol. Cell. Neurosci. 63, 101–113.

Guirado, R., Carceller, H., Castillo-Gómez, E., Castrén, E., and Nacher, J. (2018).

Automated analysis of images for molecular quantification in immunohistochemistry. Heliyon 4.

Guirado, R., Perez-Rando, M., Sanchez-Matarredona, D., Castrén, E., and Nacher, J. (2014a). Chronic fluoxetine treatment alters the structure, connectivity and plasticity of cortical interneurons. Int. J. Neuropsychopharmacol. 17, 1635–1646.

Guirado, R., Perez-Rando, M., Sanchez-Matarredona, D., Castillo-Gómez, E., Liberia, T., Rovira-Esteban, L., et al. (2014b). The dendritic spines of interneurons are dynamic structures influenced by PSA-NCAM expression. Cereb. Cortex 24, 3014–3024.

Guirado, R., Sanchez-Matarredona, D., Varea, E., Crespo, C., Blasco-Ibáñez, J. M., and Nacher, J. (2012). Chronic fluoxetine treatment in middle-aged rats induces changes in the expression of plasticity-related molecules and in neurogenesis. BMC Neurosci. 13, 5.

Gulyas, A. I., Miettinen, R., Jacobowitz, D. M., and Freund, T. F. (1991). Calretinin-immunoreacti cells in the rat hippocampus. I. A new type of neuron specifically associated with the mossy fibre system - revealed. Eur.J.Neurosci.Suppl. 4, 158.

Gutierrez, H., and Davies, A. M. (2007). A fast and accurate procedure for deriving the Sholl profile in quantitative studies of neuronal morphology. J. Neurosci. Methods 163, 24–30.

Hájos, N., Katona, I., Naiem, S. S., Mackie, K., Ledent, C., Mody, I., et al. (2000). Cannabinoids inhibit hippocampal GABAergic transmission and network oscillations. Eur. J. Neurosci. 12, 3239–3249.

Hall, C. S. (1934). Emotional behavior in the rat. I. Defecation and urination as measures of individual differences in emotionality. Journal of Comparative Psychology. 18, 385-403.

Harauzov, A., Spolidoro, M., DiCristo, G., De Pasquale, R., Cancedda, L., Pizzorusso, T., et al. (2010). Reducing intracortical inhibition in the adult visual cortex promotes ocular dominance plasticity. J. Neurosci. 30, 361–371.

Harrison, P. J., and Weinberger, D. R. (2005). Schizophrenia genes, gene expression, and neuropathology: On the matter of their convergence. Mol. Psychiatry 10, 40–68.

Hassouna, I., Ott, C., Wüstefeld, L., Offen, N., Neher, R. a., Mitkovski, M., et al. (2016). Revisiting adult neurogenesis and the role of erythropoietin for neuronal and oligodendroglial differentiation in the hippocampus. Mol. Psychiatry 21, 1752–

1767.

Heidbreder, C. A., and Groenewegen, H. J. (2003). The medial prefrontal cortex in the rat: Evidence for a dorso-ventral distinction based upon functional and anatomical characteristics. Neurosci. Biobehav. Rev. 27, 555–579.

Hensch, T. K., and Fagiolini, M. (2000). Inhibitory threshold for critical-period activation in primary visual cortex. Nature 404, 183–186.

Hildebrandt, H., and Dityatev, A. (2015). Polysialic acid in brain development and synaptic plasticity. In: SialoGlyco chemistry and biology I. Topics in current chemistry, volume 366. Springer, Berlin, Heidelberg.

Hildebrandt, H., Mühlenhoff, M., and Gerardy-Schahn, R. (2010). Polysialylation of NCAM. In: Structure and function of the neural cell adhesion molecule NCAM. Advances in experimental medicine and biology, volume 663. Springer, New York, NY.

Hildebrandt, H., Mühlenhoff, M., Oltmann-Norden, I., Röckle, I., Burkhardt, H., Weinhold, B., et al. (2009). Imbalance of neural cell adhesion molecule and polysialyltransferase alleles causes defective brain connectivity. Brain 132, 2831–2838.

Hildebrandt, H., Mühlenhoff, M., Weinhold, B., and Gerardy-Schahn, R. (2007). Dissecting polysialic acid and NCAM functions in brain development. J. Neurochem. 103 Suppl, 56–64.

Holtmaat, A. J. G. D., Trachtenberg, J. T., Wilbrecht, L., Shepherd, G. M., Zhang, X., Knott, G. W., et al. (2005). Transient and persistent dendritic spines in the neocortex in vivo. Neuron 45, 279–291.

Hoover, W. B., and Vertes, R. P. (2007). Anatomical analysis of afferent projections to the medial prefrontal cortex in the rat. Brain Struct. Funct. 212, 149–179.

Hotulainen, P., and Hoogenraad, C. C. (2010). Actin in dendritic spines: Connecting dynamics to function. J. Cell Biol. 189, 619–629.

Hylin, M. J., Orsi, S. A., Moore, A. N., and Dash, P. K. (2013). Disruption of the perineuronal net in the hippocampus or medial prefrontal cortex impairs fear conditioning. Learn. Mem. 20, 267–273.

Jedlicka, P., Vlachos, A., Schwarzacher, S. W., and Deller, T. (2008). A role for the spine apparatus in LTP and spatial learning. Behav. Brain Res. 192, 12–19.

John, N., Krügel, H., Frischknecht, R., Smalla, K. H., Schultz, C., Kreutz, M. R., et al. (2006). Brevican-containing perineuronal nets of extracellular matrix in dissociated hippocampal primary cultures. Mol. Cell. Neurosci. 31, 774–784.

Jones, F. S., and Jones, P. L. (2000). The tenascin family of ECM glycoproteins: Structure, function, and regulation during embryonic development and tissue remodeling. Dev. Dyn. 218, 235–259.

Karagiannis, A., Gallopin, T., David, C., Battaglia, D., Geoffroy, H., Rossier, J., et al. (2009). Classification of NPY-expressing neocortical interneurons. J. Neurosci. 29, 3642–3659.

Katona, I., and Freund, T. F. (2012). Multiple functions of endocannabinoid signaling in the brain. Annu. Rev. Neurosci. 35, 529–558.

Keck, T., Scheuss, V., Jacobsen, R. I., Wierenga, C. J., Eysel, U. T., Bonhoeffer, T., et al. (2011). Loss of sensory input causes rapid structural changes of inhibitory neurons in adult mouse visual cortex. Neuron 71, 869–882.

Kelley, L. L., Koury, M. J., Bondurant, M. C., Koury, S. T., Sawyer, S. T., and Wickrema, A. (1993). Survival or death of individual proerythroblasts results from differing erythropoietin sensitivities: a mechanism for controlled rates of erythrocyte production. Blood 82, 2340–2352.

Kerner, B. (2009). Glutamate neurotransmission in psychotic disorders and substance abuse. Open Psychiatr. J. 3, 1–8.

Kevenaar, J. T., and Hoogenraad, C. C. (2015). The axonal cytoskeleton: from organization to function. Front. Mol. Neurosci. 8, 1–12.

Killcross, S., Robbins, T. W., and Everitt, B. J. (1997). Different types of fear-conditioned behaviour mediated by separate nuclei within amygdala. Nature 388, 377–380.

Kim, S., Lee, S., Ryu, S., Suk, J. G., and Park, C. (2002). Comparative analysis of the anxiety-related behaviors in four inbred mice. Behav. Processes 60, 181–190.

Klausberger, T., and Somogyi, P. (2008). Neuronal diversity and temporal dynamics: the unity of hippocampal circuit operations. Science 321, 53–57.

Klingmüller, U., Bergelson, S., Hsiao, J. G., and Lodish, H. F. (1996). Multiple tyrosine residues in the cytosolic domain of the erythropoietin receptor promote activation of STAT5. Proc. Natl. Acad. Sci. U. S. A. 93, 8324–8.

Kolb, B., and Gibb, R. (2015). Plasticity in the prefrontal cortex of adult rats. Front. Cell.

Neurosci. 9, 1–11.

Kosaka, T., and Heizmann, C. W. (1989). Selective staining of a population of parvalbumin-containing GABAergic neurons in the rat cerebral cortex by lectins with specific affinity for terminal N-acetylgalactosamine. Brain Res. 483, 158–163.

Kröcher, T., Malinovskaja, K., Jürgenson, M., Aonurm-Helm, A., Zharkovskaya, T., Kalda, A., et al. (2013). Schizophrenia-like phenotype of polysialyltransferase ST8SIA2-deficient mice. Brain Struct. Funct. 220, 71–83.

Krocher, T., Rockle, I., Diederichs, U., Weinhold, B., Burkhardt, H., Yanagawa, Y., et al. (2014). A crucial role for polysialic acid in developmental interneuron migration and the establishment of interneuron densities in the mouse prefrontal cortex. Development 141, 3022–3032.

Kubota, Y. (2014). Untangling GABAergic wiring in the cortical microcircuit. Curr. Opin. Neurobiol. 26, 7–14.

Kwon, S. E., and Chapman, E. R. (2011). Synaptophysin regulates the kinetics of synaptic vesicle endocytosis in central neurons. Neuron 70, 847–854.

Lachance-Touchette, P., Choudhury, M., Stoica, A., Di Cristo, G., and Cossette, P. (2014). Single-cell genetic expression of mutant GABAA receptors causing Human genetic epilepsy alters dendritic spine and GABAergic bouton formation in a mutation-specific manner. Front. Cell. Neurosci. 8, 1–10.

Lasztóczi, B., and Klausberger, T. (2014). Layer-specific GABAergic control of distinct gamma oscillations in the CA1 hippocampus. Neuron 81, 1126–1139.

Lee, C. C., Huang, C. C., and Hsu, K. Sen (2011). Insulin promotes dendritic spine and synapse formation by the PI3K/Akt/mTOR and Rac1 signaling pathways. Neuropharmacology 61, 867–879.

Lévi, S., Le Roux, N., Eugène, E., and Poncer, J. C. (2015). Benzodiazepine ligands rapidly influence GABAA receptor diffusion and clustering at hippocampal inhibitory synapses. Neuropharmacology 88, 199–208.

Lewis, D. A., Hashimoto, T., and Volk, D. W. (2005). Cortical inhibitory neurons and schizophrenia. Nat. Rev. Neurosci. 6, 312–324.

Longair, M. H., Baker, D. A., and Armstrong, J. D. (2011). Simple neurite tracer: Open source software for reconstruction, visualization and analysis of neuronal processes. Bioinformatics 27, 2453–2454.

Lorenzo Bozzelli, P., Alaiyed, S., Kim, E., Villapol, S., and Conant, K. (2018). Proteolytic remodeling of perineuronal nets: effects on synaptic plasticity and neuronal population dynamics. Neural Plast. 2018.

Lucassen, P. J., Pruessner, J., Sousa, N., Almeida, O. F. X., Van Dam, A. M., Rajkowska, G., et al. (2014). Neuropathology of stress. Acta Neuropathol. 127, 109–135.

Luine, V., and Frankfurt, M. (2013). Interactions between estradiol, BDNF and dendritic spines in promoting memory. Neuroscience 239, 34–45.

Luscher, B., Shen, Q., and Sahir, N. (2011). The GABAergic deficit hypothesis of major depressive disorder. Mol. Psychiatry 16, 383–406.

Malinow, R., Hayashi, Y., Maletic-Savatic, M., Zaman, S. H., Poncer, J. C., Shi, S. H., et al. (2010). Introduction of green fluorescent protein (GFP) into hippocampal neurons through viral infection. Cold Spring Harb. Protoc. 2010.

Maragakis, N. J., and Rothstein, J. D. (2004). Glutamate transporters: Animal models to neurologic disease. Neurobiol. Dis. 15, 461–473.

Margolis, R. K., Rauch, U., Maurel, P., Margolis, R. U. (1996). Neurocan and phosphacan: Two major nervous tissue- specific chondroitin sulfate proteoglycans. Perspect Dev Neurobiol. 3, 273–290.

Marín, O. (2012). Interneuron dysfunction in psychiatric disorders. Nat. Rev. Neurosci. 13, 107–120.

Markram, H., Toledo-Rodriguez, M., Wang, Y., Gupta, A., Silberberg, G., and Wu, C. (2004). Interneurons of the neocortical inhibitory system. Nat. Rev. Neurosci. 5, 793–807.

Masuda, S., Nagao, M., Takahata, K., Konishi, Y., Gallyas, F., Tabira, T., et al. (1993). Functional erythropoietin receptor of the cells with neural characteristics: Comparison with receptor properties of erythroid cells. J. Biol. Chem. 268, 11208–11216.

Matuszko, G., Curreli, S., Kaushik, R., Becker, A., and Dityatev, A. (2017). Extracellular matrix alterations in the ketamine model of schizophrenia. Neuroscience 350, 13–22.

Mauney, S. A., Athanas, K. M., Pantazopoulos, H., Shaskan, N., Passeri, E., Berretta, S., et al. (2013). Developmental pattern of perineuronal nets in the human prefrontal cortex and their deficit in schizophrenia. Biol. Psychiatry 74, 427–435.

McAuley, E. Z., Scimone, A., Tiwari, Y., Agahi, G., Mowry, B. J., Holliday, E. G., et al. (2012). Identification of sialyltransferase 8B as a generalized susceptibility gene for psychotic and mood disorders on chromosome 15q25-26. PLoS One 7.

McEwen, B. S. (1999). Stress and hippocampal plasticity. Annu. Rev. Neurosci. 22, 105–122.

McKinney, R. A. (2010). Excitatory amino acid involvement in dendritic spine formation, maintenance and remodelling. J. Physiol. 588, 107–116.

Mikkonen, M., Soininen, H., Tapiola, T., Alafuzoff, I., and Miettinen, R. (1999). Hippocampal plasticity in Alzheimer's disease: changes in highly polysialylated NCAM immunoreactivity in the hippocampal formation. Eur. J. Neurosci. 11, 1754–1764.

Miskowiak, K., O'Sullivan, U., and Harmer, C. J. (2007). Erythropoietin Enhances Hippocampal Response during Memory Retrieval in Humans. J. Neurosci. 27, 2788–2792.

Morawski, M., Reinert, T., Meyer-Klaucke, W., Wagner, F. E., Tröger, W., Reinert, A., et al. (2015). Ion exchanger in the brain: Quantitative analysis of perineuronally fixed anionic binding sites suggests diffusion barriers with ion sorting properties. Sci. Rep. 5, 1–9.

Morikawa, S., Ikegaya, Y., Narita, M., and Tamura, H. (2017). Activation of perineuronal net-expressing excitatory neurons during associative memory encoding and retrieval. Sci. Rep. 7, 1–9.

Morishita, H., Cabungcal, J. H., Chen, Y., Do, K. Q., and Hensch, T. K. (2015). Prolonged period of cortical plasticity upon redox dysregulation in fast-spiking interneurons. Biol. Psychiatry 78, 396–402.

Morishita, H., and Hensch, T. K. (2008). Critical period revisited: impact on vision. Curr. Opin. Neurobiol. 18, 101–107.

Moser, M. B., Trommald, M., and Andersen, P. (1994). An increase in dendritic spine density on hippocampal CA1 pyramidal cells following spatial learning in adult rats suggests the formation of new synapses. Proc. Natl. Acad. Sci. 91, 12673–12675.

Müller, C., and Remy, S. (2014). Dendritic inhibition mediated by O-LM and bistratified interneurons in the hippocampus. Front. Synaptic Neurosci. 6, 1–15.

Mühlenhoff, M., Rollenhagen, M., Werneburg, S., Gerardy-Schahn, R., and Hildebrandt,

H. (2013). Polysialic acid: Versatile modification of NCAM, SynCAM 1 and neuropilin-2. Neurochem. Res. 38, 1134–1143.

Mühlenhoff, M., Oltmann-Norden, I., Weinhold, B., Hildebrandt, H., and Gerardy-Schahn, R. (2009). Brain development needs sugar: The role of polysialic acid in controlling NCAM functions. Biol. Chem. 390, 567–574.

Murphy, D. D., Cole, N. B., Greenberger, V., and Segal, M. (1998). Estradiol increases dendritic spine density by reducing GABA neurotransmission in hippocampal neurons. J. Neurosci. 18, 2550–2559.

Nacher, J., Guirado, R., and Castillo-Gómez, E. (2013). Structural plasticity of interneurons in the adult brain: Role of PSA-NCAM and implications for psychiatric disorders. Neurochem. Res. 38, 1122–1133.

Nacher, J., Guirado, R., Varea, E., Alonso-Llosa, G., Röckle, I., and Hildebrandt, H. (2010). Divergent impact of the polysialyltransferases ST8SiaII and ST8SiaIV on polysialic acid expression in immature neurons and interneurons of the adult cerebral cortex. Neuroscience 167, 825–837.

Nacher, J., Blasco-Ibáez, J. M., and McEwen, B. S. (2002a). Non-granule PSA-NCAM immunoreactive neurons in the rat hippocampus. Brain Res. 930, 1–11.

Nacher, J., Lanuza, E., and McEwen, B. S. (2002b). Distribution of PSA-NCAM expression in the amygdala of the adult rat. Neuroscience 113, 479–484.

Nadam, J., Navarro, F., Sanchez, P., Moulin, C., Georges, B., Laglaine, A., et al. (2007). Neuroprotective effects of erythropoietin in the rat hippocampus after pilocarpine-induced status epilepticus. Neurobiol. Dis. 25, 412–426.

Nelson, S. B., and Valakh, V. (2015). Excitatory/Inhibitory balance and circuit homeostasis in autism spectrum disorders. Neuron 87, 684–698.

Newcomer, J. W., Farber, N. B., and Olney, J. W. (2000). NMDA receptor function, memory, and brain aging. Dialogues Clin. Neurosci. 2, 219–232.

Oliva, A., Jiang, M., Lam, T., Smith, K. L., and Swann, J. W. (2000). Novel hippocampal interneuronal subtypes identified using transgenic mice that express green fluorescent protein in GABAergic interneurons. J. Neurosci. 20, 3354–3368.

Oltmann-Norden, I., Galuska, S. P., Hildebrandt, H., Geyer, R., Gerardy-Schahn, R., Geyer, H., et al. (2008). Impact of the polysialyltransferases ST8SiaII and ST8SiaIV on polysialic acid synthesis during postnatal mouse brain development. J. Biol. Chem.

283, 1463–1471.

Ostrowski, D., and Heinrich, R. (2018). Alternative erythropoietin receptors in the nervous system. J. Clin. Med. 7, 24.

Ott, C., Martens, H., Hassouna, I., Oliveira, B., Erck, C., Zafeiriou, M.P., et al. (2015). Widespread expression of erythropoietin receptor in brain and its induction by injury. Mol. Med. 21, 803–815.

Pan, F., Aldridge, G. M., Greenough, W. T., and Gan, W. B. (2010). Dendritic spine instability and insensitivity to modulation by sensory experience in a mouse model of fragile X syndrome. Proc. Natl. Acad. Sci. 107, 17768–17773.

Pannese, E. (1999). The golgi stain: Invention, diffusion and impact on neurosciences. J. Hist. Neurosci. 8, 132–140.

Pantazopoulos, H., and Berretta, S. (2016). In sickness and in health: Perineuronal nets and synaptic plasticity in psychiatric disorders. Neural Plast. 2016.

Paxinos, G., and Franklin, K. B. J. (2008). The Mouse Brain in Stereotaxic Coordinates (3rd. Edition). Academic Press.

Perez-Rando, M., Castillo-Gomez, E., Bueno-Fernandez, C., and Nacher, J. (2018). The TrkB agonist 7,8-dihydroxyflavone changes the structural dynamics of neocortical pyramidal neurons and improves object recognition in mice. Brain Struct. Funct. 223, 2393–2408.

Perez-Rando, M., Castillo-Gómez, E., Guirado, R., Blasco-Ibañez, J. M., Crespo, C., Varea, E., et al. (2017a). NMDA Receptors Regulate the Structural Plasticity of Spines and Axonal Boutons in Hippocampal Interneurons. Front. Cell. Neurosci. 11:166.

Pérez-Rando, M., Castillo-Gómez, E., Bellés, M., Carceller, H., and Nácher, J. (2017b). The activation of NMDA receptors alters the structural dynamics of the spines of hippocampal interneurons. Neurosci. Lett. 658, 79–84.

Petridis, A. K., El Maarouf, A., and Rutishauser, U. (2004). Polysialic acid regulates cell contact-dependent neuronal differentiation of progenitor cells from the subventricular zone. Dev. Dyn. 230, 675–684.

Pettit, D. L., and Augustine, G. J. (2000). Distribution of Functional Glutamate and GABA Receptors on Hippocampal Pyramidal Cells and Interneurons. J. Neurophysiol. 84, 28–38.

Pham, K., Nacher, J., Hof, P. R., and McEwen, B. S. (2003). Repeated restraint stress

suppresses neurogenesis and induces biphasic PSA-NCAM expression in the adult rat dentate gyrus. Eur. J. Neurosci. 17, 879–886.

Pizzorusso, T., Medini, P., Berardi, N., Chierzi, S., Fawcett, J. W., and Maffei, L. (2002). Reactivation of ocular dominance plasticity in the adult visual cortex. Science. 298, 1248–1251.

Porrero, C., Rubio-Garrido, P., Avendaño, C., and Clascá, F. (2010). Mapping of fluorescent protein-expressing neurons and axon pathways in adult and developing Thy1-eYFP-H transgenic mice. Brain Res. 1345, 59–72.

Prut, L., and Belzung, C. (2003). The open field as a paradigm to measure the effects of drugs on anxiety-like behaviors: A review. Eur. J. Pharmacol. 463, 3–33.

Purves, D., Brannon, E. M., Cabeza, R., Huettel, S. A., LaBar, K. S., Platt, M. L., and Woldorff, M. G. (2008). Principles of cognitive neuroscience, volume 83. Sinauer Associates.

Qiao, H., Li, M. X., Xu, C., Chen, H. Bin, An, S. C., and Ma, X. M. (2016). Dendritic spines in depression: what we learned from animal models. Neural Plast. 2016, 20–24.

Radley, J. J., Sisti, H. M., Hao, J., Rocher, A. B., McCall, T., Hof, P. R., et al. (2004). Chronic behavioral stress induces apical dendritic reorganization in pyramidal neurons of the medial prefrontal cortex. Neuroscience 125, 1–6.

Rajmohan, V., and Mohandas, E. (2007). The limbic system. Indian J. Psychiatry 49, 132–139.

Ramón y Cajal S (1909). Histologie du système nerveux de l'homme et des Vertébrés. At <http://cataleg.ub.edu/record=b1267770~S1*cat>.

Rochefort, N. L., and Konnerth, A. (2012). Dendritic spines: From structure to in vivo function. EMBO Rep. 13, 699–708.

Rotaru, D. C., Lewis, D. A., and Gonzalez-Burgos, G. (2012). The role of glutamatergic inputs onto parvalbumin-positive interneurons: Relevance for schizophrenia. Rev. Neurosci. 23, 97–109.

Rudolph, U., and Knoflach, F. (2011). Beyond classical benzodiazepines: Novel therapeutic potential of GABAA receptor subtypes. Nat. Rev. Drug Discov. 10, 685–697.

Rutishauser, U. (2008). Polysialic acid in the plasticity of the developing and adult vertebrate nervous system. Nat. Rev. Neurosci. 9, 26–35.

Saghatelyan, A. K., Dityatev, A., Schmidt, S., Schuster, T., Bartsch, U., and Schachner, M. (2001). Reduced perisomatic inhibition, increased excitatory transmission, and impaired long-term potentiation in mice deficient for the extracellular matrix glycoprotein tenascin-R. Mol. Cell. Neurosci. 17, 226–240.

Santos, M. S., Li, H., and Voglmaier, S. M. (2009). Synaptic vesicle protein trafficking at the glutamate synapse. Neuroscience 158, 189–203.

Sargin, D., El-Kordi, A., Agarwal, A., Müller, M., Wojcik, S. M., Hassouna, I., et al. (2011). Expression of constitutively active erythropoietin receptor in pyramidal neurons of cortex and hippocampus boosts higher cognitive functions in mice. BMC Biol. 9, 27.

Schaefer, N., Rotermund, C., Blumrich, E. M., Lourenco, M. V., Joshi, P., Hegemann, R. U., et al. (2017). The malleable brain: plasticity of neural circuits and behavior – a review from students to students. J. Neurochem. 142, 790–811.

Scheuss, V., and Bonhoeffer, T. (2014). Function of dendritic spines on hippocampal inhibitory neurons. Cereb. Cortex 24, 3142–3153.

Scheyltjens, I., and Arckens, L. (2016). The current status of somatostatin interneurons in inhibitory control of brain function and plasticity. Neural Plast. 2016, 8723623.

Schindelin, J., Arganda-Carreras, I., Frise, E., Kaynig, V., Longair, M., Pietzsch, T., et al. (2012). Fiji: an open source platform for biological image analysis. Nat. Methods 9, 676–682.

Schuster, T., Krug, M., Stalder, M., Hackel, N., Gerardy-Schahn, R., and Schachner, M. (2001). Immunoelectron microscopic localization of the neural recognition molecules L1, NCAM, and its isoform NCAM180, the NCAM-associated polysialic acid, beta1 integrin and the extracellular matrix molecule tenascin-R in synapses of the adult rat hippocampus. J. Neurobiol. 49, 142–158.

Seamans, J. K., Lapish, C. C., and Durstewitz, D. (2008). Comparing the prefrontal cortex of rats and primates: Insights from electrophysiology. Neurotox. Res. 14, 249–262.

Seki, T., and Arai, Y. (1999). Different polysialic acid-neural cell adhesion molecule expression patterns in distinct types of mossy fiber boutons in the adult hippocampus. J. Comp. Neurol. 410, 115–125.

Seki, T., and Arai, Y. (1993). Distribution and possible roles of the highly polysialylated neural cell adhesion molecule (NCAM-H) in the developing and adult central nervous system. Neurosci. Res. 17, 265–290.

Selten, M., van Bokhoven, H., and Nadif Kasri, N. (2018). Inhibitory control of the excitatory/inhibitory balance in psychiatric disorders. F1000Research 7, 23.

Sharma, N., Classen, J., and Cohen, L. G. (2013). Neural plasticity and its contribution to functional recovery. Handb. Clin. Neurol. 110, 3–12.

Sharma, V., Gilhotra, R., Dhingra, D., and Gilhotra, N. (2011). Possible underlying influence of p38MAPK and NF-κB in the diminished anti-anxiety effect of diazepam in stressed mice. J. Pharmacol. Sci. 116, 257–263.

Sheng, N., Yang, J., Silm, K., Edwards, R. H., and Nicoll, R. A. (2017). A slow excitatory postsynaptic current mediated by a novel metabotropic glutamate receptor in CA1 pyramidal neurons. Neuropharmacology 115, 4–9.

Shi, Z., Hodges, V. M., Dunlop, E. A., Percy, M. J., Maxwell, A. P., El-Tanani, M., et al. (2010). Erythropoietin-induced activation of the JAK2/STAT5, PI3K/Akt, and Ras/ERK pathways promotes malignant cell behavior in a modified breast cancer cell line. Mol. Cancer Res. 8, 615–626.

Sholl, B. D. a (1953). Dendritic organization in the neurons of the visual and moter cortices of the cat. J Anat 87, 387–406.

Sigel, E., and Ernst, M. (2018). The benzodiazepine binding sites of GABAA receptors. Trends Pharmacol. Sci. 39, 659–671.

Sirén, A. L., Faßhauer, T., Bartels, C., and Ehrenreich, H. (2009). Therapeutic potential of erythropoietin and its structural or functional variants in the nervous system. Neurotherapeutics 6, 108–127.

Sirén, A. L., Knerlich, F., Poser, W., Gleiter, C. H., Bruck, W., and Ehrenreich, H. (2001). Erythropoietin and erythropoietin receptor in human ischemic/hypoxic brain. Acta Neuropathol. 101, 271–276.

Soghomonian, J. J., and Martin, D. L. (1998). Two isoforms of glutamate decarboxylase: Why? Trends Pharmacol. Sci. 19, 500–505.

Somogyi, P., and Klausberger, T. (2005). Defined types of cortical interneurone structure space and spike timing in the hippocampus. J. Physiol. 562, 9–26.

Sorg, B. A., Berretta, S., Blacktop, J. M., Fawcett, J. W., Kitagawa, H., Kwok, J. C. F., et al. (2016). Casting a wide net: Role of perineuronal nets in neural plasticity. J. Neurosci. 36, 11459–11468.

Spires, T. L. (2005). Dendritic spine abnormalities in amyloid precursor protein

transgenic mice demonstrated by gene transfer and intravital multiphoton microscopy. J. Neurosci. 25, 7278–7287.

Spruston, N. (2008). Pyramidal neurons: Dendritic structure and synaptic integration. Nat. Rev. Neurosci. 9, 206–221.

Stepanyants, A., Hof, P. R., and Chklovskii, D. B. (2002). Geometry and structural plasticity of synaptic connectivity. Neuron 34, 275–288.

Stettler, D. D., Yamahachi, H., Li, W., Denk, W., and Gilbert, C. D. (2006). Axons and synaptic boutons are highly dynamic in adult visual cortex. Neuron 49, 877–887.

Steullet, P., Cabungcal, J.-H., Cuénod, M., and Do, K. Q. (2014). Fast oscillatory activity in the anterior cingulate cortex: dopaminergic modulation and effect of perineuronal net loss. Front. Cell. Neurosci. 8, 1–10.

Stone, J. M. (2011). Glutamatergic antipsychotic drugs: A new dawn in the treatment of schizophrenia? Ther. Adv. Psychopharmacol. 1, 5–18.

Sullivan, P. F., Keefe, R. S. E., Lange, L. A., Lange, E. M., Stroup, T. S., Lieberman, J., et al. (2007). NCAM1 and neurocognition in schizophrenia. Biol. Psychiatry 61, 902–10.

Sultan, K. T., and Shi, S. H. (2018). Generation of diverse cortical inhibitory interneurons. Wiley Interdiscip. Rev. Dev. Biol. 7, 1–18.

Swanson, C. J., Bures, M., Johnson, M. P., Linden, A. M., Monn, J. A., and Schoepp, D. D. (2005). Metabotropic glutamate receptors as novel targets for anxiety and stress disorders. Nat. Rev. Drug Discov. 4, 131–144.

Takamori, S., Holt, M., Stenius, K., Lemke, E. A., Grønborg, M., Riedel, D., et al. (2006). Molecular Anatomy of a Trafficking Organelle. Cell 127, 831–846.

Tamamaki, N., Yanagawa, Y., Tomioka, R., Miyazaki, J. I., Obata, K., and Kaneko, T. (2003). Green fluorescent protein expression and colocalization with calretinin, parvalbumin, and somatostatin in the GAD67-GFP knock-In mouse. J. Comp. Neurol. 467, 60–79.

Tan, X.J., Dai, Y.B., Wu, W.F., Kim, H.J., Barros, R.P., Richardson, T.I., et al. (2012). Reduction of dendritic spines and elevation of GABAergic signaling in the brains of mice treated with an estrogen receptor ligand. Proc. Natl. Acad. Sci. 109, 1708–1712.

Tao, R., Li, C., Zheng, Y., Qin, W., Zhang, J., Li, X., et al. (2007). Positive association between SIAT8B and schizophrenia in the Chinese Han population. Schizophr. Res.

90, 108–14.

Tarsa, L., and Goda, Y. (2002). Synaptophysin regulates activity-dependent synapse formation in cultured hippocampal neurons. Proc. Natl. Acad. Sci. 99, 1012–1016.

Testa, D., Prochiantz, A., and Di Nardo, A. A. (2018). Perineuronal nets in brain physiology and disease. Semin. Cell Dev. Biol.

Thomson, A. M. (2007). Functional maps of neocortical local circuitry. Front. Neurosci. 1, 19–42.

Tian, L., Stefanidakis, M., Ning, L., Van Lint, P., Nyman-Huttunen, H., Libert, C., et al. (2007). Activation of NMDA receptors promotes dendritic spine development through MMP-mediated ICAM-5 cleavage. J. Cell Biol. 178, 687–700.

Tjia, M., Yu, X., Jammu, L. S., Lu, J., and Zuo, Y. (2017). Pyramidal neurons in different cortical layers exhibit distinct dynamics and plasticity of apical dendritic spines. Front. Neural Circuits 11, 1–10.

Toole, B. P. (2004). Hyaluronan: from extracellular glue to pericellular cue. Nat. Rev. Cancer 4, 528.

Traynelis, S. F., Wollmuth, L. P., McBain, C. J., Menniti, F. S., Vance, K. M., Ogden, K. K., et al. (2010). Glutamate receptor ion channels: structure, regulation, and function. Pharmacol. Rev. 62, 405–496.

Tremblay, R., Lee, S., and Rudy, B. (2016). GABAergic Interneurons in the Neocortex: From Cellular Properties to Circuits. Neuron 91, 260–292.

Tukker, J. J., Fuentealba, P., Hartwich, K., Somogyi, P., and Klausberger, T. (2007). Cell type-specific tuning of hippocampal interneuron firing during gamma oscillations in vivo. J. Neurosci. 27, 8184 LP-8189.

Tyan, L., Chamberland, S., Magnin, E., Camire, O., Francavilla, R., David, L. S., et al. (2014). Dendritic inhibition provided by interneuron-specific cells controls the firing rate and timing of the hippocampal feedback inhibitory circuitry. J. Neurosci. 34, 4534–4547.

Ueno, H., Suemitsu, S., Murakami, S., Kitamura, N., Wani, K., Okamoto, M., et al. (2017a). Postnatal development of GABAergic interneurons and perineuronal nets in mouse temporal cortex subregions. Int. J. Dev. Neurosci. 63, 27–37.

Ueno, H., Suemitsu, S., Okamoto, M., Matsumoto, Y., and Ishihara, T. (2017b). Parvalbumin neurons and perineuronal nets in the mouse prefrontal cortex.

Neuroscience 343, 115–127.

Ultanir, S. K., Hall, B. J., Kim, J.-E., Ghosh, A., Ellisman, M., and Deerinck, T. (2007). Regulation of spine morphology and spine density by NMDA receptor signaling in vivo. Proc. Natl. Acad. Sci. 104, 19553–19558.

Urban-Ciecko, J., and Barth, A. L. (2016). Somatostatin-expressing neurons in cortical networks. Nat. Rev. Neurosci. 17, 401–409.

Uylings, H. B. M., Groenewegen, H. J., and Kolb, B. (2003). Do rats have a prefrontal cortex? Behav. Brain Res. 146, 3–17.

Valeeva, G., Valiullina, F., and Khazipov, R. (2013). Excitatory actions of GABA in the intact neonatal rodent hippocampus in vitro. Front. Cell. Neurosci. 7, 1–12.

Van Aerde, K. I., and Feldmeyer, D. (2015). Morphological and physiological characterization of pyramidal neuron subtypes in rat medial prefrontal cortex. Cereb. Cortex 25, 788–805.

Varea, E., Guirado, R., Gilabert-Juan, J., Martí, U., Castillo-Gomez, E., Blasco-Ibáñez, J. M., et al. (2012). Expression of PSA-NCAM and synaptic proteins in the amygdala of psychiatric disorder patients. J. Psychiatr. Res. 46, 189–197.

Varea, E., Blasco-Ibáñez, J. M., Gómez-Climent, M. A., Castillo-Gómez, E., Crespo, C., Martínez-Guijarro, F. J., et al. (2007a). Chronic fluoxetine treatment increases the expression of PSA-NCAM in the medial prefrontal cortex. Neuropsychopharmacology 32, 803–812.

Varea, E., Castillo-Gómez, E., Gómez-Climent, M. Á., Blasco-Ibáñez, J. M., Crespo, C., Martínez-Guijarro, F. J., et al. (2007b). PSA-NCAM expression in the human prefrontal cortex. J. Chem. Neuroanat. 33, 202–209.

Varea, E., Nácher, J., Blasco-Ibáñez, J. M., Gómez-Climent, M. Á., Castillo-Gómez, E., Crespo, C., et al. (2005). PSA-NCAM expression in the rat medial prefrontal cortex. Neuroscience 136, 435–443.

Vazquez-Sanroman, D. B., Monje, R. D., and Bardo, M. T. (2017). Nicotine self-administration remodels perineuronal nets in ventral tegmental area and orbitofrontal cortex in adult male rats. Addict. Biol. 22, 1743–1755.

Walsh, R. N., and Cummins, R. a (1976). The Open-Field Test: a critical review. Psychol. Bull. 83, 482–504.

Wang, D., and Fawcett, J. (2012). The perineuronal net and the control of CNS plasticity.

Cell Tissue Res. 349, 147–160.

Weinhold, B., Seidenfaden, R., Röckle, I., Mühlenhoff, M., Schertzinger, F., Conzelmann, S., et al. (2005). Genetic ablation of polysialic acid causes severe neurodevelopmental defects rescued by deletion of the neural cell adhesion molecule. J. Biol. Chem. 280, 42971–42977.

Wen, T. H., Binder, D. K., Ethell, I. M., and Razak, K. A. (2018). The Perineuronal "safety" net? Perineuronal net abnormalities in neurological disorders. Front. Mol. Neurosci. 11, 1–17.

Witthuhn, B. A., Quelle, F. W., Silvennoinen, O., Yi, T., Tang, B., Miura, O., et al. (1993). JAK2 associates with the erythropoietin receptor and is tyrosine phosphorylated and activated following stimulation with erythropoietin. Cell 74, 227–236.

Wu, C., and Sun, D. (2015). GABA receptors in brain development, function, and injury. Metab. Brain Dis. 30, 367–379.

Wüstefeld, L., Winkler, D., Janc, O. a., Hassouna, I., Ronnenberg, A., Ostmeier, K., et al. (2016). Selective expression of a constitutively active erythropoietin receptor in GABAergic neurons alters hippocampal network properties without affecting cognition. J. Neurochem. 136, 698–705.

Xerri, C. (2008). Imprinting of idyosyncratic experience in cortical sensory maps: Neural substrates of representational remodeling and correlative perceptual changes. Behav. Brain Res. 192, 26–41.

Yabe, U., Sato, C., Matsuda, T., and Kitajima, K. (2003). Polysialic acid in human milk: CD36 is a new member of mammalian polysialic acid-containing glycoprotein. J. Biol. Chem. 278, 13875–13880.

Yamada, J., Ohgomori, T., and Jinno, S. (2015). Perineuronal nets affect parvalbumin expression in GABAergic neurons of the mouse hippocampus. Eur. J. Neurosci. 41, 368–378.

Yamada, J., and Jinno, S. (2013). Spatio-temporal differences in perineuronal net expression in the mouse hippocampus, with reference to parvalbumin. Neuroscience 253, 368–379.

Yang, S. Y., Huh, I. S., Baek, J. H., Cho, E. Y., Choi, M. J., Ryu, S., et al. (2015). Association between ST8SIA2 and the risk of schizophrenia and bipolar I disorder across diagnostic boundaries. PLoS One 10, 1–12.

Yu, X., Shacka, J. J., Eells, J. B., Suarez-Quian, C., Przygodzki, R. M., Beleslin-Cokic, B., et al. (2002). Erythropoietin receptor signalling is required for normal brain development. Development 129, 505–516.

Yuste, R. (2011). Dendritic spines and distributed circuits. Neuron 71, 772–781.

Zhang, S., Wang, J., and Wang, L. (2010). Structural plasticity of dendritic spines. Front. Biol. China 5, 48–58.

Zhang, S. (2005). Rapid reversible changes in dendritic spine structure in vivo gated by the degree of ischemia. J. Neurosci. 25, 5333–5338.

Zuber, C., Lackie, P. M., Catterall, W. A., and Roth, J. (1992). Polysialic acid is associated with sodium channels and the neural cell adhesion molecule N-CAM in adult rat brain. J. Biol. Chem. 267, 9965–9971.